NRC·CNRC

Literature Review and Experimental Testing of Hydrogen/Diesel Blends for Heavy-Duty Compression Ignition Engines Operating at Typical Locomotive Engine Load Conditions

Prepared for:

Innovation Centre
Transport Canada, Ottawa, Ontario

Prepared by:

Hongsheng Guo[1], Richard Fréchette[2], Simon Lafrance[1], Brian Liko[1], Shouvik Dev[1]
[1]Energy, Mining and Environment Research Centre
[2]Automotive and Surface Transportation Research Centre
National Research Council Canada, Ottawa, Ontario

June 30, 2023

National Research Council Canada | Conseil national de recherches Canada

Canada

Disclaimer

This report is intended to provide the literature review, and testing results and analysis of a laboratory experimental investigation on a heavy-duty hydrogen-diesel dual fuel compression ignition engine, which was carried out at the National Research Council Canada (NRC). The contents of this report are for reference but not intended to be a comprehensive guidance to development, application and regulations of hydrogen engine technologies. The report reflects the views of the authors only and does not reflect the views or policies of Transport Canada and NRC. Neither NRC nor Transport Canada assumes liability for any decisions based upon the information and/or from references in this report. NRC and Transport Canada, or their employees, assume no legal liability for the utilization of the information in this report. Neither NRC nor Transport Canada assumes any legal liability for any damage or other liability whatsoever including any consequential damage even if NRC or Transport Canada or any of the NRC and Transport Canada representatives/employees have been advised of the possibility of such damages resulting from selection or use of the information, apparatuses, methods, processes or similar items described in this report. NRC and Transport Canada do not endorse products or companies. References and hyperlinks in this report to any specific commercial entity, product, process, or service by trade name, trademark, manufacturer, or otherwise, does not constitute or imply an endorsement, recommendation, or favoring by NRC and Transport Canada and shall not be used for advertising or service endorsement purposes. Trade or company names appear in this report only because they are essential to the objectives of the report. NRC and Transport Canada do not exercise any editorial control over the information that may be found in these references. The analysis and opinions presented are solely those of report authors and do not reflect those of other Government of Canada departments or agencies.

Abstract

Achieving Canada's 2030 and 2050 greenhouse gas (GHG) emissions goals means supporting new innovations that can drive emission reductions from the current fleet today, while also supporting the long-term transition to zero-carbon technologies tomorrow. During combustion, diesel engines produce air pollutant emissions including (PM) and nitrogen oxides (NOx) in addition to greenhouse gas (GHG) emissions. To be able to fulfill the GHG reduction requirements, diesel locomotives will have to reduce their GHG and air pollutant emissions. Fuel switching from diesel to low/zero carbon fuels is a means of reducing GHG emissions from locomotives in the short to medium term. Hydrogen can be a life-cycle low carbon energy carrier if it is produced by renewable energy, and therefore has the potential to reduce GHG emissions in industrial applications such as rail. Modifying a diesel engine to integrate hydrogen in the mix could help switch from diesel to life-cycle low carbon fuel and achieve reductions in GHG and pollutant emissions. This project conducted a literature review and experimental investigation of the feasibility of hydrogen application in a heavy-duty compression ignition diesel engine using dual fuel combustion technology to decrease the use of conventional diesel and reduce GHG emissions.

The literature review investigated the current use of hydrogen-diesel co-combustion engines in rail and other modes, its maintenance and retrofit effort, and its mechanics of combustion. Hydrogen only creates water when it is burned but it may also cause other issues. When co-burned with diesel, hydrogen can help reduce carbon dioxide (CO_2) emissions, although the percentage of CO_2 reduction tends to be lower than the percentage of hydrogen used. PM and carbon monoxide (CO) emissions are lower due to a more complete combustion of the mix but the higher combustion temperature usually increases the level of NOx emissions in the process. Two hydrogen injection processes, direct and indirect, were investigated. Both injection methods can have their pros and cons that have to be considered. Indirect injection is cheaper to integrate but is more limited in the range of mix and controls available. Direct injection offers more control and mix range but is more expensive and requires intrusive modification that could jeopardize the warranty and useful life of the equipment. The cost of modification, operating cost, and maintenance requirements are also discussed in this review but information about them is very limited due to the lack of studies on that subject. Comparisons are done with the trucking industries but even if hydrogen mix is seemingly more common for this mode, it remains very rare.

Considering the gaps in current scientific studies, lack of information related to the economics, as well as no real-life integration of hydrogen-diesel dual fuel combustion, the literature review suggested that currently the technology readiness level (TRL) for full integration of hydrogen-diesel co-combustion in a locomotive falls within the TRL 2-3 range.

The experimental investigation was conducted at three typical engine operating conditions, i.e. 25, 50 and 75% of full engine load, and a constant engine speed of 1000 rpm. The maximum diesel displacement ratios (hydrogen energy fraction) reached during the investigation were 50% displacement at the 25% engine load condition, 40% displacement at the 50% engine load condition, and 25% displacement at the 75% engine load condition. These displacement limits were chosen because of the capabilities of the test facility setup. The results reveal that increasing diesel displacement ratio with hydrogen almost linearly reduced CO_2 emissions. CO_2 was the dominant contributor to overall GHG emissions in hydrogen-diesel dual fuel combustion, and hence, the net GHG emissions, which included a mix of carbon dioxide (CO_2), methane (CH_4) and nitrous oxide (N_2O), also linearly reduced with increasing diesel displacement ratio. When 50, 40 and 25% of diesel was replaced by hydrogen at the three engine operating conditions, GHG emissions were also reduced by 50, 40 and 25%, respectively, compared to the original diesel-only operation. Increasing diesel displacement ratio also significantly reduced PM/smoke and CO emissions.

However, it was noted that cylinder peak pressure rise rate increased with increasing diesel displacement ratio, which is a limiting factor that prevents further increasing diesel displacement ratio by hydrogen in applications. Increasing diesel displacement ratio also increased NOx emissions.

Table of Contents

Table of Figures

List of Tables

Acronyms and Abbreviations

Φ: Injection timing

θ: Crank angle

γ: Specific heat ratio

ATDC: After top dead center

BSEC: Brake specific energy consumption

bTDC: Before the top dead center

BTE: Brake thermal efficiency

BMEP: Brake mean effective pressure

CA: Crank angle

CA05: Start of combustion, define as the crank angle at which 5% of cumulative heat is released

CA10: Crank angle at which 10% of cumulative heat is released

CA10-90: Combustion duration, defined as the difference between CA90 and CA10

CA50: Combustion phasing, defined as crank angle at which 50% of cumulative heat is released

CA90: Crank angle at which 90% of cumulative heat is released

CAD: Crank angle degree

CI: Compression ignition

CR: Compression ratio

DI: Direct injection

EGR: exhaust gas recirculation

GHG: Greenhouse gas

HC: Hydrocarbon

HDDF: hydrogen diesel dual fuel

HES/%H_2: Hydrogen energy share/hydrogen energy fraction

H2DDI: Hydrogen-diesel dual direct injection

ICE: Internal combustion engine

IMEP: Indicated mean effective pressure

ISFC: indicated specific fuel consumption

ITE: Indicated thermal efficiency

LHV: Low heating value

LFL: Lower flammability limit

LL: Low Load

Lpm: liter per minute

MFB: Mass Fraction burned

ML: Medium Load

NL: Nominal Load

NOx: Nitrogen oxides, shorthand for nitric oxide (NO) and nitrogen dioxide (NO_2)

P: Cylinder pressure

PM: particulate matter

RME: Rapeseed methyl ester

RME7: Rapeseed methyl ester 7% volume

SI: Spark injection

SODI: Start of diesel injection

V: Cylinder volume

1. Introduction

Locomotives have long lifespans and operate in service for several decades. Achieving Canada's 2030 and 2050 greenhouse gas (GHG) emissions goals, therefore, means supporting new innovations that can drive emission reductions from the current fleet today, while also supporting the long-term transition to zero-emission technologies tomorrow.

Electrification is often raised as the method to reduce GHG emissions from transportation sector and help Canada reach its climate change goals. However, non-catenary electrification is still unfeasible for freight transportation by 20 to 30 years, or even longer, due to the limit in the energy density of batteries. It has been predicted that freight transportation will still rely on fuel-based internal combustion engines until 2050. Fuel switching from diesel to low/zero carbon fuels is an effective and reliable way which can help the rail industry reduce GHG emissions in the short to medium term.

Hydrogen is a carbon-free energy carrier. It can be a life-cycle low carbon energy carrier if it is produced by renewable energy. Therefore, hydrogen has the potential to greatly reduce GHG emissions in industrial applications, especially in the freight transportation industry.

Although fuel cells for locomotives are being developed, it is expected that they will take more than decades to reach commercial-scale production. In the interim, stakeholders in the hydrogen industry have suggested converting diesel engines to run on a hydrogen-diesel mixture. If successful, this could help to kick-start a hydrogen economy without waiting for commercial hydrogen fuel cell vehicles, and enable quicker uptake of hydrogen within the existing internal combustion engine locomotive fleet.

Dual fuel combustion is able to replace a significant amount of diesel with low/zero carbon fuels, such as natural gas/renewable natural gas, ammonia and hydrogen, in compression ignition internal combustion engines. The National Research Council (NRC) has conducted investigations on natural gas/ammonia/syngas/biogas-diesel dual fuel combustion in compression ignition engines. The results from these previous investigations suggested that replacing diesel with these low/zero carbon fuels using dual fuel combustion technology helps reduce GHG and particulate matter (PM) emissions. As a carbon-free energy carrier, hydrogen not only generates zero carbon dioxide (CO_2) emissions at the tailpipe but also has higher flame propagation speed and wider flammability limit range than natural gas, biogas, syngas and ammonia, which suggests that hydrogen-diesel dual fuel combustion may perform better than natural gas/ammonia/syngas/biogas-diesel dual fuel combustion in terms of fuel slip, (i.e. some fuel components are not burned inside engine cylinders and therefore leave as exhaust and crankcase emissions), which is a primary concern for dual fuel engines. Therefore, it is hypothesized that hydrogen-diesel dual fuel combustion in compression ignition engines would notably reduce tailpipe GHG and PM emissions, while maintaining diesel-like efficiency. In addition, depending on the level of modification, dual fuel combustion can easily and automatically be switched back to diesel-only operation should hydrogen be unavailable.

Industry has done some work to examine the feasibility and business case for this technology for trucks, but not for rail. If this type of technology is feasible, then it could open a path for the rail sector to start decarbonizing earlier and start incorporating hydrogen into their operations before zero-emission fuel cell technologies are commercially available. Because of this opportunity, Transport Canada (TC) is interested in understanding the design of hydrogen-diesel dual fuel combustion engines, and experimental testing of emissions from such heavy-duty engines under locomotive operating loads.

Diesel locomotives are typically operated via "notches", which are the rate at which the locomotive's power is applied. These traditionally go from idle condition (negligible load), notch 1 (low load), up to notch 8 (high

load). A study done by GHD Limited and Transport Canada (GHD Limited, 2018) investigated the duty cycle profile of various locomotive operations in Canada. The table below summarizes the most up-to-date duty cycle information for each locomotive category in Canada. The distribution of time spent in each notch will be used as a reference to compare against the experimental results of the testing conducted by NRC for this project.

Table 1. Locomotive Duty Cycle Information (Adapted from GHD Limited, 2018).

Notch	Class I Mainline Freight	Regional Mainline Freight	Class I Road Switcher	Class I Yard Switcher	Intercity	Commuter
Idle	48.0%	67.4%	71.4%	80.7%	63.7%	76.6%
N1	8.6%	8.3%	7.7%	7.3%	6.0%	3.3%
N2	6.8%	4.9%	6.9%	6.3%	5.0%	1.9%
N3	5.8%	4.1%	4.8%	3.1%	3.5%	1.7%
N4	4.6%	3.5%	2.8%	1.4%	3.2%	1.7%
N5	3.5%	2.0%	1.5%	0.5%	3.0%	1.1%
N6	3.2%	2.0%	0.8%	0.3%	3.3%	0.8%
N7	2.1%	1.6%	0.5%	0.1%	2.3%	0.5%
N8	13.6%	6.2%	1.7%	0.3%	9.4%	12.4%
Unaccounted	3.8%	0.0%	1.9%	0.0%	0.6%	0.0%

Although it is not possible to infer the distribution of total fuel consumed across notches from this table, it is useful to observe the amount of time spent at various load conditions.

In order to examine the feasibility, benefits, and challenges of deploying hydrogen-diesel co-combustion in rail, the NRC (1) conducted a literature review of the current use of the technology in rail and other modes from which it could be adapted to rail, and (2) tested the combustion and emissions performance of hydrogen-diesel dual fuel combustion using a heavy-duty compression ignition engine test cell under loading conditions of 25, 50, and 75% of full engine load.

The information obtained from this study aims to provide context to decision-makers about converting diesel engines to run on a hydrogen-diesel mixture, such as the ease with which it might be implemented in the near-term and how much it might compete with other options that require large investments to convert locomotives such as fuel cells.

2. Literature Review

The Energy, Mining and Environment (EME) and Automotive and Surface Transportation (AST) Research Centres of the National Research Council Canada performed a literature review of the use of hydrogen-diesel co-combustion engines in rail, or other appropriate modes from which co-combustion for rail could be adapted. The research is intended to derive the technological maturity of hydrogen-diesel co-combustion for locomotives and its position on the spectrum between being used as a drop-in replacement or requiring significant conversion to be viable. This section presents the findings of a literature review on the subject.

2.1 Objectives and Methodology of Literature Review

The literature provided:

- A review of the current use of hydrogen-diesel co-combustion engines in rail, or other appropriate modes from which co-combustion could be adapted to rail.
- An overview of how hydrogen is injected into a cylinder for co-combustion.
- A description of mechanics of combustion within the cylinder during co-combustion, with an assessment of the challenges as the hydrogen ratio increases and approaches 100%.
- An assessment of the modifications to a full-scale locomotive engine, fuel lines, and engine controls that would be necessary to enable a diesel engine to incorporate hydrogen in co-combustion.
- An assessment of the costs associated with performing the modifications as set out above.
- Any insights into changes of maintenance requirements for diesel-hydrogen engines compared to diesel engines and associated costs.

2.1.1 Literature Review Scope

The scope of this research is to identify potential GHG saving through hydrogen addition with current locomotives in place in the world. The scope is on large engines such as locomotive and semi-trucks. This study does not examine topics related to:

- Embrittlement in engine due to hydrogen use.
- Embrittlement in feeding system.
- Hydrogen emission in the exhaust system.
- Fueling hydrogen and hydrogen availability.
- Engine-specific maintenance.

These and other topics would be the subject of further study.

2.1.2 Literature Scan Methodology

A literature scan was completed by the NRC's National Science Library using various publication databases and sources. This report presents the results of searching in the following scientific databases: Scopus and ProQuest (Advanced Technologies & Aerospace Collection, and Materials Science & Engineering Collection), Cordis Europa, and the UIC Publications database. In order to identify as many relevant papers as possible, the search was conducted at a very broad and high-level on the concept of hydrogen fuel cell powered locomotives. The document searches were further refined based on their relevance in relation to:

- hydrogen mixing techniques,
- hydrogen mixing percentages,
- engine loads with hydrogen,
- GHG and pollutant changes,
- costs of transformation, and,
- real life integration.

2.1.3 Reference Summary

The findings from the literature scan are summarized as follows:

- 52 references mentioning different concepts and designs of hydrogen diesel in co-combustion
- 2 literature reviews on hydrogen-diesel co-combustion
- 6 references mentioning current projects related to co-combustion
- 6 references related to experimentations on co-combustion
- 11 references mentioning cost, maintenance or modifications related to co-combustion.

References that mentioned cost, modifications or maintenance linked to co-combustion of diesel hydrogen in the databases were extremely limited. The search was expanded to include articles that were not related to trains but with trucks and stationary systems. The bibliographies from each paper were reviewed to identify additional references and sources of interest were integrated into this literature review. Some additional criteria was developed to create a better literature scan and achieve a better scope of the current situation and the coming challenges. As a high-level summary, the findings were:

- No studies that retrofitted locomotive engines specifically
- 2 studies that retrofitted heavy-duty engines (not locomotive specific)
- No studies that conducted any in-service or field testing
- 13 studies that were research/lab testing
- An analysis of the relative technology readiness levels of the co-combustion

2.2 Review of Hydrogen-Diesel Co-Combustion Engines

Co-combustion, also known as dual fuel combustion, is the process by which a significant amount of diesel is replaced with low/zero carbon fuels, such as natural gas/renewable natural gas, ammonia and hydrogen, in compression ignition internal combustion engines. The NRC has conducted investigations on natural gas, ammonia, syngas, and biogas dual fuel combustion with diesel in compression ignition engines. The results from these previous investigations suggested that replacing diesel with these low/zero carbon fuels using dual fuel combustion technology helps reduce GHG and particulate matter (PM) emissions. As a carbon-free energy carrier, hydrogen not only generates zero CO_2 emissions but also has higher flame propagation speed and wider flammability limit range than natural gas, biogas, syngas and ammonia, which suggests that hydrogen-diesel dual fuel combustion may perform better than natural gas/ammonia/syngas/biogas-diesel dual fuel combustion in terms of fuel slip, which is a primary concern for dual fuel engines. Therefore, it is hypothesized that hydrogen-diesel dual fuel combustion in compression ignition engines would notably reduce GHG and PM emissions, while maintaining diesel-like efficiency. In addition, if need be, dual fuel combustion can easily and automatically be switched back to diesel-only operation should hydrogen be unavailable.

There are 26,000 locomotives in the US using diesel at the moment and there are millions more trucks and other engines that require diesel to work. Replacing these diesel engines with more environmentally friendly equipment will take a long time. The option to upgrade them with a more accessible solution could be a quick and cheap option. Replacing a portion of diesel fuel with hydrogen could help reduce CO_2 emissions from these engines.

The upgrade proposed by this study is to introduce different levels of hydrogen into diesel engines operating at various engine loads. It is predicted that the results will be different in terms of GHG, PM, NOx, and other pollutant emissions. Currently, without hydrogen, there are noticeable emissions of those pollutants and GHG that can vary according to load and engine. The predicted impacts include efficiency benefits, but also an increased risk of knocking in the engine.

2.3 Previous Literature Reviews

Through this literature scan, two literature reviews conducted by other researchers on this topic were discovered. Both published in 2017, they give a good summary of the situation at the time. Some of their findings and final analysis will be discussed in the next two sections.

2.3.1 A comprehensive Review on Utilization of Hydrogen in a Compression Ignition Engine under Dual Fuel Mode (Chintala & Subramanian, 2017)

A literature summary of performance, combustion and emission characteristics of hydrogen-diesel dual-fuel engines at different loads are given in Table 2. It could be concluded from the table that the utilization of hydrogen in compression ignition (CI) engines under dual-fuel mode yields both the benefits of thermal efficiency improvement and emissions (carbon based) reduction significantly.

Table 2: Summary of effects of hydrogen on performance, combustion and emission characteristics of dual-fuel engines.

Description of the parameter	**With increasing H2 energy share at higher and moderate loads**	**With increasing H2 energy share at lower loads**
Thermal efficiency	Increases (higher than base diesel mode)	Decreases
Exergy efficiency	Increases at higher load Fluctuating trend at moderate loads	Fluctuating trend
Volumetric efficiency	Decreases	Decreases
Exhaust gas temperature	Increases	Increases
In-cylinder peak pressure	Increases	Decreases
In-cylinder peak temperature	Increases	Decreases
Start of combustion	Advances	Retards
Heat release rate	Increases	Decreases
Ignition delay	Decreases/fluctuating trend	Fluctuating trend
Combustion duration	Decreases	Increases
Combustion efficiency	Increases	Decreases
Rate of pressure rise	Increases	Decreases
HC emissions	Decreases	Decreases
CO emissions	Decreases	Decreases
Smoke/PM emissions	Decreases	Decreases
CO2 emissions	Decreases	Decreases

NOx emissions	Increases	Increases

A literature summary on performance, combustion and emission characteristics of dual-fuel engines with compression ratio reduction and water injection strategies is given in Table 3.

Table 3: Comparative summary of water injection and compression ratio reduction strategies under dual-fuel mode at high load condition

Description of the parameter	Conventional dual-fuel mode	Water addition strategy	CR reduction strategy
Thermal efficiency	Increases	Decreases	Decreases
In-cylinder peak pressure	Increases	Decreases	Decreases
In-cylinder peak temperature	Increases	Decreases	Decreases
Start of combustion	Advances	Retards	Retards
Heat release rate	Increases	Decreases	Decreases
Ignition delay	Decreases	Increases	Increases
Combustion duration	Decreases	Increases	Increases
Rate of pressure rise	Increases	Decreases	Decreases
HC emissions	Decreases	Increases	Increases
CO emissions	Decreases	Increases	Increases
Smoke/PM emissions	Decreases	Increases	Increases
NOx emissions	Increases	Decreases	Decreases

The following conclusions are drawn based on the literature information from this literature review and the two tables above related to hydrogen based dual-fuel engines.

- With increasing hydrogen energy share in a dual-fuel engine, thermal efficiency of the engine increases significantly at high and moderate loads whereas the efficiency decreases at low loads.
- As hydrogen is a carbon free energy carrier, all carbon based emissions such as hydrocarbon (HC), carbon monoxide (CO), carbon dioxide (CO2), and smoke/particulate matter (PM) in diesel engines under dual-fuel mode decreases substantially at all loads.
- Nitrogen oxides (NOx) emissions increase drastically with hydrogen addition in a dual-fuel engine at high and moderate loads due to high in-cylinder temperature.
- In-cylinder pressure and in-cylinder temperature increase significantly with increase in hydrogen energy share in a dual-fuel engine at high and moderate loads.
- Start of combustion in a CI engine under dual-fuel mode advances with increase in amount of hydrogen substitution. Beyond a critical energy share of hydrogen, auto-ignition of premixed hydrogen-air mixture could occur, which may result in combustion with knocking.

- High levels of NOx emissions, abnormal combustion at high hydrogen energy shares, and limited hydrogen energy share are the major problems associated with hydrogen dual-fuel operation.
- The aforementioned three problems could be resolved by low temperature combustion strategies including water injection and reduction of compression ratio of the engine.

2.3.2 A review of Hydrogen as a Compression Ignition Engine Fuel (Dimitriou & Tsujimura, 2017)

This review is interesting because the authors published it a year prior to publishing the results of their own experiment (Dimitriou et al., 2018). Their experiment will be shown in section 2.5.1.4.

The review found that hydrogen supply in compression ignition engines provides significant reductions in HC, CO, CO_2 and smoke levels which, under optimum conditions, can reach reductions of over 50%. High hydrogen rates tend to have an apparent effect on the combustion process which is depicted as a sharp increase in heat release rate and brake thermal efficiency. However, the increased in-cylinder temperatures due to the high combustion temperature of hydrogen result in a significant growth of NOx emissions, particularly at high load conditions.

Applying exhaust gas recirculation (EGR) can compensate the increased pressure and heat release rate resulting from the hydrogen enrichment, leading to NOx emissions decreasing with increasing EGR ratio. However, increasing EGR rate is most often associated with a penalty in smoke, CO and HC emissions due to the lower O_2 levels in the cylinder chambers. Despite the penalty, the combination of hydrogen fuel with EGR under optimum parameters have been found to provide a simultaneous reduction of all emissions compared to the neat diesel operation.

This reference concluded that hydrogen supply has been demonstrated to significantly reduce smoke and part of the harmful diesel engine emissions, NOx emissions are still a critical issue in hydrogen-diesel co-combustion operations. The study states that this challenge needs to be resolved in order to bring back the reliability and interest of blending diesel with hydrogen in compression ignition engines. Further extensive research is required to assess whether low-temperature combustion techniques can assist in NOx reduction while maintaining a knock-free operation.

The main findings of this review (Dimitriou & Tsujimura, 2017) are summarized in the Table 4. This table provide the test condition and the impact on emissions of pollutants. White boxes indicate that this parameter wasn't studied in this test.

Table 4: Summary of the impact on the performance and emissions behaviour of hydrogen/diesel dual-fuel engines compared to the diesel-only operation as derived from the literature survey.

Reference		Positive			Negative			No change				**Comments**
	Year	**Test conditions**			**Performance (increase is a positive outcome)**		**Emissions (decrease is a positive outcome)**					
		Load	**EGR**	**H2 supply**	**BTE**	**BSFC**	**PM**	**HC**	**NOx**	**CO**	**CO2**	
(Varde & Frame, 1983)	1983	82%, 100%	No	14%-17%								

(Lilik et al., 2010)	2010	25%, 75%	0-13%	2.5%-15%								1800rpm
		25%, 75%	0-13%	2.5%-15%								3600rpm
(Saravanan & Nagarajan, 2009a)	2009	25%, 100%	No	9.4%-37%								
		50%, 75%	No	9.4%-37%								
(Saravanan & Nagarajan, 2009b, 2010)	2009	25%	No	2-9.5 lpm								
		50%, 75%	No	2-9.5 lpm								
		100%	No	2-9.5 lpm								
(Zhou et al., 2014)	2014	10%	No	10%-40%								
		30%	No	10%-40%								
		50%	No	10%-40%								
		100%	No	10%-40%								
(Sandalcı & Karagöz, 2014)	2014	100%	No	0-46%								
(Masood et al., 2007; Saravanan & Nagarajan, 2008)	2008	20% - 100%	No	10%-100%								
(Saravanan & Nagarajan, 2008)	2008	100%	No	0-38.6%								Variation of injection timing
(Saravanan & Nagarajan, 2008)	2008	0% - 100%	No	0-100%								NOx reduced for H2>30%
(Tsujimura & Suzuki, 2017)	2017	3-9bar IMEP	No	0-90%								NOx increase for high loads
(Suzuki & Tsujimura, 2015)	2015	Partial	0-36%	50-78%								
(Suzuki et al., 2015)	2015	4.5-10.5 bar IMEP	0-29%	0-83%								
(Talibi et al., 2017)	2017	8.5-11 bar IMEP	0-3% O2 red	0-40%								
(Bose & Maji, 2009)	2009	20%, 40%, 60%, 80%	0-20%	0.15 kg/hr								

(Wu & Wu, 2012)	2012	10%-60%	0-40%	0-20%								
(Shin et al., 2011)	2011	5.9 bar IMEP	2%-31%	2%-10%								
(Chaichan, 2015)	2015	0.1-0.7	0-15%	0-20%0-20%								
(Gatts et al., 2012)	2012	10%-70%	No	0-92%								
(SinghYadav et al., 2012)	2012	0.5-3kW	0-20%	40mg/hr								
(Christodoulou & Megaritis, 2014)	2014	2.5-5 bar IMEP	No	0-8%								
(Tomita et al., 2001)	2001	0.3. 0.4, 0.5	No	0-80%								Advanced injection timing
(Chintala & Subramanian, 2016)	2016		No	0-36%								Water addition
(Chintala & Subramanian, 2015)	2015	100%	No	0-36%								Water addition
(Mathur et al., 1992)	2015	0-100%	No	20-50 lpm								Diluents addition
(Guo et al., 2011)	2011	4 bar IMEP	0-60%	0-15%								Varied CR
(Park et al., 2015)	2015	0.35-0.43 bar IMEP	0-43%	0-70%								PCCI, additional EGR- low NOx
(Geo et al., 2008)	2008	25%-100%	No	0-28%								Biofuels
(Samuel & McCormick, 2010)	2010	5.3 bar IMEP	No	1.2-2.8 lpm								NOx increase for H2 rate
(Deb et al., 2015)	2015	5.2 kW	No	0-42%								
(Karagöz et al., 2015)	2015	10%-100%	No	30%								NOx increased for full load

2.4 Current Use of Hydrogen-Diesel Co-combustion Engines in Rail and Trucks

This section summarizes the current use of hydrogen-diesel co-combustion engines in rail and trucks.

2.4.1 Trains

The review did not find any published results reporting on in-service conversions of diesel locomotives to diesel-hydrogen co-combustion. The majority of the planned conversions in the locomotive area involve conversion to hydrogen cells by removing the entire diesel engine block and putting the necessary

equipment for the conversion into it. Figure 1 provides an example that should soon be realized at the Sierra Northern railway. (Casey, 2021)

Many projects involve the replacement of diesel locomotives with hydrogen fuel cell locomotives such as a project with 14 locomotives in Germany (Day, 2022) and even a project already underway in the United States using Canadian hydrogen cells (Lagerquist, 2022). These projects are just a few examples of projects already in place or very advanced in the field of hydrogen fuel cell trains, which are numerous compared to co-combustion trains, which are mainly present in laboratories for the moment.

There is, however, a German-funded project in Namibia, Africa to convert two diesel-electric locomotives to operate in co-combustion. The project was last announced in October 2022. The locomotives will operate in tandem with an in-between car carrying hydrogen. This project is expected to take 18 months (Geerts, 2022).

2.4.2 Trucks

There seems to be more conversion in the field of ground transportation trucks. Some companies have converted one or more of their vehicles and some are working on projects for new engines specifically designed to run on a hydrogen-diesel fuel blend. The Ladgewood company has been using semi-trailers converted to co-combustion for more than a year. (Nielsen, 2021) The article mentions modifications to the engine to keep all the manufacturer's warranty and uses a hydrogen-diesel blend to reduce GHGs by up to 40%. This project was accomplished by Vancouver-based Hydra Energy.

The company dynaCERT is commercializing a kit to adapt a diesel truck engine to use hydrogen in the combustion process. (dynaCERT, 2023). This kit claims to be able to use hydrogen with a diesel engine and achieve up to 88.7% reduction in NOx, 46.7% in CO, 9.6% in CO_2 and 55.3% in PM. However, no references were found that described real-world use of these kits. The company HYDI is also selling a similar product. (HYDI, 2023); it claims reductions up to 25% for CO, 14% for fuel usage and 70% for PM but has not been verified through independent testing. DynaCERT and HYDI use hydrogen generated on the vehicle through the electrolysis process with electricity supplied to the equipment by the vehicle. The studies do not mention the quantity of electricity require to manage that system, so it is hard to estimate the level of efficiency of these systems.

The Cummins Company has designed a combustion engine for the combustion of agnostic fuels that allows hydrogen to run. (Zarich, 2022) This engine, however, will not be available until 2027. However, it will have the announced advantage of being less expensive than an electrical system based on batteries or hydrogen fuel cells. The company MAN is also presenting a similar engine able to use dual fuel (Schaffelhofer, 2022), and so is Volvo with its Volvo Penta engine. (Schultz, 2022) Both companies' promise CO_2 reduction with their new engines being developed in the coming years.

2.5 How Hydrogen Is Injected into a Cylinder for Co-Combustion, Mechanics of Combustion within the Cylinder during Co-Combustion and Modifications Required

This section will examine five examples of hydrogen-diesel dual-fuel (HDDF) engines found in the literature. These examples were selected due to their details on their approaches, experiments and results.

There are mainly two types of injections studied: indirect injection via the air intake manifold (also known as port injection), and direct injection (DI) into the cylinder by the use of an additional injector, see on Figure 2.

Indirect injection is made by injecting hydrogen through the air flow in the manifold. This process allows a simple setup and hydrogen is mixed with air. This process doesn't allow a specific timing to introduce hydrogen in the piston. The mix enters the piston at the normal timing of a four-stroke engine.

Compared to widely studied hydrogen port injection in a diesel engine, the hydrogen DI concept executes a near top dead centre (TDC) injection to cause hydrogen mixing controlled combustion (Liu et al., 2020).

2.5.1 Port Injection through Air Intake

Port injection is more popular in experimentation. However, the lack of mixing control may limit broader experimentations with higher level of hydrogen in the mix because it cannot be injected at chosen timings.

2.5.1.1 Hydrogen supplement co-combustion with diesel in compression ignition engine (Hamdan et al., 2015)

This section will review the testing conducted in (Hamdan et al., 2015), seen in Figure 3. Hydrogen is injected into the air-intake manifold at atmospheric pressure. A pressure regulator, a volumetric rotameter and a throttle valve are used to control the hydrogen flow rate. The flow rate of air is measured using a calibrated orifice meter with a pressure transducer arrangement. The pressure transducer has an uncertainty of ±0.1 Pa. The engine specifications are shown in Table 5.

Table 5: E6 Engine specifications.

Number of cylinders	1
Bore	76.2 mm
Stroke	111.1 mm
Swept volume	0.507 L
Max. speed	50 rev/s (3000 RPM)
Max. power, diesel (CR = 20.93)	9.0 kW, naturally aspirated
Compression ratio (CR)	Max. CR 22
Injection timing	Variable, 20°–45° btdc

Effect of engine speed:

The effect of hydrogen addition is investigated under variable engine speed (1080 RPM to 1800 RPM) and is compared against base-case study for pure diesel. The results under variable engine speed are shown in Figure 4 where diesel is injected at 35° before top dead center (btdc). As shown in Figure 4a, the thermal efficiency increases as engine speed increases and then drops after reaching an optimum value. The behavior in Figure 4a is expected since at the beginning, the increase in the engine speed leads to upsurge in the turbulence levels that leads to better mixing and more intensified combustion. Then an optimum point is reached, after which any further increase in the engine speed leads to a reduction in the volumetric efficiency due to limitations in the breathing ability of the engine cylinder, the high opening/closing frequency of the intake valves and the associated difficulty and complexity of the air suction process. As a result,

further increase of the engine speed decreases the power output and leads to a fall in the thermal efficiency. The combustion with hydrogen supplement shows better efficiency when compared to the pure diesel case. This is expected since hydrogen has higher flame temperature and faster flame speed when compared to the pure diesel combustion. The specific fuel consumption is shown in Figure 4b, which shows that the presence of hydrogen reduces the specific fuel consumption rate since the lower heating value (LHV) of hydrogen is two and half times higher than diesel. In other words, more energy is released per hydrogen molecule than per molecule of diesel hydrocarbon. This effect is more pronounced at part load (low engine speed), but the study does not provide an explanation as to why.

As shown in Figure 4c, the exhaust temperature is higher in the presence of hydrogen when compared to pure diesel case. The increase in exhaust temperature is due to (a) the high heating value of hydrogen and (b) the high flame temperature when compared to diesel. Since it is difficult to measure the flame temperature inside the internal combustion engine, the exhaust temperature is used as an indicator to the flame temperature. Hence a higher exhaust temperature implies a higher flame temperature. As shown in Figure 4d, a high flame temperature will produce more NOx. The NOx is produced during the combustion process when nitrogen and oxygen are present at elevated temperatures.

For PM emissions, a direct correlation with the exhaust gas opacity (in percentage) is used to reflect qualitatively the PM emissions levels. Increasing the engine speed leads to a shorter residence time in the combustion chamber with less fuel air mixing which leads to higher smoke in the exhaust, hence opacity increases. The PM emissions are shown in Figure 4e. The higher the combustion temperature with hydrogen supplement, the higher the NOx emissions and the lower the PM emissions compared to pure diesel. Increasing the hydrogen addition enhances the premixed flame combustion and leads to a higher combustion temperature, which tends to decrease the formation of unburned carbon in the exhaust.

Effect of hydrogen flow rate:

The effect of amount of hydrogen added when it is burned with diesel is shown in Figure 5 where diesel is injected at 35° btdc. For current engines, the results show that as hydrogen supplement increases, the engine efficiency increases, which is expected since hydrogen presence will upsurge the combustion temperature and enhances mixing due to the higher flame speed of hydrogen when compared to diesel. As shown in Figure 5a for engine speed of 1260 RPM, the thermal efficiency increases with the increase of hydrogen flow rate from 0 to 8 LPM. The specific fuel consumption for fixed engine speed of 1260 RPM and different hydrogen flow rate is shown in Figure 5b, from which it is clear that as hydrogen flow rate increases, the specific fuel consumption decreases. This reduction in specific fuel consumption is expected since the lower heating value (LHV) of hydrogen is two and half times higher than LHV of diesel.

The temperature of the exhaust gases with respect to hydrogen flow rate is shown in Figure 5c. As expected, the increase of hydrogen supplement fuel causes rise in the flame temperature and hence an increase in the exhaust gases temperature. The increase in combustion temperature tends to increase NOx emissions, as shown in Figure 5d, since NOx is produced when nitrogen and oxygen are present at elevated temperatures.

The increase in the combustion temperature and increase in the NOx are associated with a decrease in the exhaust opacity from 54% at 0% hydrogen to 40% at 2 LPM, as may be seen in Figure 5e. As hydrogen is admitted with the intake air, further hydrogen addition tends to reduce the air admitted to the engine which tends to decrease the NOx formation as seen in Figure 5d and increases in the smoke formation as seen in Figure 5e.

Effect of diesel injection timing:

The effects of diesel fuel injection timing on engine performance while being supported with hydrogen supplement are shown in Figure 6. As shown in Figure 6a, at engine speed of 1260 RPM with hydrogen supplement of 4 LPM, the engine efficiency decreases with the advance in injection timing (early injection) from 20° to 40° btdc. Early injection will cause too much pressure rise before end of compression stroke which reduces output power and hence reduces engine efficiency. The specific fuel consumption for fixed engine speed of 1260 RPM and flow of 4 LPM of hydrogen supplement fuel is shown in Figure 6b. The specific fuel consumption increases as injection timing is advanced since as stated earlier advancing injection timing will reduce output power.

The effect of early injection on exhaust temperature is limited to a small decrease due to the reduction in the temperature at the end of expansion stroke, which is observed in Figure 6c. The NOx emissions are shown in Figure 6d which shows that as injection timing is advanced, the NOx emissions increase which is due to the high rise in the peak temperature and pressure of the engine during the compression stroke. As the injection timing becomes more advanced, the pressure and temperature at time of injection becomes less and less. This tends to increase the ignition delay period of the diesel fuel and hence more mass of fuel is being injected without burning. This tends to increase the smoke formation in the exhaust as shown in Figure 6e.

Summary of findings

In this work, an experimental investigation has been conducted to examine the effect of the presence of hydrogen supplement on the performance of dual fuel diesel engine. The hydrogen is introduced to the engine at atmospheric conditions by injecting the hydrogen to the air-intake manifold. It is found that the presence of 4 LPM hydrogen supplement boosts the engine efficiency for engine speed range of 1080 RPM to 1800 RPM. Also, the engine efficiency at an engine speed of 1260 RPM continues increasing with the increase of hydrogen supplement flow rate. The engine runs smoothly with the presence of hydrogen and no knocking is detected during above testing conditions. In parallel to the thermal efficiency boosting, the results demonstrate an increase in NOx Emissions and a decrease in PM emissions.

Finally, this article has no mention of any cost and modification or operation.

2.5.1.2 Influence of hydrogen co-combustion with diesel fuel on performance, smoke and combustion phases in the compression ignition engine (Juknelevicius et al., 2019)

The main objective of this study, shown in Figure 7, was to examine the impact of hydrogen addition to a compression ignition engine fueled with either rapeseed methyl ester (RME) or 7% RME blended diesel fuel (RME7) on combustion phases and ignition delay as well as smoke and exhaust toxic emissions. Tests were performed on an engine modified to work in dual fuel mode with gaseous and liquid fuel (Figure 7). The single cylinder stationary compression ignition engine Andoria S320 was used for this purpose. It was equipped with the high-pressure common rail fuel pump Bosch CR/CP1S3 driven by the 2.2 kW electric motor GL-90L2-4. Another electric motor was used as the starter for this engine. After starting up the engine, it transmits energy to a power generator. The engine was set to operate at a constant speed of 965 rpm ±0.83%. The generated electric power was supplied to the power grid and was measured. The technical specifications of the engine are given Table 6.

Table 6: Engine specifications

Number of cylinders	1

Bore diameter (mm)	120
Piston stroke (mm)	160
Displacement (cm³)	1810
Compression ratio	17
Rated power (kW/HP)	13.2/18
Rated speed (rpm)	1500
Peak torque (Nm)	84.4
Peak torque speed (rpm)	1200
Length of connecting road (mm)	275
Intake valve opening	23° bTDC
Intake valve closing	40° aBDC
Exhaust valve opening	46° bBDC
Exhaust valve closing	17° aTDC

Combustion properties

The positive trends in maximum combustion pressure were observed with increase of HES within all ranges of loads and both tested fuels (Figure 8). In fact, at the low load (LL) the maximum pressure fluctuates within the ranges of 4.88–5.08 MPa and 4.79–5.04 MPa with RME7 and RME, respectively. The negligible influence of hydrogen fraction at the LL and partially at the medium load (ML) to nominal loads (NL) with low HES was probably caused by low hydrogen fraction in the engine combustion chamber, which was below the lower flammability limit (LFL) for hydrogen. As hydrogen affects the combustion duration, the start of diesel injection timing φ was set at fixed position during tests of hydrogen–diesel mixture, as that makes it possible to compare and analyze combustion phases with various HES. Experiments revealed that the hydrogen–diesel mixture combustion leads to higher in-cylinder peak pressure with HES over 20% as depicted in Figure 8b.

ISFC decreases with increase of HES. RME at medium and nominal loads has the highest decrease of ISFC by 23.3% in comparison to 19.8% for RME7 (Figure 9). Hydrogen, due to high flame speed and short quenching distance, extends the flammability limits of the RME–hydrogen mixture, and allows for RME to be completely combusted, especially under higher loads, which leads to a reduction in ISFC as stated by (Baltacioglu et al., 2016). The main reason that ISFC is remarkably reduced, is due to the relatively high calorific value of hydrogen. Hence, higher hydrogen addition will result in lower ISFC. Additionally, as observed, the engine load is limited by abnormal combustion (knocking), which might appear at nominal loads and HES higher 35%. At those conditions, knock can be easily transformed to heavy knock and form extremely high in-cylinder pressure pulsations (over 1MPa), leading to increased heat transfer rate to the piston crown, both of which can quickly damage the piston.

Figure 9 compares ISFC against HES at various engine loads for RME and RME7. Under all conditions, a general reduction in ISFC is seen with increasing HES. At 35% HES, knocking becomes an issue.

Figure 10 compares the indicated thermal efficiency (ITE) against HES at various engine loads for RME and RME7. Indicated thermal efficiency (ITE) is inversely proportional to ISFC, it takes the lower heating value (LHV) for entire combustible mixture consisted of RME, DF and hydrogen into account. Although,

ISFC decreases as presented in Figure 9, ITE is approximately at the same level in between 0.33 and 0.36 except test with RME at low load as shown in Figure 10.

Hydrogen addition to these fuels increases the LHV of the entire combustible fuel charge trapped in the engine cylinder. A higher fuel LHV usually results in higher combustion temperature, and hence affects other combustion parameters and exhaust emissions.

- In-cylinder peak combustion pressure increases significantly by approximately 15% at medium and nominal loads with hydrogen increase from 20 to 33%.
- The combustion duration CA0–10 at the Figure 11 (considered as ignition lag) and CA10–90 at the Figure 12 (main combustion phase) shorten with increase of hydrogen energy share (HES).
- Presence of hydrogen also contributes to the decrease in Indicated Specific Fuel Consumption (ISFC) due to higher LVH for the total in-cylinder fuel charge caused by the higher LHV of hydrogen. Increase in ISFC does not affect brake thermal engine efficiency, which is at stable level of 0.35 ± 0.015.
- Hydrogen energy share of less than 15% decreases the NO emissions, but higher hydrogen dose increases it significantly at nominal load.
- Negative correlation of hydrogen addition on unburnt HC and CO at the Figure 13 and Figure 14 is observed only at partial loads. The engine working at full load generates maximal emissions of HC and CO while HES is around 20%.
- In all tests NO, HC and CO emissions from RME7 combustion were higher in comparison to pure RME.
- The smokiness decreased steadily with increase of HES.
- The amount of hydrogen that could be added was limited because of combustion knock occurring at nominal load with HES of nearly 35%.

Smokiness is a parameter which characterizes exhaust gases from the CI engine. Smokiness depicts transparency of exhaust gases contaminated with condensed unburnt fuel and soot, which are considered as major substances causing smoke. Unburnt hydrocarbon-based molecules and soot are usually inline with each other, and they are mostly formed as result of both local oxygen deficiency and short time for complete combustion as it is observed for HC and CO emissions. As seen in Figure 15, smokiness is in negative trend with HES. It means that hydrogen assisted diesel fuels provide unfavorable conditions for soot formation. Among all the exhaust emissions tested, smokiness is the parameter which significantly decreases with increase in HES.

2.5.1.3 Performance and emission studies on port injection of hydrogen with varied flow rates with Diesel as an ignition source (Saravanan & Nagarajan, 2010)

The engine used for the experimental investigation was a single cylinder, four stroke, water cooled, direct injection diesel engine, with a rated power of 3.7 kW at a rated speed of 1500 rpm Table 7. The technical specifications of the test engine are given in Table 7. The engine was coupled to an electrical dynamometer for loading and was mounted on the test bed with suitable connections for crankcase ventilation. An electronic control unit (ECU) was used to control the injection timings and durations of the hydrogen injection. The electronic control unit acquires the signal from an infrared sensor that indicates the crankshaft position. The injection timings of the hydrogen injector were varied from 5° crank angle (CA) before gas exchange top dead centre (BGTDC) to 25° CA after gas exchange top dead centre (AGTDC) in steps of 5° CA. The injection durations were fixed as 30° CA, 60° CA and 90° CA. Based on the above, 21 combinations

of injection timings and injection duration (as shown in Table 7) were obtained from which the optimized timings for hydrogen injection were determined. The hydrogen flow rate for the optimized injection timings was maintained at 5.5 liter per minute (lpm). The optimum timing was found to be 5° CA BGTDC with injection duration of 30° CA based on the performance, combustion and emission characteristics (as highlighted in Table **8**8). Further, to optimize the hydrogen flow rate, the hydrogen flow was varied from 2 lpm to 9.5 lpm with optimized injection timings. Figure 16 shows the schema of the experimental setup.

Table 7: Engine specifications.

Make and model	Kirloskar, AV1 make, naturally aspirated engine
General	4-Stroke/vertical
Type	Compression ignition
Number of cylinder(s)	One
Bore	80 mm
Stroke	110 mm
Swept volume	553 cc
Clearance volume	36.87 cc
Compression ratio	16.5: 1
Static injection timings	23° BITDC
Nozzle opening pressure	200–205 bar
BMEP at 1500 rpm	5.42 bar
Type of injector	3 hole injector
Rated output	3.7 kW at 1500 rpm
Rated speed	1500 rpm
Combustion chamber	Hemispherical open
Type of cooling	Water cooled

Table 8: Start of injection timings and injection duration for hydrogen operation in port injection.

S. No.	Start of injection		Injection duration	
	Crank angle (°)	Time (ms)	Crank angle (°)	Time (ms)
1	5° BGTDC	0.56	30	3.33
2	5° BGTDC	0.56	60	6.66
3	5° BGTDC	0.56	90	9.99
4	GTDC	1.11	30	3.33
5	GTDC	1.11	60	6.66
6	GTDC	1.11	90	9.99

7	5° AGTDC	1.67	30	3.33
8	5° AGTDC	1.67	60	6.66
9	5° AGTDC	1.67	90	9.99
10	10° AGTDC	2.22	30	3.33
11	10° AGTDC	2.22	60	6.66
12	10° AGTDC	2.22	90	9.99
13	15° AGTDC	2.78	30	3.33
14	15° AGTDC	2.78	60	6.66
15	15° AGTDC	2.78	90	9.99
16	20° AGTDC	3.33	30	3.33
17	20° AGTDC	3.33	60	6.66
18	20° AGTDC	3.33	90	9.99
19	25° AGTDC	3.89	30	3.33
20	25° AGTDC	3.89	60	6.66
21	25° AGTDC	3.89	90	9.99
22	23° BITDC		Diesel	

The engine was injected with diesel fuel and hydrogen simultaneously, with diesel acting as the pilot fuel. This, in turn, automatically reduces the diesel quantity by the governor. Figure 17 shows the valve timing of the hydrogen injection. The schematic view of the experimental set up is shown in Figure 16.

Brake thermal efficiency

Figure 18 depicts the variation of brake thermal efficiency for port injection at different injection timings and injection durations. Brake thermal efficiency is defined as the rate of energy required to produce a unit kilowatt power. Based on the performance, the optimum injection timing and injection duration for hydrogen port injection were found to be 5° CA BGTDC and 30° CA (injection parameter set #1), respectively, since the efficiency at these points is higher in the entire load spectrum.

Figure 19 shows the variation of brake thermal efficiency with load at optimized start of injection and injection duration. The brake thermal efficiency is 26.2% for hydrogen flow of 7.5 lpm compared to 21.6% in the case of diesel at 75% load. A further increase in efficiency to 26.7% is obtained with hydrogen flow rate of 9.5 lpm. Similarly, at full load with 7.5 lpm of hydrogen flow, the brake thermal efficiency is 24.7% as compared to 23.4% for diesel. At full load, the efficiency obtained is 24.1% with a hydrogen flow rate of 9.5 lpm, but a mild knock was observed. Hence the optimum flow rate was found to be 7.5 lpm. The

flammability limits of premixed hydrogen flames are much broader than the hydrocarbon fuels. Hence, a chamber fumigated with hydrogen can enhance burning of the diesel fuel, which increases efficiency.

Specific energy consumption

Figure 20 depicts the variation of specific energy consumption at all loads with optimized start of injection and injection duration for port injected hydrogen fuel. The specific energy consumption was found to be 13.72 MJ/kW h for a hydrogen flow rate of 7.5 lpm compared to diesel of 16.67 MJ/kW h at 75% load; a further reduction in SEC to 13.5 MJ/kW h is obtained with hydrogen flow rate of 9.5 lpm. At full load, with hydrogen flow rate of 7.5 lpm, the lowest SEC is 14.54 MJ/kW h compared to diesel of 15.41 MJ/kW h. For the flow rate of 9.5 lpm the SEC is 14.9 MJ/kWh at full load. The specific energy consumption is almost constant from 75% of load to full load. This is due to the presence of rich air fuel mixture compared to part load. With 7.5 lpm of hydrogen flow rate the overall SEC is better than other hydrogen flow rates. In general, in the hydrogen operated dual fuel engine the SEC reduces due to the uniformity in mixture formation in hydrogen which in-turn assists the diesel combustion, thereby improving the combustion of Diesel. The specific energy consumption is almost constant from 75% of load to full load. This is because, at high load conditions, a rich air fuel mixture is present, and, as a result of the rich air fuel mixture, there is no significant improvement in efficiency, which ultimately makes the energy consumption remain constant. Table 9 shows the energy share ratio of Diesel and hydrogen in port injection.

Emissions

The NO_X emissions are found to be similar at 75% load and full load for both hydrogen and diesel operation. However, the emissions are lower at lower loads in hydrogen dual fuel operation due to lean mixture operation. The smoke emissions reduce by 44% in hydrogen diesel dual fuel operation compared to diesel operation. The CO and HC for hydrogen operation at optimized conditions are the same as that of diesel emissions. The engine operated smoothly with hydrogen except at full load that resulted in knocking especially at high hydrogen flow rates. These experimental results can be used as a base for the dual fuel applications and can be further extended to automotive applications. It can further be extended to neat hydrogen applications.

2.5.1.4 Combustion and emission characteristics of a hydrogen-diesel dual-fuel engine (Dimitriou et al., 2018)

In this study, the implementation of hydrogen fuel was tested at low and medium operating loads in a heavy-duty hydrogen-diesel dual-fuel engine. The paper provided a detailed experimental analysis of the effects of hydrogen energy share ratio and various combustion strategies such as exhaust gas recirculation, diesel injection pressure and diesel injection patterns.

The test setup included a heavy-duty multi-cylinder compression-ignition engine which was operated in a dual-fuel mode with hydrogen and diesel. The experimental analysis presented was focussed on two engine operating conditions of 20 kW and 40 kW, representing low and medium engine loads, respectively, at a fixed speed of 1,500 rpm. The target of this experimental study was to achieve the maximum H2 energy share ratios for each engine load, enabling smooth operation and minimum carbon emissions while controlling NOx and soot emissions by means of exhaust gas recirculation and advanced injection strategies. Details of the engine setup and specifications at shown at Figure 21 and Table 9.

Table 9: Engine specifications

Engine type	Inline-4
Displacement (L)	5.2
Bore × Stroke (mm)	115 × 125
Compression ratio	17.5:1
Fuel (port injection)	Hydrogen
Fuel (direct injection)	Diesel

Four injectors were used to supply the engine with hydrogen fuel into a dedicated gas fuel chamber prior the intake manifold of the engine. Hydrogen fuel was homogeneously delivered to the four cylinders of the engine after passing an air-hydrogen mixer. The hydrogen supply system consisted of compressed gas cylinders, pressure regulators and flow rate measurement devices as shown in Figure 22. The hydrogen injection pressure was set to 4 bar (gauge) for all experiments in this paper while the injection quantity was controlled by the frequency and period of the hydrogen injectors' valves opening times. Compressed nitrogen (N2) gas was used to purge the hydrogen gas out of the engine system at the end of the experimental procedure for safety reasons.

A multi-cylinder compression ignition engine has been tested at low and medium loads under different hydrogen-diesel energy share ratios. The effects of exhaust gas recirculation, diesel injection pressure and injection strategy have been analysed and the main conclusions are drawn below:

- For low load conditions, smooth operation without pre-ignition was achieved for H_2 energy share ratios of up to 98%, (see at Figure 23). At medium loads, the maximum H_2 energy share ratio dropped to 85% (Figure 24). Higher rates led to pre-ignition and cylinder-to-cylinder unbalanced operation.
- A simultaneous reduction of all harmful emissions and BTE of the same level as in the conventional diesel engine were observed at low load conditions. Carbon and NOx emissions were reduced by over 90% while the soot emissions were 85% lower than the conventional diesel engine when an H_2 energy share ratio of 98% was applied. For H_2 energy share ratios lower than 93%, NOx emission was increased compared to the conventional engine. See at Figure 21.
- At medium engine loads, a similar trend on carbon and soot emissions were observed. However, the NOx emission was increased by up to four times compared to the conventional diesel engine. This increase is the result of the high in-cylinder temperatures generated by the combustion of a high energy content fuel. See at Figure 26.
- Exhaust gas recirculation provided a significant reduction of NOx emission by up to 75%. However, the introduction of high EGR rates deteriorated the soot oxidation process and engine-out soot emissions. At medium loads, a simultaneous reduction of NOx and soot emissions compared to the conventional diesel operation could not be achieved.
- The improved fuel atomization as a result of the increase of the diesel injection pressure shifted the combustion phase closer to TDC and enhanced the BTE of the engine. As a result, NOx emission increased while soot formation was reduced.
- An increased pre-injection rate, as well as a long dwell angle, was found to provide a positive effect on the combustion efficiency because of the advanced, high-intensity combustion near the TDC.
- Emissions of unburned H2 levels in exhaust were observed, along with the presence of other combustion by-products of CO_2, CO, soot, and NO_x. H_2 in the exhaust was found to increase when H_2 in the fuel mixture increased from 0% through to 40% of the mix then reduced linearly when H_2

fuel mixture was increased from 40% to 100% of the mix. This situation is problematic for both safety and global warming, given that hydrogen is an indirect contributor to GHG (Consultancy, 2022; Warwick et al., 2022).

It is clear from the above conclusions that the addition of hydrogen fuel can provide dramatic reductions in carbon emissions of CI engines. However, the primary challenge is the control of the in-cylinder combustion temperature at medium and high load conditions. Exhaust gas recirculation can contribute to this, but it comes with a penalty on soot emission. The study suggests that alternative technologies such as water injection and low-temperature combustion techniques seem to be unavoidable for the hydrogen-diesel co-combustion to enable simultaneous reduction of NOx, soot and carbon emissions.

2.5.2 Direct Injection

The slower burning rate is expected to hinder a rapid pressure rise and subsequent pressure ringing (i.e. knocking) and to reduce NOx emissions, which are problematic in premixed combustion dominant, hydrogen port injection dual-fuel diesel engines. This study directly compares the in-cylinder pressure, efficiency and engine-out emissions of port injected and direct injected hydrogen-diesel dual-fuel combustion in the same engine. The tests were performed in a single-cylinder engine equipped with three injection systems including a hydrogen port injector, a hydrogen direct injector and a common-rail diesel direct injector. The engine was operated at intermediate load using a fixed total energy input of 820 J with hydrogen energy fraction of 50%. The results show that mixing-controlled combustion of the hydrogen in direct injection mode leads to lower in-cylinder pressure and thus lower engine efficiency. However, the severe pressure rising observed for the hydrogen port injection is avoided and engine-out NOx emission is reduced, indicating the hydrogen DI is more stable, its combustion is cleaner and a higher hydrogen utilisation can be achieved.

2.5.2.1 Direct injection of hydrogen main fuel and diesel pilot fuel in a retrofitted single-cylinder compression ignition engine (Liu et al., 2022)

The schematic diagram of the engine test facility is shown in Figure 27 (Liu et al., 2022). Hydrogen is fuelled by a retrofitted injector that was modified from a gasoline direct injector (GDI, Bosch 026,150,533), accommodated in the modified glow-plug hole of the production engine head at 45° to the engine head plane. The original injector, replaced by the GDI, features 6 holes with a diameter of approximately 160 μm and included angle of 70° as measured by X-ray computed tomography imaging. This commercial GDI injector was chosen because of its sealing integrity at desired hydrogen feed pressure. The hydrogen injector, as illustrated in the bottom right image in Figure 28, is modified with an added cap on top of the original injector tip. The added cap has a single hole with a 1 mm diameter. The direction of the hydrogen jet is aligned with the injector body as illustrated in Figure 28 (bottom-right). As the original liquid-fuelling injector body was used for gaseous hydrogen injection without fuel-passing lubrication, one droplet of engine oil has been added to the injector feed before each day of the experiments for needle lubrication. Injector failure was not observed the entire test.

Table 10: Engine configuration details.

Engine Details		
Displacement Volume	497.8 cm³	
Bore	83 mm	
Stroke	92 mm	
Compression ratio	17.7	
Swirl ratio	1.4	
Valves	2 intakes, 2 exhaust	
Piston	55 mm diameter top-hat cylindrical bowl	
Intake	Naturally aspirated, unthrottled	
Injection System Details		
	Hydrogen	**Diesel**
Injector	Modified Bosch spray-guided GDI injector	Bosch CRI2 150° included angle
Number of holes	6 x 160 µm. Injector cap has a 1 mm diameter axially drilled hole	7 x 134 mm
Flow rate	1.44 g/s at 200 MPa H2 pressure	800 cm³/min at 10 MPa pressure Discharge coefficient 0.86 Bosch K-Factor 1.5
Pump	Zenobalti Hydrogen Boost Pump System (ZB-1301) Haskel Hydrogen Pump (AG-62-86,979)	Bosch CP3, commonrail

Setup is shown at Figure 27 and Figure 28 (Liu et al., 2022). A parametric study was conducted with constant mid-point combustion phasing and engine speed. In the study, a range of hydrogen injection timings 180-0° (bTDC) and hydrogen energy fractions 20-90% were tested, with the remaining energy supplied by diesel. The in-cylinder pressure was measured to determine the apparent heat release rate, indicated mean effective pressure and efficiency, combustion phasing and combustion noise. The engine-out emissions of CO_2 and NOx were measured and analysed. The main findings and conclusions of this experimental study are as follows.

- The best result demonstrated in the article is 78% CO_2 reduction. The maximum IMEP of 943 kPa was achieved with 57.2% indicated efficiency at 90 °CA bTDC hydrogen injection timing, which is 27% greater than the diesel baseline. This suggests that at high hydrogen content, substantial efficiency increases may be possible, however they may also lead to more

unpredictable combustion as this peak IMEP range was only observed under very precise crank angle injection timings (Figure 29).

- Two combustion modes emerge for the H2DDI, with primarily premixed combustion for early to intermediate 180-60° (bTDC) hydrogen injection timing, and primarily mixing-controlled diffusion combustion with flame crossover point around 40 ° (bTDC) for late injection timings of 20-0 ° (bTDC). For this study, premixed combustion cases exhibit higher peak in-cylinder pressure, peak aHRR, IMEP and efficiency but also higher NOx. A premixed combustion is mixing the hydrogen with air prior to injection. In a diffusion combustion, the fuel and the oxidant are separated by a thin interface where they mix together.
- A trade-off between engine performance quantified by IMEP and efficiency, and low NOx emissions emerges (Figure 30). The maximum IMEP, efficiency and NOx are attained at 40° (bTDC) hydrogen injection timing, at which the hydrogen charge is intermediate between well-mixed and stratified, enabling fast flame propagation.
- Higher hydrogen energy fraction produces higher NOx emissions greater than three times the diesel baseline for 90% hydrogen energy fraction and 90° (bTDC) injection timing (Figure 30). However, varying hydrogen direct injection timing enables reduction of NOx, even below the diesel baseline, for very late hydrogen injection timing for 80 to 90% hydrogen energy fraction. Regardless, there is an associated reduction in IMEP and efficiency as the combustion phasing cannot be fixed but retarded.
- 40° (bTDC) injection timing at 90% hydrogen energy fraction emerges as a good balance of IMEP and NOx, with 843 kPa IMEP (13.3% above diesel baseline) and 90 g/kWh CO_2 (85.9% below diesel baseline). At this condition, the estimated combustion noise is 93.6 dB at 3.5 dB below the diesel baseline. The combustion characteristics at this point are intermediate between premixed and mixing controlled combustion, with a blend of well-mixed and stratified charge.

Finally, this article has no mention of any cost and modification or operation. Since they used off-the-shelves equipment for the modifications, cost should not be significant.

2.5.2.2 Performance and combustion characteristics of a direct injection SI hydrogen engine (Mohammadi et al., 2007)

Figure 31 (Mohammadi et al., 2007) shows the configuration of the combustion chamber, together with injector and spark plug arrangements. The test engine used was a single-cylinder four-cycle natural aspirated SI engine with a bore diameter of 102 mm and a stroke of 105 mm, which was converted from a direct-injection diesel engine (Yanmar NFD-170). In this study, a flat-head piston was used to form the disc-shaped combustion space, and compression ratio was fixed at 11.5:1. Hydrogen gas from a high-pressure vessel was supplied to an electro-magnetically actuated gas injector (Westport Innovation Inc.), and hydrogen flow rate was precisely measured by a mass flow controller (Oval, F-123S). The gas injector has seven nozzle holes with a hole diameter of 0.52 mm. Injection timing and duration can be adjusted by an electronic control system (Morigiken). Injection pressure was regulated at 8 MPa, which might ensure the sufficient penetration of fuel jet and afford a fast fuel–air mixing even at injection timing near top dead center. A passenger-car spark-plug (NGK C7HA) was installed on the cylinder head as ignition source and ignition timing was preciously detected by a current monitor (Pearson 110). In the study, the distance between the spark plug and injection nozzle tip is approximately 30 mm. This distance is the minimum distance that can be achieved due to the cylinder head geometry.

Figure 32 (Mohammadi et al., 2007) shows the schematic of the experimental setup for controlling engine speed, ignition timing and fuel–air ratio, and for measuring engine performance, combustion process and exhaust emissions.

Table 11: Engine specifications

Engine type	Spark-ignition 4-stroke cycle
Bore×Stroke	102mm×105mm
Displacement	857 cc
Compression ratio	11.5:1
Combustion chamber	Disc shape
Swirl ratio	2.6
Intake valve opening angle	360◦ATDC
Intake valve closing angle	580◦ATDC
Exhaust valve opening angle	130◦ATDC
Exhaust valve closing angle	380◦ATDC
Injector nozzle	0.52mm x 7 mm

A direct-injection spark ignition hydrogen engine was developed and attention was paid on the effects of injection timing on the engine performance, combustion characteristics and NOx emission under a wide range of engine loads. The results reveal that:

- In-cylinder injection of hydrogen during the intake stroke prevents backfire. However, thermal efficiency and output power are limited by knock due to reduction in volumetric efficiency. See at Figure 33.
- Hydrogen injection at compression stroke prevents knock and gives an increase in thermal efficiency and maximum output power. Injection timing was further retarded to a CA at 100°BTDC and the results are shown in Figure 35, compared with results of a CA at 130°BTDC in Figure 34. Retarding the injection timing lowers NOx concentration, typically for the higher equivalence ratios. This indicates that NOx formation depends on the heterogeneity in the fuel–air mixture. A study carried out by one of the authors shows that for an equivalence ratio < 0.7, combustion of heterogeneous mixture gives higher emission, however, for equivalence ratio > 0.7 emission of homogeneous mixture's combustion is much higher than that for heterogeneous mixture (Shioji et al., 1995).
- Hydrogen injection at later stage of compression stroke can achieve a thermal efficiency higher than 38.9% and a brake mean effective pressure of 0.95 MPa. Under high engine output conditions, late injection of hydrogen offers a great reduction in NOx emissions due to lean operation. A maximum thermal efficiency value of 38.9% was achieved at 80°BTDC (Figure 36). As can be seen in the NOx results, NOx emissions for 80°BTDC at a brake mean effective pressure of 0.8MPa are 60% lower than that for 130°BTDC. This is due to an increase in heterogeneity of fuel–air mixture caused by retard in the injection timing. Above results reveal that optimization of injection timing is an effective method to obtain high thermal efficiency and low NOx emissions for a given engine load.

As indicated in the study, employing direct-injection technology in a hydrogen engine is very effective to control the abnormal combustion of hydrogen and achieve high thermal efficiency and output power.

However, the authors believe that further investigation is required for better performance. Although late injection results in lower NOx emissions, utilization of other techniques such as exhaust gas recirculation and after-treatment methods are required to bring the NOx emission to an acceptable level. In addition, optimization of combustion chamber geometry; injection parameters such as injection pressure and nozzle hole numbers/arrangement; swirl intensity, etc. are indeed important to achieve an engine performance level competitive to that in the modern direct-injection diesel engines.

2.5.3 Complimentary Research

This section details other research of interest that was not included in the main discussion of the report. These articles are shown to supplement the review with the main key findings.

(Deb et al., 2015) analysed the performance and emissions of a dual fuel H_2-diesel with different amount of H_2 from 0 to 42% of input energy at 1500 RPM. Increase of thermal efficiency (15% with the addition of 42% entrance energy by hydrogen instead of diesel) and improved combustion because of a wider hydrogen flammability limit. Reduction of 18.6% energy consumption with 42% H_2 addition and also reduction of CO_2, CO, UHC and soot by 40%, 33%, 89% and 33% respectively. NOx increases to 500% with 42% H_2 addition. Adding more than 42% H_2 leads to knocking phenomena in the engine.

(Saravanan & Nagarajan, 2008) studied hydrogen as an air-enrichment medium with diesel as an ignition source in a stationary diesel engine system to improve engine performance and reduce emissions. Results suggest that the stationary engines can be operated with less fuel than neat diesel operations, resulting in lower smoke levels and particulate emissions. Hydrogen (H_2)-enriched air systems in diesel engines enable the realization of higher brake thermal efficiency, resulting in lower specific energy consumption (SEC). NO_X emissions are reduced from 2762 to 515ppm with 90% hydrogen enrichment at 70% engine load. At full load, NO_X emission marginally increases compared to diesel operation, while both smoke and particulate matter are reduced by about 50%. The brake thermal efficiency increases from 22.78% to 27.9% with 30% hydrogen enrichment. Thus, using hydrogen-enriched air in a diesel engine produces less pollution and better performance.

(Saravanan et al., 2008) injected hydrogen into the intake manifold by using a hydrogen gas injector while keeping diesel as in the conventional mode as an ignition source for hydrogen combustion. The flow rate of hydrogen was set at 5.5 lpm at all load conditions. The injection timing was kept constant at top dead center (TDC) and injection duration was adjusted to find the optimized injection condition. Experiments were conducted on a single cylinder, four stroke, water-cooled, direct injection diesel engine coupled to an electrical generator. At 75% load the maximum brake thermal efficiency for hydrogen operation at injection timing of TDC and with injection duration of 30° CA is 25.66% compared with 21.59% for diesel. The oxides of nitrogen (NOx) emission are 21.7 g/kWh for hydrogen compared with diesel of 17.9 g/kWh. Smoke emissions reduced to 1 Bosch smoke number (BSN) in hydrogen compared with diesel of 2.2 BSN. Hydrogen operation in the dual fuel mode with diesel exhibits a better performance and reduction in emissions (except NOx) compared to diesel in the entire load spectra.

(Bose & Maji, 2009) conducted an experiment using a diesel–hydrogen blend. A timed manifold induction system which is electronically controlled has been developed to deliver hydrogen on to the intake manifold. The solenoid valve is activated by the new technique of taking signal from the rocker arm of the engine instead of cam actuation mechanism. In the investigation, hydrogen-enriched air has been used in a diesel engine with hydrogen flow rate of 0.15 kg/h. As diesel is substituted and hydrogen is inducted, the NO*x* emission is increased. In order to reduce NO*x* emission an EGR system has been developed. In the

EGR system a lightweight EGR cooler has been used instead of a bulky heat exchanger. In this experiment performance parameters such as brake thermal efficiency, volumetric efficiency, and brake specific energy consumption (BSEC) are determined and emissions such as oxides of nitrogen, carbon dioxide, carbon monoxide, hydrocarbon, smoke and exhaust gas temperature are measured. Dual fuel operation with hydrogen induction coupled with exhaust gas recirculation results in lowered emission level and improved performance level compared to the case of neat diesel operation.

(Karagöz et al., 2015) sprayed hydrogen via gas injector from intake port and used diesel fuel as ignition source. Hydrogen's energy content was stabilized at 30% in overall fuels and all tests were performed in 1100 rpm stable engine speed. Also, in different engine loads (40%, 60%, 75% and 100%) intake air enriched with hydrogen's effect on diesel engine's performance, emissions and combustion were examined. Obtained results show that in part load conditions where air is enriched with hydrogen, NOx emissions and soot emissions can be taken under control. However, on full load condition (100% engine load), with hydrogen addition, dramatic rise of NOx emissions was observed. Working normal conditions with hydrogen + diesel fuel, it is noted that engine load affects NOx emissions significantly. On full load conditions, enriched with hydrogen, even though there is some rise in THC emissions, there are reductions in CO_2 and CO emissions. Furthermore, peak in-cylinder gas pressure and peak heat release rate have risen in hydrogen enriched condition. This peak pressure is easily managed with the current engine.

(Roy et al., 2010) carried out an experiment at a constant pilot injection pressure and pilot quantity for different fuel-air equivalence ratios, hydrogen substitution from 20% to 80% and at various injection timings without and with charge dilution. The experimental strategy was to optimize the injection timing to maximize engine power at different fuel-air equivalence ratios without knocking and within the limit of the maximum cylinder pressure. The engine was tested first with hydrogen-operation condition up to the maximum possible fuel-air equivalence ratio of 0.3. A maximum IMEP of 908 kPa and a thermal efficiency of about 42% were obtained. The equivalence ratio could not be further increased due to knocking of the engine. The emission of CO was only about 5 ppm, and that of HC was about 15 ppm. However, the NOx emissions were high, 100–200ppm or more. The charge dilution by N_2 was then performed to obtain lower NOx emissions. 100% reduction of NOx was achieved with 60% N_2 dilution maintaining 10% higher IMEP than hydrogen operation. Charge dilution uses inert gas to closely approach the thermodynamically ideal engine cycle. Hydrogen has very high diffusivity. This ability to disperse in air is advantageous for the formation of a uniform mixture of fuel and air, and to curb the hydrogen leak problems. Hydrogen has very low density. This results in a problem when used in an internal combustion engine. A very large volume is necessary to store enough hydrogen to give a vehicle an adequate driving range. Due to the dilution by N_2 gas, higher amount of energy could be supplied from hydrogen without knocking, and about 13% higher IMEP was produced than without charge dilution.

(Santoso et al., 2013) investigated hydrogen utilization to replace diesel engine fuel at low load operation. Hydrogen cannot be used directly in a diesel engine due to its high auto ignition temperature. To investigate the combustion characteristics of this dual fuel engine, a single cylinder diesel research engine was converted to utilize hydrogen as fuel. Hydrogen was introduced to the intake manifold using a mixer before entering the combustion chamber. The engine was run at a constant speed of 2000 rpm and 10 Nm load. Hydrogen was introduced at the flow rate of 21.4, 36.2, and 49.6 liters per minute. Specific energy consumption, indicated efficiency, and cylinder pressure were investigated. At this low load, the hydrogen enrichment reduced the cylinder peak pressure and the engine efficiency. The reaction progress variable and combustion rate of reaction were slower as shown by the CFD.

2.5.4 Further Research Potential

Both manifold injection and direct injection processes achieve interesting results for different reasons. Manifold injection is interesting for its simplicity to integrate as it is easy and cheap to install and use, but has its limitations. Due to the use of low-pressure air intake, a high ratio of hydrogen cannot be achieved, which limits the potential to reduce GHG emissions. Direct injection remains more interesting to achieve higher mix but are more expensive to integrate.

This technology also brings other questions and potential research on the subject. Even if not required for this current review, the following four subjects could be investigated. They were not discussed in any of the articles cited in the review and are all linked to the usage of hydrogen.

2.5.4.1 Is hydrogen slip a significant issue in hydrogen - diesel co-combustion engines?

Fuel slip is a phenomenon that some fuel components, such as hydrogen, are not completely burned inside engine cylinders and therefore leave the engine as part of the exhaust. This is a concern for almost all gaseous fuel – diesel co-combustion engines. Unfortunately, none of the review references has investigated the issue of hydrogen slip for hydrogen – diesel co-combustion engines. This could be a future research subject.

2.5.4.2 The importance of examining the carbon intensity of hydrogen production

There are no specifications about the sources of hydrogen in the articles cited in this literature review. To know more about it, some article discusses the impact of this energy carrier. (Howarth & Jacobson, 2021) Hydrogen is often viewed as an important energy carrier in a future decarbonized world. Currently, most hydrogen is produced by steam reforming of methane in natural gas (known as “gray hydrogen”), with high carbon dioxide emissions. Increasingly, many propose using carbon capture and storage to reduce these emissions, producing so-called “blue hydrogen,” frequently promoted as low emissions. However, greenhouse gas emissions from the production of blue hydrogen are still quite high, particularly due to the release of fugitive methane. At 3.5% emission rate of methane from natural gas and a 20-year global warming potential, total carbon dioxide equivalent emissions for blue hydrogen are only 9%-12% less than for gray hydrogen. While carbon dioxide emissions are lower, fugitive methane emissions for blue hydrogen are higher than for gray hydrogen because of an increased use of natural gas to power the carbon capture. Perhaps surprisingly, the greenhouse gas footprint of blue hydrogen is more than 20% greater than burning natural gas or coal for heat and some 60% greater than burning diesel oil for heat, again with the default assumptions. In a sensitivity analysis in which the methane emission rate from natural gas is reduced to a low value of 1.54%, greenhouse gas emissions from blue hydrogen are still greater than from simply burning natural gas and are only 18%-25% less than for gray hydrogen. The analysis assumes that captured carbon dioxide can be stored indefinitely, which has not been demonstrated. The study referenced in this section shows that the impact that the hydrogen production process has on lifecycle emissions associated with using hydrogen as a fuel must be carefully considered when the goal is to reduce GHG emissions. The carbon intensity of the source hydrogen must be carefully examined and assumptions based on based on generalized labels should be avoided.

2.5.4.3 What is the cold weather effect of the modification and the behaviour with cold air, diesel and hydrogen intake?

The current literature review did not have the goal to investigate the cold and very cold environment for a HDDF. That been said, no articles were found that mentioned or studied how HDDF engines are affected

in the cold in terms of starting the engine, the efficiency, the emissions and the impact on the engines structure and longevity. Knowing that some experiments change or modify the glow plug for the addition of hydrogen injectors, this could affect the capacity for a very cold start. It is difficult, without any available studies, to predict what the behaviour of the hydrogen diesel mix dealing with cold hydrogen, cold diesel, and cold air intake, will be. Further studies could be done to address this topic.

2.5.4.4 What is the effect of metal embrittlement due to contact with hydrogen, especially in a hot environment like an ICE?

(Okonkwo et al., 2023) discusses embrittlement. It is a process, by which various metals, mainly high-strength steels, become brittle and crack after being exposed to hydrogen. It is caused by the ingress of either molecular or atomic hydrogen into a metal lattice (Laadel et al., 2022). However, the exact mechanism of hydrogen embrittlement is not clear. The capacity of the material to deform or stretch under load is limited due to a metallurgical interaction between atomic hydrogen and the crystallographic structure. As a result, when stressed or loaded, it becomes “brittle” and the metal will fracture or break at a far lower strain or stress than expected. Hydrogen embrittlement is particularly dangerous because of its reduced breaking strength and the vulnerability of material to hydrogen embrittlement increases as its tensible strength increases. Embrittlement caused by very minute amounts of hydrogen, which is undetectable by typical loss-of-ductility bend tests, has been a major source of concern for materials and system designers. This atomic level embrittlement occurs at hydrogen levels as low as 10 ppm (Zan et al., 2015).

2.6 Assessment of the Scale of Effort Required to Modify/Retrofit an Engine to Include Hydrogen-Diesel Co-Combustion

In this literature review, all main articles covered using either direct injection (Liu et al., 2020), (Dimitriou et al., 2018) or port injection (Mohammadi et al., 2007) and (Saravanan & Nagarajan, 2010) used off the shelf injectors with minor modifications and did not mention any additional maintenance.

While the following articles described the modifications implemented (if any), there was no mention of the cost associated with those modifications or maintenance.

It was not possible to find references discussing the cost of the modifications required to operate a locomotive in co-combustion. No article was found about this, and no article mentions the costs they had to face for their own modifications. Discussion has taken place with an organization in Alberta on this issue for road vehicles. This company mentioned conversion costs of approximately $50,000 for a road vehicle, which does not include the storage and transportation of hydrogen.

For (Talibi et al., 2014), hydrogen gas was supplied from a compressed hydrogen gas bottle and was injected into the engine inlet manifold 350 mm upstream of the inlet valves. The flow of H2 was controlled using a Bronkhorst thermal massflow controller (F201-AV-70K), to an accuracy of ±0.08 L/min.

For (Sathishkumar & Ibrahim, 2021), the flow rate of air was calculated on a volume basis using displacement type flow meter, which was erected on the surge tank. Hydrogen induction in the engine was carried out using a separate line, which consists of hydrogen cylinder, regulator, hydrogen mass flow meter, needle valve, water trap and flame arrestor. The flow rate of hydrogen was measured on the mass basis using a thermal mass flow meter; a needle valve helped to control the hydrogen flow rate as desired; a flame arrestor and water trap were used for safety purpose to resist the backfire travelling from the engine to hydrogen cylinder. Diesel fuel flow measurement was carried on the mass basis directly. A hydrogen

leak test was performed before the commencement of any experiments in the HDDF mode using a hydrogen gas detector.

For (Chintala & Subramanian, 2017), manifold injection system has offered significant benefits such as controlling of gaseous fuel injection timing and duration, better mixing characteristics of fuel with air, low temperature exposure to hydrogen injector (as the gas injector generally mount at a larger distance from the combustion chamber), and cited only minor engine hardware modifications (retrofitting of hydrogen gas injector).

For (Das, 2002), several existing petroleum-fuelled engine configurations have been modified and it has been found that the converted system does not need substantial hardware modifications.

(Saravanan & Nagarajan, 2010) noted that the dual fuel mode of operation with hydrogen has numerous advantages such as smooth engine operation with little modification for fuel induction or injection.

(Dhole et al., 2014) observed that at high load, thermal efficiency increases. The best amount of H2 at energy basis is 20% at high load. At part loads, the amount of NOx emission reduces but UHC and CO increase. Results show that there is no need for any modifications on the engine while hydrogen addition is low.

(de Morais et al., 2013) noted that the addition of H2 to 20% doesn't need any modifications in the engine. At 75% load, maximum SFC reduction occurs and if H2 is obtained from clean upstream sources, CO2 emission will reduce to 12%.

2.7 Insights into Changes of Maintenance Requirements for Diesel-Hydrogen Engines Compared to Diesel Engines and Associated Costs of Running with Hydrogen

One article cites the common operating cost approach for a co-combustion vehicle (El Hannach et al., 2019):

For this specific case study, each vehicle is replaced every 5 years. Consequently, the price of a new vehicle is added to the analysis every 5 years. The annual maintenance fees are assumed to be the same for both diesel and hydrogen-diesel vehicles. It anticipated, however, that maintenance costs will be less for the converted trucks. Preliminary internal studies show that the diesel particulate filter is activated less frequently with the dual-fuel system, although further analyses are required to validate this finding and to estimate an associated reduction in maintenance costs. The conversion cost of the vehicle is discarded as being minimal and it doesn't require any additional maintenance events over its lifetime period. The cost analysis of the waste hydrogen cycle is simplified to one parameter that reflects the combined cost of capture, purification, compression, transport, and distribution of the hydrogen. The value is varied in this work between C$1/kg and C$4/kg in order to cover a realistic range and analyze its specific impact on the LCA outcomes. The US Department of Energy (DOE) cost target for hydrogen for fuel cell vehicle application is $4/kg by 2020.

Since the cost of truck conversion to dual-fuel mode was deemed negligible in this article, and the costs related to maintenance and services are considered to be the same for both fuel options. The total cost of the technology over the whole life cycle will largely depend on the price of hydrogen and the ratio of diesel displacement. Figure 33 (El Hannach et al., 2019) provides a summary of the total cost assessments for

different displacement ratio and hydrogen price scenarios. The price of hydrogen should be less than C$3.6/kg in order to be competitive with the cost of pure diesel in this vehicle application.

Although the conversion of trucks into co-combustion system is more current than in the rail industry, there is no mention of the real cost of conversion and the maintenance requirements. Since this system is fairly new, it could explain the lack of maintenance description to maintain it in good working condition. Upcoming new dual-fuel engines from Volvo and Cummins might give a good look at the difference in maintenance over the next decade.

3. Testing Report

The Energy, Mining and Environment (EME) Research Centre of the National Research Council Canada were tasked by Transport Canada (TC) to experimentally test the combustion and emissions performance of a heavy-duty diesel engine under locomotive-like engine conditions. Efficiency, GHG, and pollutant emissions were observed from a hydrogen-diesel dual fuel engine under loading conditions of 25, 50, and 75% of full engine load. These load levels reflect typical locomotive operating loads from notches 1-2, 4-6, and 7-8, respectively. This section summarizes the test cell setup, testing procedure and results of the testing. The information from this testing will supplement the literature review by providing additional insights into the change in emissions, engine efficiency, and the factors that limit how much diesel can be substituted with hydrogen.

3.1 Objective

The scope and data of the experimental testing will include:

- GHG emissions, including carbon dioxide (CO_2), nitrous oxide (N_2O) and methane (CH_4);
- Criteria air contaminants, including nitrogen oxides (NOx), particulate matter (PM), carbon monoxide (CO) and unburned hydrocarbons (UHC);
- Fuel consumption rate (diesel and hydrogen);
- Engine efficiency;
- Peak engine cylinder pressure and peak pressure rise rate.

The results of the dual fuel operation at different hydrogen energy fractions will be compared to those of conventional diesel combustion.

3.2 Engine and Test Cell Setup

The testing was conducted on a single-cylinder, four-stroke, heavy-duty (HD) diesel engine. Figure 38 shows the schematic of the experimental test bench and Table 12 lists the relevant specifications of the engine. The test engine was a Caterpillar 3401 diesel engine which was modified to suit hydrogen-diesel dual-fuel combustion. The engine was also outfitted with a Ganser common rail diesel injection system to directly inject diesel into the engine cylinder. The diesel flow rate was measured by a Bronkhorst mini CORI-FLOW™ mass flow meter (model M−14). The engine was supplied with pressurized air (up to 5.5 bar) and the intake air could be conditioned through a heating and cooling system to a range of temperatures from 10 to 80 °C. Surge tanks were used before the intake manifold and after the exhaust manifold to reduce the pressure oscillations during the test and simulate the intake pressure condition. An exhaust back

pressure valve was installed downstream of the exhaust surge tank to simulate the back pressure condition. A turbine-type mass flow meter was used to measure the intake air flow rate (manufactured by Sierra Instruments Inc.). The hydrogen was supplied through a compressed gas cylinder outfitted with a single-stage regulator. The flow rate of hydrogen was measured by a Bronkhorst thermal mass flow meter. The final hydrogen pressure before the injectors were regulated to approximately 6.5 bar by using a Bronkhorst electronic pressure controller. A gas chamber was installed before the gaseous injection system to reduce pressure pulsations in the flow. A port fuel injection (PFI) system consisting of eight solenoid gas injectors (SP014, Clean Air Power™) was used to inject hydrogen into the intake port. The injection timings, pulse widths, and injector pressures of both diesel and hydrogen were controlled by National Instruments (NI) hardware (PXI-1031 chassis) and LabVIEW-based software.

An eddy current dynamometer was connected to the test engine in order to control the engine load according to the experimental requirements. An AVL encoder with a speed ranging from 50 to 20,000 revolutions per minute (RPM) and a resolution of 0.01 crank angle degree (CAD) was used to determine the angular position of the crankshaft and engine speed. In-cylinder pressure was measured using a Kistler Piezo-Star 6125C pressure transducer, which was flush-mounted on the cylinder head. The collected pressure signals were amplified by the Kistler charge-amplifier and then inputted to the AVL combustion analyzer. In-cylinder pressure measurements were conducted at a resolution of 0.2 CAD for 100 consecutive cycles. Exhaust gases were sampled after the exhaust surge tank and transferred to the emission analyzers using a heated sample line (maintained at 191 °C). The exhaust gas compositions were measured by a set of California Analytical Instruments 600 series analyzers for emissions of CO, CO_2, HC and NOx, and a MKS Fourier-Transform Infra-Red (FTIR) series 2000 multi-gas analyzer for emissions of N_2O and CH_4 over three minutes for each steady-state test condition. PM were measured by an AVL smoke meter (415S). The measured filter smoke number (FSN) was converted to mass concentration (m_{soot}) by (Christian et al., 1993):

$$m_{soot} = \frac{1}{0.405} \times 4.95 \times FSN \times \exp(0.38FSN) \quad (1)$$

The intake pressure and temperature, exhaust gas pressure and temperature, lubricating oil pressure and temperature, cooling water temperature, engine speed and load, and flow rates of hydrogen, diesel, and air were also simultaneously recorded by a data acquisition (DAQ) system based on the LabVIEW platform over three minutes for each steady-state test condition.

Table 12: Engine specifications (*ATDC stands for after top dead center).

Engine model	Caterpillar 3401
Number of cylinders	1
Bore × Stroke (mm × mm)	137.2 × 165.1
Conn. rod length (mm)	261.62
Compression ratio	16.25
Displacement (L)	2.44
Intake valve opening (IVO)	-358.3 ºATDC*
Intake valve closing (IVC)	-169.7 ºATDC
Exhaust valve opening (EVO)	145.3 ºATDC
Exhaust valve closing (EVC)	348.3 ºATDC
Maximum power output	74.6 kW (@2100 rpm)

Testing was carried out using hydrogen supplied by Messer Canada Inc. and a commercial Canadian ultra-low sulfur diesel (ULSD). The lower heating value (LHV) of hydrogen is 120 MJ/kg and that of diesel is 43.45 MJ/kg. Other properties of diesel fuel are listed in Table 13.

Table 13: Properties of diesel.

Property	Diesel
Density (kg/m^3)	824.6 (@ 15 ^{o}C)
Cetane number	44.9
LHV (MJ/kg)	43.45
90% distillation temperature (^{o}C)	279.7
Hydrogen content (mass%)	12.38
Carbon content (mass%)	83.39

3.3 Test Conditions, Procedure and Methodology

The load and speeds of locomotive engines change from idling to different notches, with idling at low load and low engine speed and notch 8 at full load and high engine speed (GHD Limited, 2018). Due to the limited time, the testing of this project was only conducted under three typical engine load conditions, i.e. 25, 50 and 75% of full engine load, which correspond to brake mean effective pressures (BMEPs) of 4.05, 8.10 and 12.15 bar, respectively, and a constant engine speed of 1000 rpm. The 25, 50 and 75% of full engine load for the test engine are generally similar to the load levels of a locomotive engine at notches 1 or 2, notches 4~6 and notches 7 or 8, respectively. The BMEP is torque divided by engine displacement volume, i.e.

$$BMEP = \frac{2\pi n_R T}{V_d} \tag{2}$$

where n_R is the number of crank revolutions for each power stroke (n_R=2 for a four-stroke engine and 1 for a two-stroke engine), T is the torque measured by the dynamometer, and V_d is the displacement volume.

The testing was first conducted at a fixed SODI timing that gave the combustion phasing of about 8 CAD ATDC (after top dead center) for diesel-only combustion at each engine load condition, but the timing varied when load changed. At each load condition, the testing started with conventional diesel-only combustion (no hydrogen introduction), and then hydrogen energy fraction was gradually increased to 5, 10, 20% and higher, until the maximum hydrogen flow meter (0.5 kg/h) range, or the peak cylinder pressure of 150 bar or the peak pressure rise rate of 15 bar/CAD, both of which are the limit that the engine hardware can afford, was reached. The hydrogen energy fraction is defined as

$$\%H2 = \frac{m_{H2} \times LHV_{H2}}{m_D \times LHV_D + m_{H2} \times LHV_{H2}} \times 100 \tag{3}$$

where m represents mass flow rate, LHV is lower heating value, and subscripts D and $H2$ represent diesel and hydrogen, respectively. The maximum hydrogen energy fraction reached during the test was 50, 40 and 25% at BMEPs of 4.05, 8.10 and 12.15 bar, respectively, due to the limit of the flow meter range. At each engine load and hydrogen energy fraction condition, the engine was allowed to reach steady state operation (defined by exhaust temperature variation within ±2 ^{o}C). Then data was collected and averaged

for a three-minute period. In addition to emission data, cylinder pressure, diesel and hydrogen flow rates, exhaust temperature, engine load/speed and efficiency were also collected and averaged during the three-minute period. The details of engine load, SODI and hydrogen energy fractions during the fixed SODI test are listed in Table 14.

Table 14: Engine parameters at fixed SODI testing.

BMEP (bar)	SODI (CAD ATDC)	%H2 (%)
4.05	-7.0	0, 5, 10, 20, 30, 40 ,50
8.10	-10.0	0, 5, 10, 20, 30, 40
12.15	-13.0	0, 5, 10, 20, 25

Then, a test on the effect of SODI timing was conducted at three different hydrogen energy fractions of 0, 10 and 25% for each of the three investigated engine loads. At each engine load and hydrogen energy fraction condition, a SODI timing sweep was conducted to examine if an appropriate diesel injection timing adjustment is beneficial to the combustion and emission performance of hydrogen-diesel dual fuel combustion compared to the diesel-only case. Table 15 lists the details of load, SODIs and hydrogen energy fractions during the SODI timing sweep.

Table 15: Engine parameters during SODI timing sweep testing.

BMEP (bar)	SODI (CAD ATDC)	%H2 (%)
4.05	-4, -5.5, -6, -7, -8. -9, -10, -11	0
	-4, -5, -6, -7, -8	10
	-4, -5, -6, -7	25
8.10	-6.5, -8, -10, -12, -14, -16, -18, -19	0
	-6.5, -8, -10, -12, -14, -16, -17.5	10
	-6.5, -8, -10, -12, -14, -16	25
12.15	-8.5, -10, -12, -14, -16, -18, -20, -21	0
	-8.5, -10, -12, -14, -16, -18, -19	10
	-8.5, -10, -11, -12, -13	25

The cylinder pressure was used to calculate the net heat release rate (HRR_{net}) using Eq. (4), where P is the cylinder pressure, V is the cylinder volume, θ is the engine crank angle, and γ is the specific heat ratio.

$$HRR_{net} = \frac{\gamma}{\gamma - 1} P \frac{dV}{d\theta} + \frac{1}{\gamma - 1} V \frac{dP}{d\theta} \quad (4)$$

Based on the heat release rate calculated by Eq. 4, four specific parameters, CA05, CA10, CA50, and CA90, are defined. They are the crank angles at which 5%, 10%, 50% and 90% of cumulative heat is released, respectively. CA05, CA50 and the difference between CA90 and CA10 (CA10-90) are referred as the start of combustion, the combustion phasing and the combustion duration, respectively.

The pressure rise rate was calculated from the pressure profiles using Eq. (5), where Δθ is 0.2 CAD.

$$\left(\frac{dP}{d\theta}\right)_n = \frac{P_{n+1} - P_n}{\Delta\theta} \quad (5)$$

3.4 Results and Discussion

The testing results of fixed SODI are presented and discussed first in this section, followed by the results of SODI sweep.

3.4.1 Fixed Start of Diesel Injection (SODI)

The results of the effect of hydrogen energy fraction on combustion and emission performance at fixed SODI are presented and discussed first.

3.4.1.1 Engine combustion performance

Figure 39 shows the net heat release rate as a function of crank angle at BMEPs of 4.05 and 12.15 bar. The result at the BMEP of 8.10 bar is between those of 4.05 and 12.15 bar and is therefore not shown. It is noted that hydrogen-diesel dual fuel combustion is qualitatively similar to conventional diesel combustion. There are two peaks on the heat release curve. However, the introduction of hydrogen modifies the values of both peaks. The first peak on the heat release rate curve is due to the reaction during the premixed combustion stage, and the second peak is caused by the diesel diffusion and hydrogen/air premixed combustion. At the BMEP of 4.05 bar, the heat release rate value of the first peak slightly increases with the introduction of hydrogen from zero to 20%, which might be because hydrogen promotes the ignition process of diesel. Further increasing hydrogen energy fraction to 50% causes the heat release rate value of the first peak to decrease at BMEP of 4.05 bar. This might be due to the significantly decreased diesel involved in the premixed ignition process when hydrogen fraction is higher. The second peak of heat release rate is due to the diesel diffusion and hydrogen/air premixed combustion. The effect of hydrogen energy fraction on the heat release rate of the second peak at BMEP of 4.05 bar is qualitatively opposite to that on the first peak. When increasing hydrogen energy fraction from zero to 20%, the heat release rate of the second peak slightly decreases at BMEP of 4.05 bar, since decreased diesel is involved and the contribution of hydrogen/air premixed combustion is negligible due to extra low equivalence ratio. With further increasing hydrogen energy fraction to 50%, the heat release rate of the second peak increases, because more hydrogen/air premixed combustion starts to contribute to the heat release at this stage when hydrogen energy fraction is higher.

Due to the quickly increased peak pressure rise rate with increasing hydrogen energy fraction (will be shown later), the maximum hydrogen energy fraction reached during the test was 25% at BMEP of 12.15 bar. Qualitatively, the effect of the introduction of small amount of hydrogen on the heat release rate value of the first peak is similar to that for BMEP of 4.05 bar. However, the introduction of small amount of hydrogen significantly advances the position and increases the heat release rate value of the second peak. This might be because the second heat release peak is dominated by hydrogen/air premixed combustion which is intensified with increasing hydrogen energy fraction at a high load condition when equivalence ratio of hydrogen/air mixture becomes relatively high.

Figure 40 displays the variations of the start of combustion (CA05) and the combustion duration (CA10-90) as a function of hydrogen energy fraction for the three investigated engine load conditions. It is noted that

the increase in hydrogen energy fraction has negligible effect on the start of combustion at BMEPs of 4.05 and 8.10 bar, but slightly advances the start of combustion at BMEP of 12.15 bar.

Combustion duration does not change significantly when a small fraction of hydrogen is introduced, but then decreases with further increasing hydrogen energy fraction at all three engine loads. This is because large amount of hydrogen increases the fraction of hydrogen/air combustion and therefore intensifies the burning rate during the second stage of heat release (second peak on the curves of Figure 39).

Figure 41 shows the variation of combustion phasing (CA50) as a function of hydrogen energy fraction. It is noted that introducing small amount of hydrogen does not significantly affect combustion phasing. However, a large amount of hydrogen advances combustion phasing at BMEPs of 8.10 and 12.15 bar, but slightly retards combustion phasing at BMEP of 4.05 bar. This result is qualitatively similar to that observed in (Li et al., 2017). The reason could be that the introduction of relatively large amount of hydrogen at low engine load slows the reactions during diesel premixed combustion stage and has a mild impact on the reactions during the diesel diffusion and hydrogen premixed combustion stage, as shown in Figure 39. As a result, the combustion phasing slightly retards although the combustion duration decreases with increasing hydrogen energy fraction at the low engine load condition investigated. However, at medium to high engine load conditions, the introduction of hydrogen dramatically enhances the reactions during diesel diffusion and hydrogen premixed combustion stage, resulting in reduced combustion duration and advancement of combustion phasing.

Figure 42 depicts the variations of peak cylinder pressure and peak pressure rise rate. It is observed that increasing hydrogen energy fraction has negligible effect on peak cylinder pressure at BMEP of 4.05 bar. This could be because increasing hydrogen energy fraction does not significantly affect or change the combustion phasing at low load condition. However, increasing hydrogen energy fraction increases the peak cylinder pressure at BMEPs of 8.10 and 12.15 bar, since combustion phasing advances and therefore more energy is released near top dead center.

Increasing hydrogen energy fraction increases peak pressure rise rate at all engine load conditions except when hydrogen energy fraction is increased from 40 to 50% at BMEP of 4.05 bar. The higher the engine load, the higher the increase rate of peak pressure rise rate with increasing hydrogen energy fraction. The peak pressure rise rate reaches about 14 bar/CAD, which was close to the limit of 15 bar/CAD, at hydrogen energy fraction of 25% and BMEP of 12.15 bar. This suggests that increased peak pressure rise rate at relatively higher engine load conditions may be a limiting factor preventing further increase of the displacement ratio of diesel. Therefore, hydrogen-diesel dual fuel combustion may not be as effective for locomotives that spend a measurable portion of their time in the higher notches, in terms of displacing diesel and reducing GHG emissions. The peak pressure rise rate slightly decreases with increasing hydrogen energy fraction from 40% to 50% at BMEP of 4.05 bar because of the retard of combustion phasing.

Figure 43 shows the variation of exhaust temperature with increasing hydrogen energy fraction. It is noted that exhaust temperature first slightly increases but then starts to decrease with increasing hydrogen energy fraction. This could be due to the combined effects of variations in combustion temperature, combustion phasing and combustion duration. Hydrogen blending increases combustion temperature (Seddiek et al., 2015), which tends to increase exhaust temperature. However, the advancement in combustion phasing (Figure 41) and decrease in combustion duration (Figure 40) tends to lower exhaust temperature. Overall, the effect of hydrogen blending on exhaust temperature is not significant. The maximum variation in exhaust temperature is less than 2.7% for all three investigated load conditions, compared to the diesel-only case.

3.4.1.2 Engine efficiency and GHG emissions

Figure 44 shows the variation of brake thermal efficiency as a function of hydrogen energy fraction. It suggests that engine efficiency does not significantly change with the introduction of hydrogen at BMEPs of 8.10 and 12.15 bar, when the diesel injection timing is fixed. This might be due to the combined effects of the advanced combustion phasing (Figure 41) that tends to decrease engine efficiency due to more energy release before top dead center and decreased combustion duration (Figure 40) that tends to improve combustion efficiency and causes more heat release near top dead center.

At a BMEP of 4.05 bar, brake thermal efficiency slightly decreases when a small amount of hydrogen is introduced. This could be due to the low combustion efficiency of hydrogen in the cold cylinder wall and crevice zones. However, brake thermal efficiency starts to increase and reaches the similar level of pure diesel combustion at hydrogen energy fraction of 50% due to gradually increased equivalence ratio of hydrogen/air mixture which improves combustion efficiency.

Methane (CH_4) and nitrous oxide (N_2O) are two strong GHGs. Figure 45 displays the variations of CH_4 and N_2O emissions when hydrogen is introduced. It is noted that increasing the hydrogen energy fraction decreases CH_4 emissions. N_2O emissions increase when a small amount of hydrogen is introduced, but do not change significantly with further increasing hydrogen energy fraction. Overall, the absolute levels of CH_4 and N_2O emissions are small.

Figure 46 depicts the variations of CO_2 and CO_2 equivalent emissions when hydrogen is introduced. CO_2 equivalent is the overall GHG and defined as:

$$CO_2 \text{ equivalent} = CO_2 + 28CH_4 + 265N_2O \quad (6)$$

where 28 and 265 are the global warming potentials of CH_4 and N_2O, respectively, for the 100-year time horizon (The Intergovernmental Panel on Climate Change (IPCC), 2015).

It is observed that CO_2 emissions almost linearly decrease with increasing hydrogen energy fraction. This is because the combustion of hydrogen does not generate any CO_2 and engine efficiency change is negligible with increasing hydrogen energy fraction.

Since the absolute levels of CH_4 and N_2O emissions are very small, the difference between CO_2 and CO_2 equivalent emissions is almost negligible. Therefore, CO_2 equivalent emissions also almost linearly decrease with increasing hydrogen energy fraction.

3.4.1.3 Pollutant emissions

Figure 47 shows the variations of nitrogen oxides (NOx) and particulate matter (PM) emissions as a function of hydrogen energy fraction at the three investigated engine load conditions. It is noted that NOx emissions slightly decrease when a small amount of hydrogen is introduced, but increase with further increasing hydrogen energy fraction at BMEPs of 4.05 and 8.10 bar. At BMEP of 12.15 bar, increasing hydrogen energy fraction increase NOx emissions. These results are qualitatively consistent with observations in literature (Li et al. 2017, Bakar et al. 2022, Juknelevicius et al. 2019, Neg et al. 2019).

PM emissions significantly decrease with increasing hydrogen energy fraction at all three engine load conditions. This is consistent with the observations of (Liu et al., 2022), since increasing hydrogen energy fraction decreases soot formation rate and increases soot oxidation rate (Guo et al., 2006).

Figure 48 displays the variations of unburned hydrocarbon (HC) and CO emissions. It is noted that HC emissions slightly increase with increasing hydrogen energy fraction. This is qualitatively consistent with

the observations of (Liu et al. 2022, Vavra et al. 2019). It is not clear what causes the slight increase in HC emissions.

CO emissions monotonically decrease with increasing hydrogen energy fraction. This might be because increasing hydrogen energy fraction increases the OH radical concentration and the temperature in the combustion zone and therefore enhances the conversion rate of CO to CO_2 via the below reaction (Frassoldati et al., 2007):

$$CO + OH = CO_2 + H \quad (7)$$

Overall, the results suggest that fuel switching from diesel to hydrogen does help reduce GHG, CO and PM emissions from the tailpipe. The maximum diesel displacement ratio with hydrogen varies with engine operating conditions, such as engine load. The lower the engine load, the more diesel that can be displaced by hydrogen. This may be beneficial to rail industry, since locomotive engines for all operations spend a significant amount of time at notches 1 and 2 or idling which are low load conditions (GHD Limited, 2018). The most benefit would likely be for locomotive operations that spend the majority of time at low-load conditions, which, referring to the statistics provided in Table 1, include Class I Road, Yard Switchers, and Commuter services operations (71.4%, 80.7%, and 76.6% respectively) (GHD Limited, 2018). Therefore, hydrogen-diesel dual fuel combustion technology has the potential to help rail industry reduce GHG and other pollutant emissions. At relatively high load conditions, the maximum diesel displacement ratio may be limited due to the higher pressure rise rate that may cause engine hardware damage. A side effect of hydrogen-diesel dual fuel combustion is the increase in NOx emissions, which would need to be addressed.

3.4.2 Sweep of Start of Diesel Injection (SODI)

The purpose of the sweep of SODI timing was to investigate if an appropriate diesel injection timing adjustment is beneficial to the combustion and emissions performance of hydrogen/diesel dual fuel combustion compared to diesel-only combustion. The sweep started from a late timing when combustion was still stable to an early timing when the peak cylinder pressure reached 150 bar or peak pressure rise rate reached about 13~15 bar/CAD.

3.4.2.1 Combustion performance

Figure 49 shows the variation of combustion phasing as a function of SODI for all three investigated engine loads. It is noted that advancing SODI advances combustion phasing. This is consistent with the general understanding, since an earlier SODI timing causes earlier start of combustion.

Combustion phasing advances as hydrogen energy fraction is increased at a fixed SODI. This has been explained during fixed diesel injection timing test.

Figure 50 depicts the variation of peak cylinder pressure as a function of SODI. It is observed that advancing SODI increases peak cylinder pressure. This is because an earlier SODI advances combustion phasing, leading to more heat release near top dead center.

Figure 51 displays the variation of peak pressure rise rate as a function of SODI. It is noted that advancing SODI increases peak pressure rise rate at all three investigated load conditions. This is also because more heat is released near top dead center with advancing SODI. Therefore, retarding SODI may help increase the limit of hydrogen energy fraction.

3.4.2.2 Engine efficiency and GHG emissions

The variation of brake thermal efficiency as a function of SODI is shown in Figure 52. It is noted that advancing SODI improves engine efficiency, since an appropriately early SODI causes more heat release near top dead center when temperature and pressure are higher. However, an overly advanced SODI causes engine efficiency to slightly deteriorate at BMEPs OF 8.10 and 12.15 bar, since more heat is released before top dead center and therefore the engine produces more negative work. This efficiency deterioration was not observed at BMEP of 4.05 bar, since SODI was not overly advanced due to the sharp increase in the pressure rise rate.

As discussed in the section on fixed diesel injection timing testing, the effect of hydrogen energy fraction on brake thermal efficiency is negligible at BMEPs of 8.10 and 12.15 bar. At a BMEP of 4.05 bar, a small amount of hydrogen slightly deteriorates engine efficiency.

Figure 53 depicts the variation of brake specific CO_2 emissions as a function of SODI. It is noted that the effect of SODI on CO_2 emissions is qualitatively opposite to that on engine efficiency, since fuel consumption decreases when engine efficiency is improved.

An increase in hydrogen energy fraction at a fixed diesel injection timing decreases CO_2 emissions at all three investigated engine load conditions, which has been discussed before.

The variation of CO_2 equivalent emissions is shown in Figure 54. Comparing Figure 53 and Figure 54, it is noted that the difference between CO_2 and CO_2 equivalent emissions is negligible, which is similar to that observed before during the discussion on fixed diesel injection timing test results. The reason is that N_2O and CH_4 emissions are negligible compared to CO2 emissions.

3.4.2.3 Pollutant emissions

Figure 55 depicts the variation of NOx emissions as a function of SODI. It is noted that retarding SODI decreases NOx emissions at BMEPs of 8.10 and 12.15 bar. This is because retarding SODI causes more combustion to occur later in the expansion stroke and therefore decreases the combustion temperature. At BMEP of 4.05 bar, NOx emissions first decrease with retarding SODI to -6 CAD ATDC, but then slightly increase with further retarding SODI from -6 to -4 CAD ATDC. It is not clear what causes the slight increase with further retarding SODI at BMEP of 4.05 bar. One possible reason might be that further retarding SODI causes incomplete combustion and therefore more hydrocarbon radicals such as CH in the reaction zone, which results in more NO formation due to the prompt NO formation route (Guo et al., 2005). Further investigation is needed in the future to confirm the fundamental mechanism behind this slight increase in NOx emissions at late SODIs.

Figure 56 shows the variation of PM emissions as a function of SODI. At BMEPs of 8.10 and 12.15 bar, retarding SODI increases PM emissions, which is consistent with the general understanding of the effect of SODI on PM emissions in compression ignition engines (Geng et al., 2021). At BMEP of 4.05 bar, retarding SODI from -11 to -8 CAD ATDC slightly increases PM emissions, but further retarding SODI from -8 to -4 CAD ATDC decreases PM emissions for diesel-only case (H2%=0). Furthermore for the 4.05 bar test, when hydrogen energy fractions are 10 and 25%, the sweeps of SODI were only conducted over ranges of SODIs later than -8 CAD ATDC due to higher pressure rise rate, and retarding SODI decreases PM emissions during the sweeps. It is not clear what the exact reason is for the decrease in PM emissions with retarding SODI to a very late timing, but a possible reason might be that soot formation rate starts to decrease when temperature becomes low at very late diesel injection timings.

Figure 57 depicts the variation of CO emissions as a function of SODI. It is observed that generally advancing SODI decreases CO emissions. This is consistent with the general understanding, since advancing SODI causes more combustion near top dead center when temperature and pressure are higher. However, at BMEP of 4.05 bar and hydrogen energy fraction of 25%, advancing SODI increases CO emissions. It might be because an overly retarded SODI causes more hydrogen to mix with diesel and therefore makes combustion more complete when hydrogen energy fraction is higher.

Overall, the results of the SODI sweep testing suggest that engine efficiency and emissions do change with changing SODI. However, there is a trade-off among different performance parameters. Appropriately advancing SODI helps improve engine efficiency and reduce GHG emissions. However, pressure rise rate increases with advancing SODI, which may limit the maximum diesel displacement ratio. NOx emissions usually also increase with advancing SODI. Therefore, appropriate adjustment of SODI may be beneficial depending on the specific targets in applications.

4. Overarching Findings and Discussion from Literature and Testing

4.1 Comparisons between the Results Observed in Literature and Testing

The results for the effect of hydrogen introduction on engine efficiency are not consistent between some of the literature and the testing in this project. Most investigations in literature (Bakar et al. 2022, Dimitriou et al. 2018, Juknelevicius et al. 2019, Li et al. 2017, Nag et al. 2019, Saravanan & Nagarajan 2010) and the testing conducted for this project suggested that the introduction of hydrogen does not significantly affect engine efficiency when diesel injection timing is fixed or not controlled. At low loads, the introduction of hydrogen might cause a slight decrease in engine efficiency, but at higher loads, engine efficiency might slightly increase. In contrast, Hamdan et al., 2015, reported a significant increase in engine efficiency with the addition of hydrogen to the engine intake manifold. A potential explanation for this may be because the investigation by Hamdan et al. did not control engine load. An increase in engine load would therefore lead to a significant increase in engine efficiency when hydrogen was introduced.

Almost all previous investigations in literature and the testing of this project suggested that the introduction of hydrogen reduced CO_2 emissions, since the combustion of hydrogen does not generate any CO_2. The percentage of CO_2 reduction depended on the variation of engine efficiency with blending hydrogen. When the variation in engine efficiency was negligible, the percentage of CO_2 reduction was almost the same as the percentage of hydrogen energy fraction. With non-negligible engine efficiency variations, the percentage of CO_2 reduction may differ compared to the percentage of hydrogen energy fraction. The investigation (Liu et al., 2022) that noted an increase in engine efficiency but only up to 78% reduction in CO_2 emissions when 90% diesel was displaced by hydrogen might imply an imbalance between the carbon in the input fuel and exhaust, suggesting that a detailed data examination might be needed.

Most previous investigations in literature and the testing of this project revealed that NOx emissions increased with increasing hydrogen energy fraction at medium to high engine loads. However, the results of NOx emissions at low loads are not consistent in literature and the testing result of this project. Some investigations (Chintala & Subramanian 2017, Christodoulou & Megaritis 2014, Geo et al. 2008, Hamdan et al. 2015, Juknelevicius et al. 2019, Karagöz et al. 2015, Lilik et al. 2010, Masood et al. 2007; Mathur et al. 1992, Saravanan & Nagarajan 2008, al.) and the testing conducted for this project, observed an increase in NOx emissions at low loads, but others (Bakar et al. 2022, Dimitriou et al. 2018, Nag et al. 2019, Saravanan & Nagarajan 2009b & 2010) noted a slight decrease in NOx emissions at low loads, when

hydrogen energy fraction was increased. The difference between the two different observations in NOx emissions at low load conditions could be due to the variations in engine design and original diesel operating conditions. The temperature and pressure inside cylinders of an engine are generally low at low load conditions. For some engines, their original design and operating conditions might allow hydrogen to be more completely burnt inside the cylinders and therefore have increased combustion temperature and NOx emissions when hydrogen energy fraction is increased at low load conditions. On the other hand, some engines' design and operating conditions might not provide a reasonable in-cylinder condition for hydrogen to be completely burnt at low loads, which might have resulted in the slight reduction in NOx emissions when hydrogen energy fraction increased. Therefore, reducing NOx emissions may come at a cost of reduced engine efficiency.

The results of the effect of hydrogen introduction on CO and PM emissions are consistent in previous investigations and the testing of this project. The introduction of hydrogen in hydrogen-diesel dual fuel engines reduced CO and PM emissions. Generally, the percentage of CO and PM emission reduction was higher than the percentage of hydrogen energy fraction, since hydrogen blending reduced CO and PM emissions due to not only the decrease in carbon intensity of the input fuel but also chemical reactions that intensify the oxidation rates of CO and PM inside cylinder, such as $CO + OH = CO_2 + H$ that intensifies the oxidation of CO due to the increased concentration of OH when hydrogen is introduced.

The effect of hydrogen on HC emissions varied among different investigations in literature and the testing of this project. However, generally the effect of hydrogen on HC emissions was not significant.

The investigation of the effect of diesel injection timing on the performance of hydrogen-diesel dual fuel engines is limited, but the results show that the performance of hydrogen-diesel dual fuel engines varied with changing diesel injection timing. Hamdan et al. (2015) noted an increase in engine efficiency when advancing diesel injection timing in limited range. The result of this project's testing revealed that there is an optimal diesel injection timing at which engine efficiency is highest when advancing the diesel injection timing. However, there was a trade-off among different performance parameters. Appropriately advancing diesel injection timing helped improve engine efficiency and reduce GHG emissions, but increased pressure rise rate and therefore limited the maximum diesel displacement ratio. NOx emissions usually also increased with advancing diesel injection timing. Therefore, diesel injection timing may be appropriately adjusted to improve the engine performance.

4.2 Assessment of Hydrogen-Diesel Combustion Feasibility for Locomotives

The literature review did not find any published results reporting on in-service conversions of diesel locomotives to diesel-hydrogen co-combustion or testing of hydrogen-diesel co-combustion, laboratory or real-world, associated with locomotives specifically. The majority of the planned conversions in the locomotive sector involve conversion to hydrogen fuel cells by removing the entire diesel engine block and putting the necessary equipment for the conversion into it, which is beyond the scope of this project. However, the literature review did find limited conversions from conventional diesel engines to hydrogen-diesel dual fuel engines for ground transportation trucks, although no detailed performance evaluation of these converted trucks has been openly reported, and no testing in cold weather conditions were found.

The port injection technology requires less engine modifications to retrofit a conventional diesel engine and a lower cost of integration while still retaining the high efficiency performance of diesel engines. It also allows the engine to easily switch back to diesel combustion mode when there is not enough hydrogen.

Therefore, most previous laboratory investigations on hydrogen-diesel dual fuel combustion in literature were for port injection. Similarly, for the reasons listed above, port fuel hydrogen injection was also chosen for the testing portion of this project. One drawback of port injection is that there is a limit in ratio of hydrogen blending, especially at higher engine load conditions. Due to the variations in engine design and operating conditions, some results from the previous investigations might differ slightly, but the potential benefits and challenges of the dual fuel technology have been revealed in a laboratory setting. However, no literature about testing port injected hydrogen-diesel dual fuel combustion in a locomotive have been found.

Investigation of the direct injection design is relatively limited. The only investigation noted in literature was from a group in Australia (Liu et al. 2021 & 2022), which investigated the combustion and emission performance of a direct injection hydrogen-diesel dual fuel engine using a single-cylinder compression ignition engine. Hydrogen was directly injected to cylinder via an injector installed to the glow plug position after the glow plug was removed. They reached a maximum hydrogen fraction of 90% and achieved a maximum of 78% reduction in CO_2 emissions. The results from this group look encouraging, but more research is needed to better understand the direct injection technology, such as the feasibility, retrofit and maintenance cost of the direct injection technology for most engines. Some of the data from this investigation might also need further examination.

Both injection types achieve very positive results in terms of reducing CO_2 and PM emissions while achieving higher efficiency in laboratories, but there are trade-offs, such as an increase in NOx emissions. Currently, no studies have addressed how to counteract this increase in NOx emission without the use of aftertreatment methods and/or exhaust gas recirculation (EGR); and, at present, both EGR and aftertreatment approaches are not capable of eliminating NOx gases completely.

It has been revealed by almost all previous investigations in literature and during the testing conducted for this project that there is a limit in the diesel displacement ratio due to knocking. This limit in diesel displacement ratio decreases when engine load increases. This means that, at low loads, higher hydrogen energy fractions can be used and thus will benefit the most from GHG reductions. Another potential method to increase the diesel displacement ratio would be to retard diesel injection timing, as testing revealed that this decreases the peak pressure rise rate, however this also increases PM and CO emissions and decreases engine efficiency.

A study into locomotive duty cycles done by GHD and TC (GHD Limited, 2018) observed that locomotives spend a significant amount of their time at idle, and that Class I road switchers, yard switchers, and commuter services operations also spend a lot of their time at lower notches. Therefore, Class I road switchers, yard switchers, and commuter services may obtain the most benefit from hydrogen-diesel combustion engines. Class I mainline and intercity passenger locomotives may derive some benefit but would be more limited because they spend more time a higher notches where it is much more difficult to have high concentrations of hydrogen in the fuel mix.

Considering the gaps in current scientific studies, lack of information related to the economics, the additional research into controlling NOx and optimizing the injection timing, as well as a lack of real-life integration on a locomotive, the literature review suggested that the technology readiness level (TRL) for full integration of hydrogen-diesel co-combustion in a locomotive falls within the TRL 2-3 range at the time of writing.

5. Final Conclusions

This project had two main objectives, first, to develop a comprehensive literature review on hydrogen-diesel dual fuel combustion for locomotive applications, and second, to conduct experimental testing of a heavy-duty hydrogen-diesel dual fuel combustion test cell engine at different locomotive operating conditions.

The literature review provided a scan of the current use of hydrogen-diesel co-combustion engines in rail, or other appropriate modes from which co-combustion could be adapted to rail, an overview of different injection methods for dual fuel combustion, a description of mechanics of hydrogen-diesel co-combustion, as well as provided an assessment of retrofit, cost and maintenance requirements for hydrogen-diesel dual fuel combustion. All the literature gathered in this review investigated hydrogen-diesel dual-fuel combustion in heavy-duty engines generally; whereas the experimental testing for this project looked at locomotive-like conditions specifically.

In the experimental testing, the combustion and emission performance of hydrogen-diesel dual fuel combustion in a heavy-duty compression ignition engine was tested under three engine load conditions, i.e. 25, 50 and 75% of full engine load and constant engine speed of 1000 rpm. These load levels are relevant to locomotive engine operating conditions from notches 1 or 2, 4 to 6, and 7 or 8 respectively. Hydrogen was introduced into the engine via engine intake port, and diesel was directly injected into the engine cylinder. The testing started at a fixed diesel injection timing, followed by an injection timing sweep.

Although the results from each source were somewhat different due to the variations in engine and operating conditions, the general trends from the literature and this project's testing are summarized below:

(1) In the experimental test, the overall GHG emissions were reduced by 50, 40 and 25% at 25, 50 and 75% engine load conditions respectively. The GHG emission reduction linearly corresponds to the rate of hydrogen substitution. This was also observed in literature. Hydrogen substitution directly reduces GHG emissions, assuming that the production of the hydrogen itself produced no additional carbon.

(2) The CH_4 and N_2O emissions were relatively small in the investigated hydrogen-diesel dual fuel engine operating conditions. Therefore, the difference between CO_2 and overall GHG emissions (CO_2 equivalent) was negligible.

(3) The effect of hydrogen energy fraction on engine efficiency was almost negligible at fixed diesel injection timings, although some literature found variation in engine efficiency at certain load conditions.

(4) The literature and testing determined that more hydrogen could be introduced into engines at low load conditions, but there were limits for the maximum hydrogen fraction at high load conditions due to pre-ignition.

- Considering this, locomotives that operate a significant amount of their time at low load conditions may obtain the most benefit from hydrogen-diesel dual-fuel combustion engines. This would include Class I road switcher, yard switchers, and commuter service locomotives.

(5) During the testing, the peak cylinder pressure did not significantly change at 25% engine load conditions, but increased at 50 and 75% engine load conditions with increasing hydrogen energy fraction at fixed diesel injection timings;

(6) The peak pressure rise rate reached the limit the engine hardware can afford at 75% of full engine load, when the hydrogen energy fraction was 25%. It may be possible to further increase the hydrogen energy fraction at 25 and 50% engine load conditions, but these were not explored in this test.

- The observations about peak pressure rise rate suggest that engines can accommodate higher hydrogen content at lower notch operating conditions in locomotive applications without major mechanical issues. However, the maximum hydrogen content may be limited when locomotives shift into higher notch conditions.

(7) Most investigations (testing included) found that NOx emissions increased with increasing hydrogen fraction. This is a side effect of hydrogen-diesel dual fuel combustion, compared to conventional diesel combustion, and needs to be addressed in future applications. The findings for NOx emissions should not be overlooked. The locomotive types that appear to be good candidates for hydrogen-diesel dual fuel combustion include switcher and commuter locomotives that operate in or around industrialized populated areas. Air quality in these areas could be very sensitive to even small increases in NOx emissions;

(8) Increasing hydrogen energy fraction generally decreased PM and CO emissions. In the testing, it was observed that PM and CO emissions decreased at fixed diesel injection timings, which is an advantage of the dual fuel combustion.

(9) The effect on HC emissions varied among different groups. In testing, the trend of the effect of hydrogen energy fraction on HC emissions was not very clear, but overall HC emissions were relatively low;

(10) Understanding the effect diesel injection timing has on engine performance is limited in literature. In the testing, a trade-off between engine efficiency and GHG and pollutant emissions was observed when changing diesel injection timing.

- With advancing diesel injection timing, engine efficiency slightly increased, and PM, CO, and other GHG emissions improved. However, NOx emissions, the peak cylinder pressure, and the peak pressure rise rate all increased at medium and high load conditions.
- With retarding diesel injection timing, the reduction in peak cylinder pressure and peak pressure rise rate may allow for the hydrogen energy fraction to increase to a certain extent.
- Therefore, appropriate adjustment of diesel injection timing may be beneficial to hydrogen-diesel dual fuel combustion depending on the specific engine tuning desired in the context of balancing the design requirements or constraints of an application's overall design package (e.g. emission aftertreatment used, use of exhaust gas recirculation, engine constraints).

(11) The technology was currently assessed at a TRL of 2-3, as it was determined there were a number of parameters that require further research. These include

- More studies related to the economics and maintenance of hydrogen-diesel combustion for locomotive engines;
- More examples of hydrogen-diesel combustion being tested outside of lab demonstrations, to help address concerns on real-life integration, and;

- More examples of engine tests under real life climatic conditions (hot weather, cold weather, varying humidity, etc.),

6. Recommendations for Future Work

Based on literature review and experimental testing of this project, following topics are recommended for further investigation in the future in order to develop and implement hydrogen-diesel dual combustion in applications:

(1) The increase in peak pressure rise rate is limiting the further increase in hydrogen energy fraction, especially at high load engine operating conditions. Therefore, it is of interest to conduct investigations to further extend the limit of hydrogen energy fraction at high load operating conditions in order to replace more diesel by hydrogen and thus to reduce more GHG emissions in applications;

(2) The increase in hydrogen energy fraction increases NOx emissions, which is a side effect in applications. In order to reduce GHG emissions while maintaining or even reducing NOx emissions, further investigation should be conducted to address this issue in future. This could include increasing the level of exhaust gas recirculation (EGR) and/or optimizing the operation and design of the aftertreatment system, such as employing selective catalytic reduction (SCR);

(3) Hydrogen leak (slip) is not only a significant safety concern and a waste of energy but also a potential indirect GHG (Derwent et al., 2006). This issue may be more significant in dual fuel combustion engine due to incomplete combustion of hydrogen in engine boundary and crevice regions. Unfortunately, to our knowledge, no investigation on hydrogen slip from hydrogen fueled internal combustion engines has been conducted in literature. Therefore, future research should be conducted on hydrogen slip, such as from exhaust and crank case, at different engine operating conditions in order to develop strategies to reduce hydrogen slip from hydrogen-diesel dual fuel engines;

(4) The use of hydrogen in internal combustion engines may cause embrittlement, which is a significant decrease of ductility of a material and makes the material brittle. Embrittlement is caused by the ingress of either molecular or atomic hydrogen into a metal lattice (Laadel et al., 2022). However, the exact mechanism of hydrogen embrittlement is not clear. The capacity of the material to deform or stretch under load is limited due to a metallurgical interaction between atomic hydrogen and the crystallographic structure. Hydrogen embrittlement is particularly dangerous because of its reduced breaking strength and the vulnerability of material to hydrogen embrittlement increases as its tensible strength increases. Embrittlement caused by very minute amounts of hydrogen, which is undetectable by typical loss-of-ductility bend tests, has been a major source of concern for materials and system designers. This issue needs further investigation in future to ensure the safe operation of engines

(5) If the hydrogen-dual fuel technology is to be used in locomotive operations, further work is required to better incentivize its uptake by railway providers.

7. References:

Baltacioglu, M. K., Arat, H. T., Özcanli, M., & Aydin, K. (2016). Experimental comparison of pure hydrogen and HHO (hydroxy) enriched biodiesel (B10) fuel in a commercial diesel engine. International Journal of Hydrogen Energy, 41(19), 8347-8353. https://doi.org/https://doi.org/10.1016/j.ijhydene.2015.11.185

Bakar R A, Widudo, Kadirgama K, Ramasamy D, Yusaf T, Kamarulzaman, M K, Sivaraos, Aslfattahi, Samylingam N L, Alwayzy S H (2022). Experimental analysis on the performance, combustion/emission characteristics of a DI diesel engine using hydrogen in dual fuel mode. Int. J. Hydrogen Energy, https://doi.org/10.1016/j.ijhydene.2022.04.129

Bose, P. K., & Maji, D. (2009). An experimental investigation on engine performance and emissions of a single cylinder diesel engine using hydrogen as inducted fuel and diesel as injected fuel with exhaust gas recirculation. International Journal of Hydrogen Energy, 34(11), 4847-4854. https://doi.org/https://doi.org/10.1016/j.ijhydene.2008.10.077

Casey, T. (2021). All Eyes On $4 Million Diesel-Killing Hydrogen Locomotive In California. Retrieved 2023-01-01 from http://sierranorthern.com/news/articles/california-energy-commission-awards-sierra-northern-railway-team-nearly-4-000-000-to-build-and-test-hydrogen-switcher-locomotive/

Chaichan, M. T. (2015). The impact of equivalence ratio on performance and emissions of a hydrogen-diesel dual fuel engine with cooled exhaust gas recirculation. International Journal of Scientific & Engineering Research, 6(6), 938-941.

Chintala, V., & Subramanian, K. (2015). An effort to enhance hydrogen energy share in a compression ignition engine under dual-fuel mode using low temperature combustion strategies. Applied Energy, 146, 174-183.

Chintala, V., & Subramanian, K. A. (2016). Experimental investigation of hydrogen energy share improvement in a compression ignition engine using water injection and compression ratio reduction. Energy Conversion and Management, 108, 106-119. https://doi.org/https://doi.org/10.1016/j.enconman.2015.10.069

Chintala, V., & Subramanian, K. A. (2017). A comprehensive review on utilization of hydrogen in a compression ignition engine under dual fuel mode. Renewable and Sustainable Energy Reviews, 70, 472-491. https://doi.org/https://doi.org/10.1016/j.rser.2016.11.247

Christian V. R., Knopf F., Jaschek A., and Schindler W. (1993). Eine neue Messmethodik der Bosch-Zahl mit erhohter Empfindlichkeit. Motortech. Z., 54, pp.16–22

Christodoulou, F., & Megaritis, A. (2014). Experimental investigation of the effects of simultaneous hydrogen and nitrogen addition on the emissions and combustion of a diesel engine. International Journal of Hydrogen Energy, 39(6), 2692-2702.

Consultancy, F.-N. (2022). Fugitive Hydrogen Emissions in a Future Hydrogen Economy.

Das, L. (2002). Hydrogen engine: research and development (R&D) programmes in Indian Institute of Technology (IIT), Delhi. International Journal of Hydrogen Energy, 27(9), 953-965.

Day, P. (2022). Hydrogen on track to replace diesel locomotives. Retrieved 2023-01-01 from https://www.reuters.com/business/energy/hydrogen-track-replace-diesel-locomotives-2022-12-07/

DdynaCERT. (2023). https://dynacert.com/page/how-it-works

de Morais, A. M., Mendes Justino, M. A., Valente, O. S., Hanriot, S. d. M., & Sodré, J. R. (2013). Hydrogen impacts on performance and CO2 emissions from a diesel power generator.

International Journal of Hydrogen Energy, 38(16), 6857-6864. https://doi.org/https://doi.org/10.1016/j.ijhydene.2013.03.119

Deb, M., Sastry, G. R. K., Bose, P. K., & Banerjee, R. (2015). An experimental study on combustion, performance and emission analysis of a single cylinder, 4-stroke DI-diesel engine using hydrogen in dual fuel mode of operation. International Journal of Hydrogen Energy, 40(27), 8586-8598. https://doi.org/https://doi.org/10.1016/j.ijhydene.2015.04.125

Derwent R, Simmonds P, O'Doherty S, Manning A, Collins W, Stevenson D (2006). Global environmental impacts of the hydrogen economy. International Journal of Nuclear Hydrogen Production and Applications, 1, 57-67

Dhole, A. E., Yarasu, R. B., Lata, D. B., & Baraskar, S. S. (2014). Mathematical modeling for the performance and emission parameters of dual fuel diesel engine using hydrogen as secondary fuel. International Journal of Hydrogen Energy, 39(24), 12991-13001. https://doi.org/https://doi.org/10.1016/j.ijhydene.2014.06.084

Dimitriou, P., Kumar, M., Tsujimura, T., & Suzuki, Y. (2018). Combustion and emission characteristics of a hydrogen-diesel dual-fuel engine. International Journal of Hydrogen Energy, 43(29), 13605-13617. https://doi.org/https://doi.org/10.1016/j.ijhydene.2018.05.062

Dimitriou, P., & Tsujimura, T. (2017). A review of hydrogen as a compression ignition engine fuel. International Journal of Hydrogen Energy, 42(38), 24470-24486. https://doi.org/https://doi.org/10.1016/j.ijhydene.2017.07.232

El Hannach, M., Ahmadi, P., Guzman, L., Pickup, S., & Kjeang, E. (2019). Life cycle assessment of hydrogen and diesel dual-fuel class 8 heavy duty trucks. International Journal of Hydrogen Energy, 44(16), 8575-8584. https://doi.org/https://doi.org/10.1016/j.ijhydene.2019.02.027

Frassoldati A, Faravelli T, Ranzi E (2007). The ignition, combustion and flame structure of carbon monoxide/hydrogen mixtures. Note 1: Detailed kinetic modeling of syngas combustion also in presence of nitrogen compounds. International Journal of Hydrogen Energy, 32: 3471 – 3485

Gatts, T., Liu, S., Liew, C., Ralston, B., Bell, C., & Li, H. (2012). An experimental investigation of incomplete combustion of gaseous fuels of a heavy-duty diesel engine supplemented with hydrogen and natural gas. International Journal of Hydrogen Energy, 37(9), 7848-7859.

Geerts, E. (2022). Namibia to develop Africa’s first hydrogen-diesel locomotive. Retrieved 2023-01-01 from https://www.railtech.com/rolling-stock/2022/10/12/namibia-to-develop-africas-first-hydrogen-diesel-locomotive/?gdpr=accept

Geng L, Xiao Y, Li S, Chen H, Chen X (2021) Effects of injection timing and rail pressure on particulate size-number distribution of a common rail DI engine fueled with fischer-tropsch diesel synthesized from coal. Journal of the Energy Institute, 95: 219-230

Geo, V. E., Nagarajan, G., & Nagalingam, B. (2008). Studies on dual fuel operation of rubber seed oil and its bio-diesel with hydrogen as the inducted fuel. International Journal of Hydrogen Energy, 33(21), 6357-6367.

GHD Limited (2018). Review of Duty Cycle Profiles for the Canadian Diesel Locomotive Fleet. Transport Canada, 11148157

Guo, H., Hosseini, V., Neill, W. S., Chippior, W. L., & Dumitrescu, C. E. (2011). An experimental study on the effect of hydrogen enrichment on diesel fueled HCCI combustion. International Journal of Hydrogen Energy, 36(21), 13820-13830.

Guo H, Liu F, and Smallwood G J (2005). A Numerical Study on NOX Formation in Laminar Counterflow CH4/Air Triple Flames. Combustion and Flame, 143: 282-298

Guo H., Liu F., Smallwood G.J., and Gülder Ö.L (2006). A Numerical Study on the Influence of Hydrogen Addition on Soot Formation in a Laminar Ethylene-Air Diffusion Flame. Combustion and Flame 145, 324-338

Hamdan, M. O., Selim, M. Y. E., Al-Omari, S.-A. B., & Elnajjar, E. (2015). Hydrogen supplement co-combustion with diesel in compression ignition engine. Renewable Energy, 82, 54-60. https://doi.org/https://doi.org/10.1016/j.renene.2014.08.019

Howarth, R. W., & Jacobson, M. Z. (2021). How green is blue hydrogen? Energy Science & Engineering, 9(10), 1676-1687. https://doi.org/https://doi.org/10.1002/ese3.956

HYDI. (2023). https://hydi.com.au/

The Intergovernmental Panel on Climate Change (IPCC). Global Warming Potential Values (https://www.ghgprotocol.org/sites/default/files/ghgp/Global-Warming-Potential-Values%20%28Feb%2016%202016%29_1.pdf)

Juknelevicius, R., Szwaja, S., Pyrc, M., & Gruca, M. (2019). Influence of hydrogen co-combustion with diesel fuel on performance, smoke and combustion phases in the compression ignition engine. International Journal of Hydrogen Energy, 44(34), 19026-19034. https://doi.org/https://doi.org/10.1016/j.ijhydene.2018.10.126

Karagöz, Y., Sandalcı, T., Yüksek, L., & Dalkılıç, A. S. (2015). Engine performance and emission effects of diesel burns enriched by hydrogen on different engine loads. International Journal of Hydrogen Energy, 40(20), 6702-6713. https://doi.org/https://doi.org/10.1016/j.ijhydene.2015.03.141

Laadel, N.-E., El Mansori, M., Kang, N., Marlin, S., & Boussant-Roux, Y. (2022). Permeation barriers for hydrogen embrittlement prevention in metals – A review on mechanisms, materials suitability and efficiency. International Journal of Hydrogen Energy, 47(76), 32707-32731. https://doi.org/https://doi.org/10.1016/j.ijhydene.2022.07.164

Lagerquist, J. (2022). First U.S. hydrogen train to use Canadian fuel cells. Retrieved 2023-01-01 from https://ca.finance.yahoo.com/news/first-us-hydrogen-train-to-use-canadian-fuel-cells-155116106.html?guccounter=1&guce_referrer=aHR0cHM6Ly93d3cuZ29vZ2xlLmNvbS8&guce_referrer_sig=AQAAAFSxIfcQV6le-y5hvSHBTH4hcZXTvBrDhehUM3E1SJ2tGIPEtKcxRyfzwVJ8D0e8PDJG_0Xs6ZEKAMZXtaaoet5WBOwCXCPvJRLbWiSWJ60RfIvookHsuoXZzGJw-ESZ5o00t7bwahF-5xzVC1u1Nlj5sIwLy2xjNGgyKNSXR42X

Li H, Liu S, Liew C, Gatts T, Wayne S, Clark N, Nuszkowski J (2017). An investigation of the combustion process of a heavy-duty dual fuel engine supplemented with natural gas or hydrogen. Int. J. Hydrogen Energy, 42:3352–3362

Liew, C., Gatts, T., Liu, S., Rapp., B., Ralston, B., Clark, N., Huang, Y. (2011). An experimental investigation of exhaust emissions of a 1999 Cummins IS,370 diesel engine supplemented with H2. Int. J. Engine Research, 13, 116-129

Lilik, G. K., Zhang, H., Herreros, J. M., Haworth, D. C., & Boehman, A. L. (2010). Hydrogen assisted diesel combustion. International Journal of Hydrogen Energy, 35(9), 4382-4398. https://doi.org/https://doi.org/10.1016/j.ijhydene.2010.01.105

Liu, X., Seberry, G., Kook, S., Chan, Q. N., & Hawkes, E. R. (2022). Direct injection of hydrogen main fuel and diesel pilot fuel in a retrofitted single-cylinder compression ignition engine. International Journal of Hydrogen Energy, 47(84), 35864-35876. https://doi.org/https://doi.org/10.1016/j.ijhydene.2022.08.149

Liu X, Srna A, Yip H L, Kook S, Chan Q N, Hawkes E R (2021). Performance and emissions of hydrogen-diesel dual direct injection (H2DDI) in a single-cylinder compression-ignition engine. Int. J. Hydrogen Energy, 4 6, 1302-1314

Liu, X., Srna, A., Yip, H. L., Kook, S., Nian, Q., & Hawkes, E. (2020). Comparison of hydrogen port injection and direct injection (DI) in a single-cylinder dual-fuel diesel engine.

Masood, M., Mehdi, S., & Ram Reddy, P. (2007). Experimental investigations on a hydrogen-diesel dual fuel engine at different compression ratios.

Mathur, H., Das, L., & Patro, T. (1992). Effects of charge diluents on the emission characteristics of a hydrogen fueled diesel engine. International Journal of Hydrogen Energy, 17(8), 635-642.

Mohammadi, A., Shioji, M., Nakai, Y., Ishikura, W., & Tabo, E. (2007). Performance and combustion characteristics of a direct injection SI hydrogen engine. International Journal of Hydrogen Energy, 32(2), 296-304. https://doi.org/https://doi.org/10.1016/j.ijhydene.2006.06.005

Nag S, Sharma P, Gupta A, Dhar A (2019). Experimental study of engine performance and emissions for hydrogen diesel dual fuel engine with exhaust gas recirculation. Int. J. Hydrogen Energy 44, 12163-12175

Nielsen, M. (2021). Prince George trucking company takes delivery of hydrogen-diesel hybrid. Retrieved 2023-01-01 from https://www.princegeorgecitizen.com/highlights/prince-george-trucking-company-takes-delivery-of-hydrogen-diesel-hybrid-4535656

Okonkwo, P. C., Barhoumi, E. M., Ben Belgacem, I., Mansir, I. B., Aliyu, M., Emori, W., Uzoma, P. C., Beitelmal, W. H., Akyüz, E., Radwan, A. B., & Shakoor, R. A. (2023). A focused review of the hydrogen storage tank embrittlement mechanism process. International Journal of Hydrogen Energy. https://doi.org/https://doi.org/10.1016/j.ijhydene.2022.12.252

Park, H., Kim, J., & Bae, C. (2015). Effects of hydrogen ratio and EGR on combustion and emissions in a hydrogen/diesel dual-fuel PCCI engine (0148-7191).

Roy, M. M., Tomita, E., Kawahara, N., Harada, Y., & Sakane, A. (2010). An experimental investigation on engine performance and emissions of a supercharged H2-diesel dual-fuel engine. International Journal of Hydrogen Energy, 35(2), 844-853. https://doi.org/https://doi.org/10.1016/j.ijhydene.2009.11.009

Samuel, S., & McCormick, G. (2010). Hydrogen enriched diesel combustion (0148-7191).

Sandalcı, T., & Karagöz, Y. (2014). Experimental investigation of the combustion characteristics, emissions and performance of hydrogen port fuel injection in a diesel engine. International Journal of Hydrogen Energy, 39(32), 18480-18489. https://doi.org/https://doi.org/10.1016/j.ijhydene.2014.09.044

Santoso, W. B., Bakar, R. A., & Nur, A. (2013). Combustion Characteristics of Diesel-Hydrogen Dual Fuel Engine at Low Load. Energy Procedia, 32, 3-10. https://doi.org/https://doi.org/10.1016/j.egypro.2013.05.002

Saravanan, N., & Nagarajan, G. (2008). An experimental investigation of hydrogen-enriched air induction in a diesel engine system. International Journal of Hydrogen Energy, 33(6), 1769-1775. https://doi.org/https://doi.org/10.1016/j.ijhydene.2007.12.065

Saravanan, N., & Nagarajan, G. (2009a). Experimental Investigation in Optimizing the Hydrogen Fuel on a Hydrogen Diesel Dual-Fuel Engine. Energy & Fuels, 23(5), 2646-2657. https://doi.org/10.1021/ef800962k

Saravanan, N., & Nagarajan, G. (2009b). An experimental investigation on manifold-injected hydrogen as a dual fuel for diesel engine system with different injection duration.

International Journal of Energy Research, 33(15), 1352-1366. https://doi.org/https://doi.org/10.1002/er.1550

Saravanan, N., & Nagarajan, G. (2010). Performance and emission studies on port injection of hydrogen with varied flow rates with Diesel as an ignition source. Applied Energy, 87(7), 2218-2229. https://doi.org/https://doi.org/10.1016/j.apenergy.2010.01.014

Saravanan, N., Nagarajan, G., Sanjay, G., Dhanasekaran, C., & Kalaiselvan, K. M. (2008). Combustion analysis on a DI diesel engine with hydrogen in dual fuel mode. Fuel, 87(17), 3591-3599. https://doi.org/https://doi.org/10.1016/j.fuel.2008.07.011

Sathishkumar, S., & Ibrahim, M. M. (2021). Investigation on the effect of injection schedule and EGR in hydrogen energy share using common rail direct injection dual fuel engine. International Journal of Hydrogen Energy, 46(20), 11494-11510. https://doi.org/https://doi.org/10.1016/j.ijhydene.2020.05.151

Schaffelhofer, F. (2022). MAN Engines: The first dual fuel hydrogen engines in use on a work boat. https://press.mantruckandbus.com/corporate/man-engines-the-first-dual-fuel-hydrogen-engines-in-use-on-a-work-boat/

Schultz, B. (2022). Volvo Penta dual-fuel hydrogen engine unveiled. https://www.dieselprogress.com/news/volvo-penta-dual-fuel-hydrogen-engine-unveiled/8024315.article

Seddiek, I. S., Elgohary, M. M., Ammar, N. R. (2015). The hydrogen-fuelled internal combustion engines for marine applications with a case study. Brodogradnja/Shipbuilding 66, 23-38

Shin, B., Cho, Y., Han, D., Song, S., & Chun, K. M. (2011). Hydrogen effects on NOx emissions and brake thermal efficiency in a diesel engine under low-temperature and heavy-EGR conditions. International Journal of Hydrogen Energy, 36(10), 6281-6291.

Shioji, M., Ikegami, M., Zhu, Q., & Sato, K. (1995). A study of a low-NOx naturalgas engine. IPC-8, 9530599, 345-350.

SinghYadav, V., Soni, S., & Sharma, D. (2012). Performance and emission studies of direct injection CI engine in duel fuel mode (hydrogen-diesel) with EGR. International Journal of Hydrogen Energy, 37(4), 3807-3817.

Suzuki, Y., & Tsujimura, T. (2015). The combustion improvements of hydrogen/diesel dual fuel engine (0148-7191).

Suzuki, Y., Tsujimura, T., & Mita, T. (2015). The performance of multi-cylinder hydrogen/diesel dual fuel engine. SAE International Journal of Engines, 8(5), 2240-2252.

Talibi, M., Hellier, P., Balachandran, R., & Ladommatos, N. (2014). Effect of hydrogen-diesel fuel co-combustion on exhaust emissions with verification using an in–cylinder gas sampling technique. International Journal of Hydrogen Energy, 39(27), 15088-15102. https://doi.org/https://doi.org/10.1016/j.ijhydene.2014.07.039

Talibi, M., Hellier, P., & Ladommatos, N. (2017). The effect of varying EGR and intake air boost on hydrogen-diesel co-combustion in CI engines. International Journal of Hydrogen Energy, 42(9), 6369-6383. https://doi.org/https://doi.org/10.1016/j.ijhydene.2016.11.207

Tomita, E., Kawahara, N., Piao, Z., Fujita, S., & Hamamoto, Y. (2001). Hydrogen combustion and exhaust emissions ignited with diesel oil in a dual fuel engine. SAE Technical Papers.

Tsujimura, T., & Suzuki, Y. (2017). The utilization of hydrogen in hydrogen/diesel dual fuel engine. International Journal of Hydrogen Energy, 42(19), 14019-14029.

Vavra J, Bortel I, and Takats M (2019). A Dual Fuel Hydrogen - Diesel Compression Ignition Engine and Its Potential Application in Road Transport. SAE Technical Paper 2019-01-0564

Varde, K., & Frame, G. (1983). Hydrogen aspiration in a direct injection type diesel engine-its effects on smoke and other engine performance parameters. International Journal of Hydrogen Energy, 8(7), 549-555.

Warwick, N., Griffiths, P., Keeble, J., Archibald, A., Pyle, J., NCAS, U. o. C. a., & Shine, K. (2022). Atmospheric implications of increased hydrogen use. Retrieved from https://www.gov.uk/government/publications/atmospheric-implications-of-increased-hydrogen-use

Wu, H.-W., & Wu, Z.-Y. (2012). Investigation on combustion characteristics and emissions of diesel/hydrogen mixtures by using energy-share method in a diesel engine. Applied Thermal Engineering, 42, 154-162.

Zan, N., Ding, H., Guo, X., Tang, Z., & Bleck, W. (2015). Effects of grain size on hydrogen embrittlement in a Fe-22Mn-0.6C TWIP steel. International Journal of Hydrogen Energy, 40(33), 10687-10696. https://doi.org/https://doi.org/10.1016/j.ijhydene.2015.06.112

Zarich, K. (2022, May 09, 2022). CUMMINS INC. DEBUTS 15-LITER HYDROGEN ENGINE AT ACT EXPO https://www.cummins.com/news/releases/2022/05/09/cummins-inc-debuts-15-liter-hydrogen-engine-act-expo

Zhou, J. H., Cheung, C. S., & Leung, C. W. (2014). Combustion, performance, regulated and unregulated emissions of a diesel engine with hydrogen addition. Applied Energy, 126, 1-12. https://doi.org/https://doi.org/10.1016/j.apenergy.2014.03.089

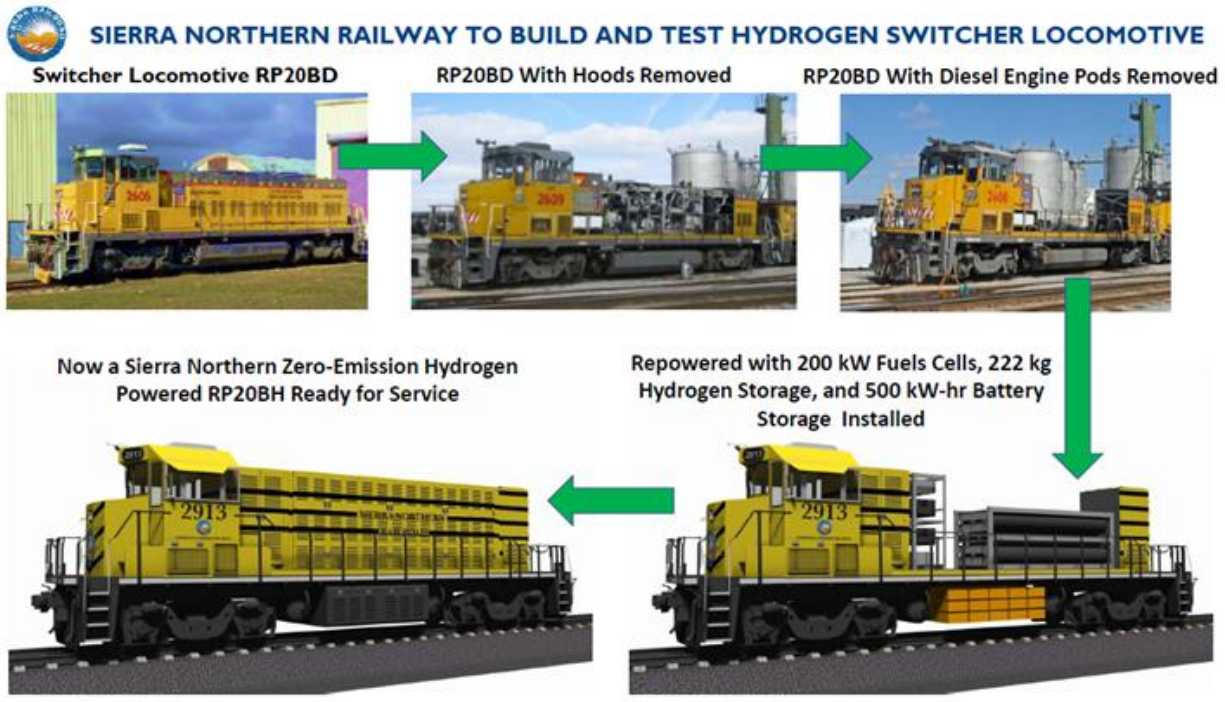

Figure 1: US locomotive fleet will switch over to diesel-killing hydrogen fuel cells and other non-diesel technologies (image courtesy of Sierra Northern Railway).

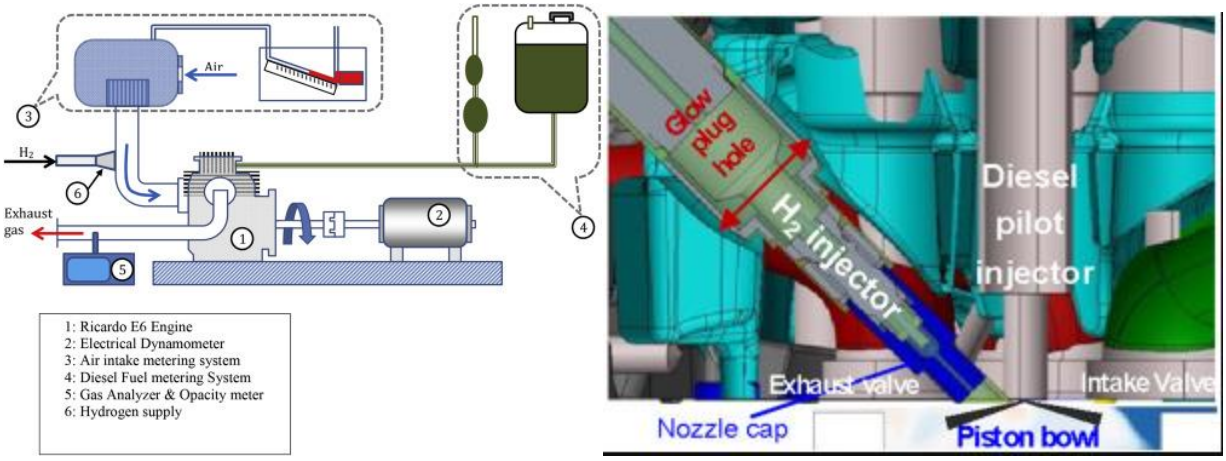

Figure 2: Indirect injection on left, direct injection on right.

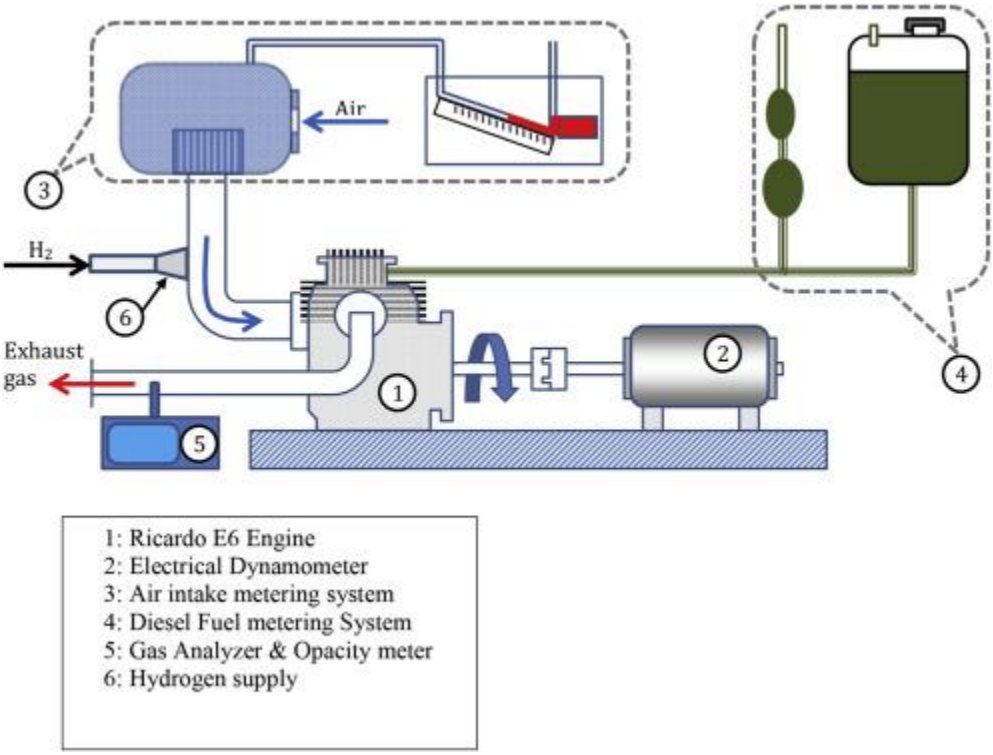

Figure 3: Schematic view of the engine test bed.

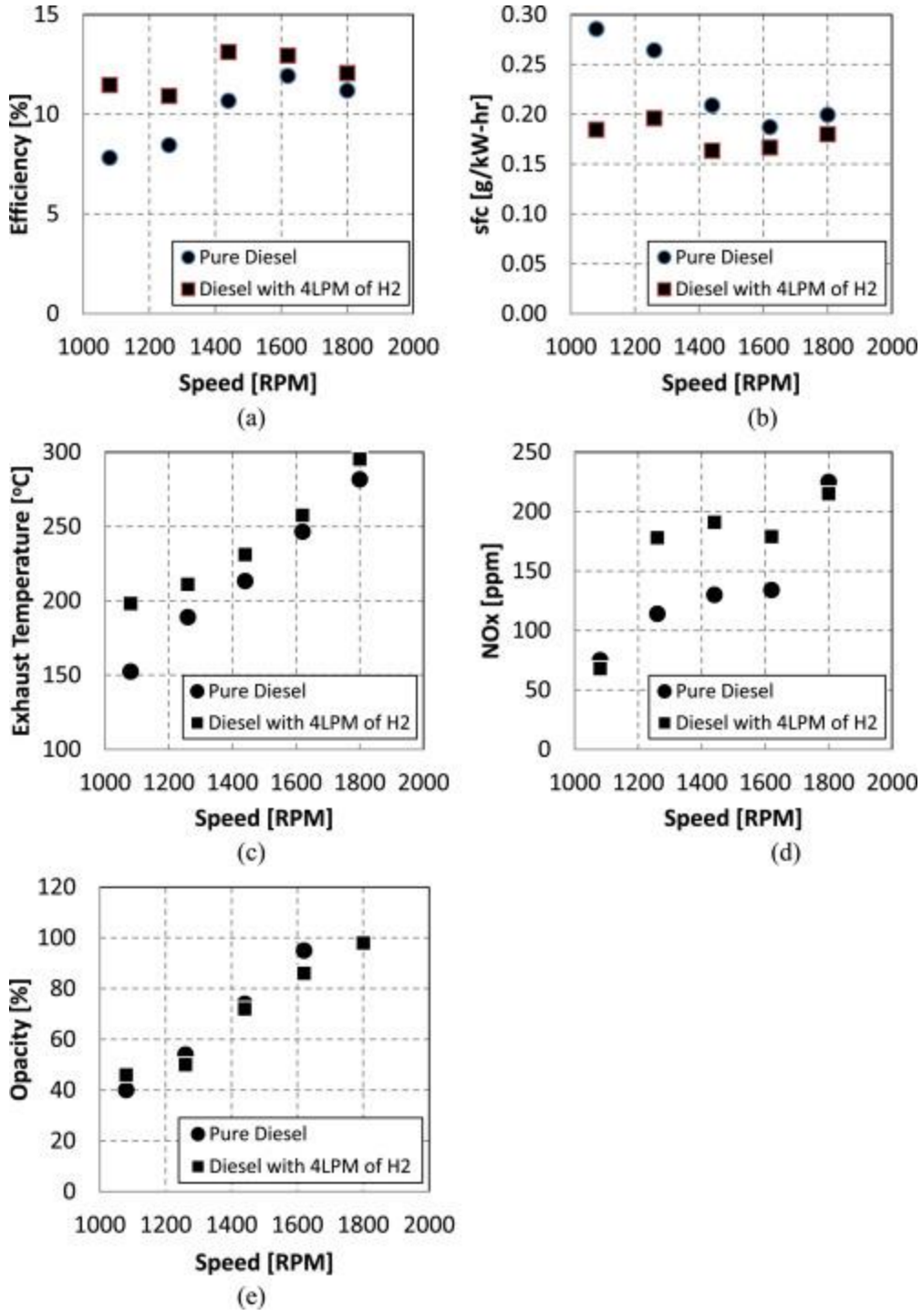

Figure 4: The effect of engine speed with the presence of 4 LPM of hydrogen supplement, where diesel is injected at 35° btdc.

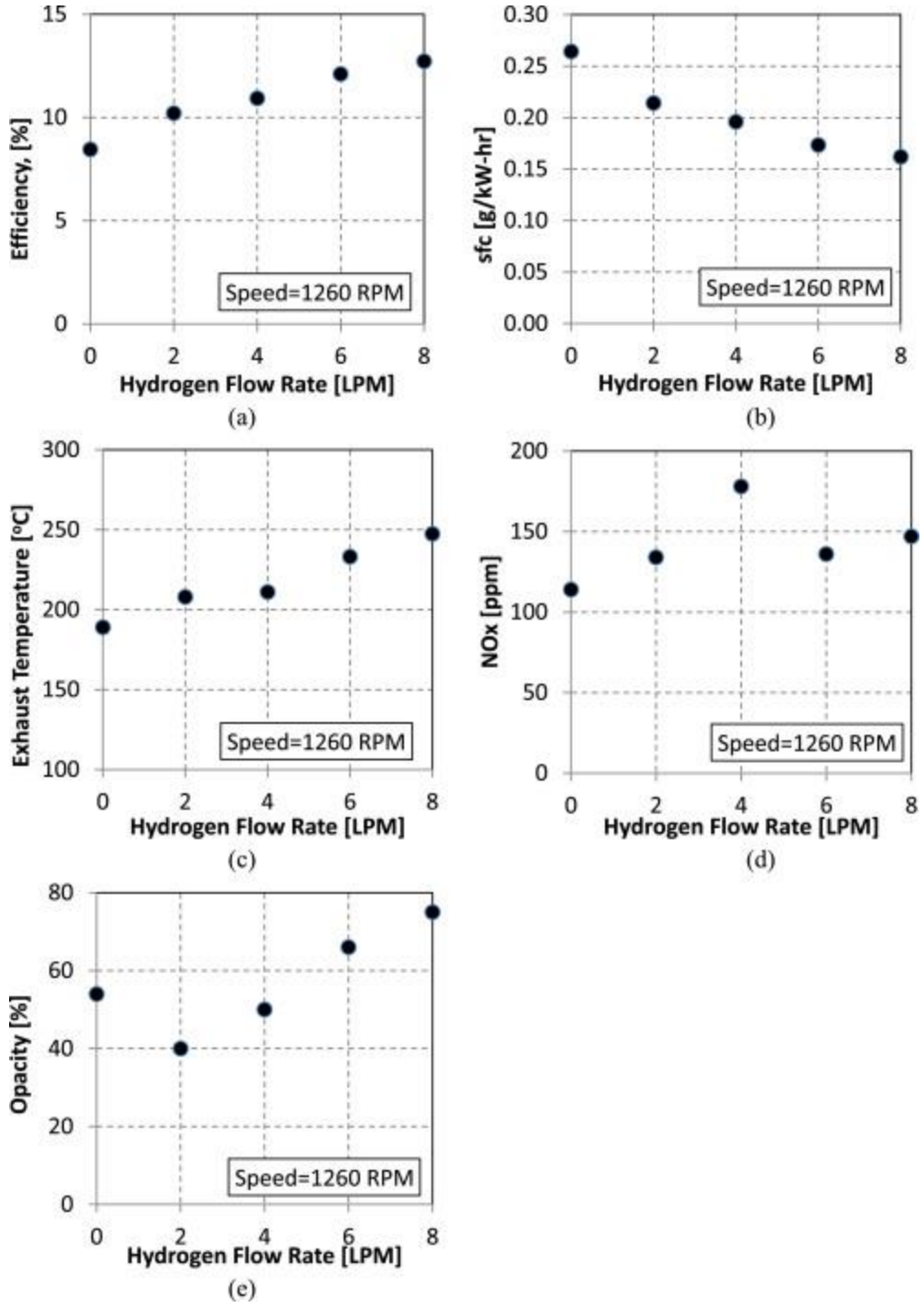

Figure 5: The effect of hydrogen supplement flow rate fixed engine speed of 1260 RPM, where diesel is injected at 35° from btdc.

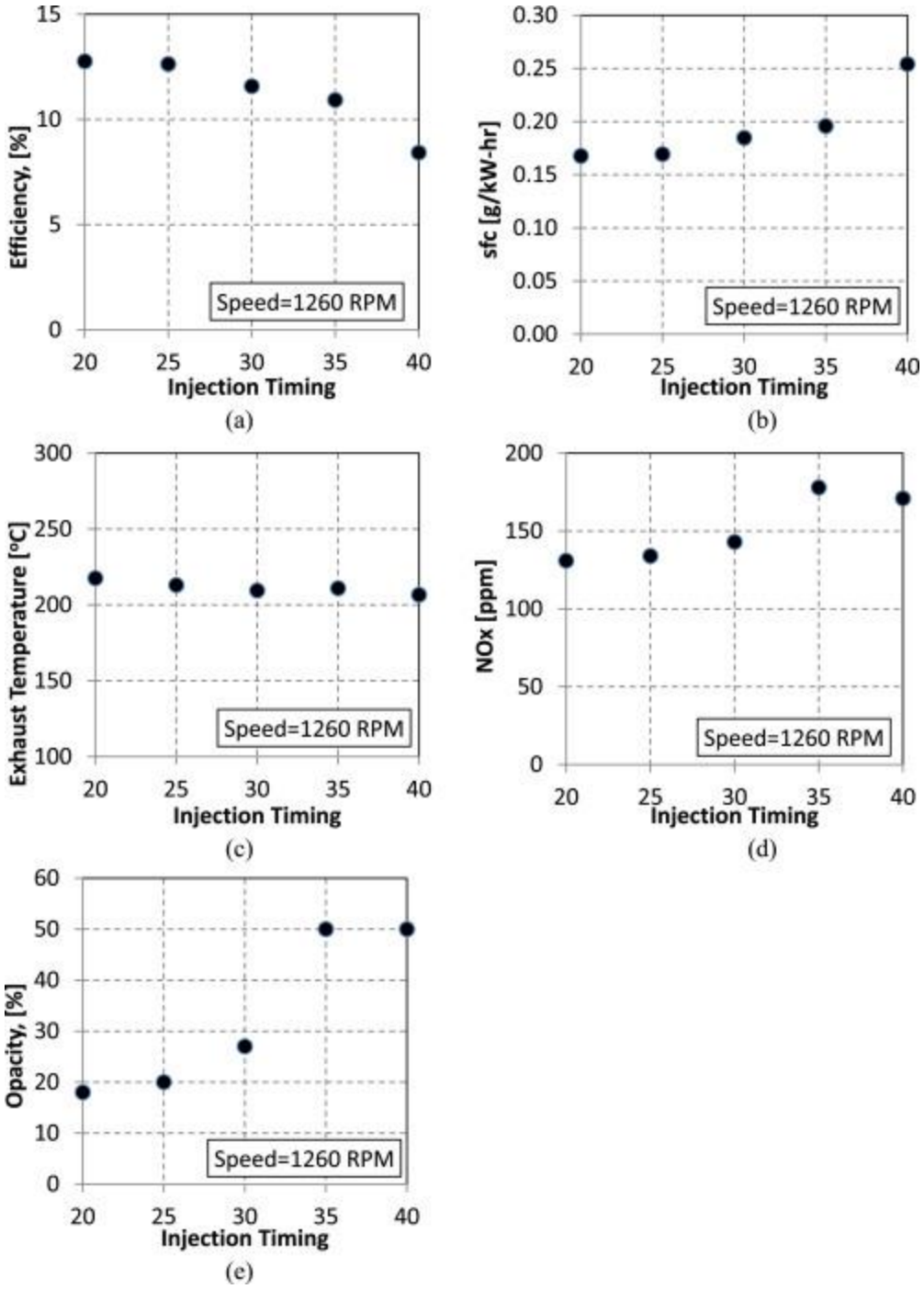

Figure 6: The early diesel injection timing with the presence of 4 LPM of hydrogen supplement.

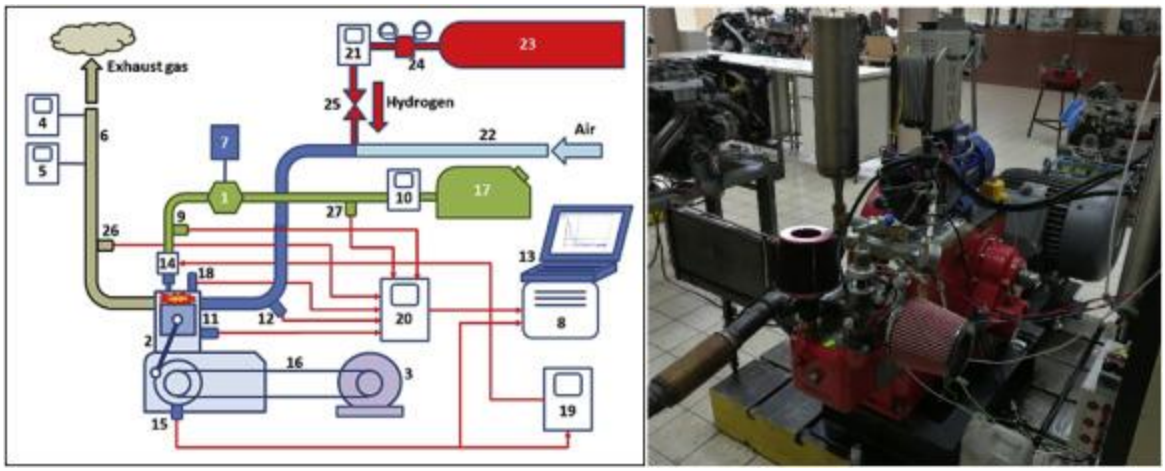

Figure 7: Test bed

Legend: 1 – DF pump, 2 – CI engine, 3 – Generator, 4 – Smoke analyzer, 5 – Exhaust gas emission analyzer, 6 – Exhaust pipe, 7 – electric motor, 8 – Data acquisition system, 9 – DF pressure sensor, 10 – DF flow meter, 11 – Engine temperature sensor, 12 – Inlet air temp. sensor, 13 – PC with SAWIR software, 14 – DF common rail injector, 15 – Crank angle encoder, 16 – Drive belt, 17 – DF tank, 18 – In-cylinder pressure sensor, 19 – DF injection controller, 20 – Amplifiers & A/D converters, 21 – Hydrogen flow meter, 22 – Air intake pipe, 23 – Hydrogen high-pressure tank, 24 – Hydrogen one-stage pressure controller, 25 – Hydrogen firebreak arrestor, 26 – Exhaust gas temperature sensor, 27 - DF temperature sensor.

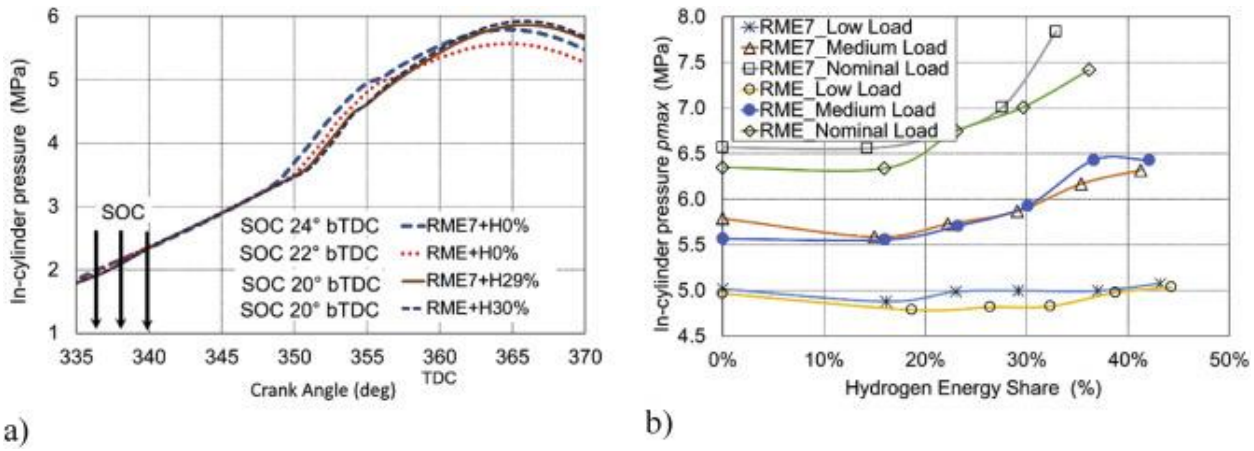

Figure 8: In-cylinder pressure at Medium Load b) In-cylinder maximum pressure pmax vs. HES.

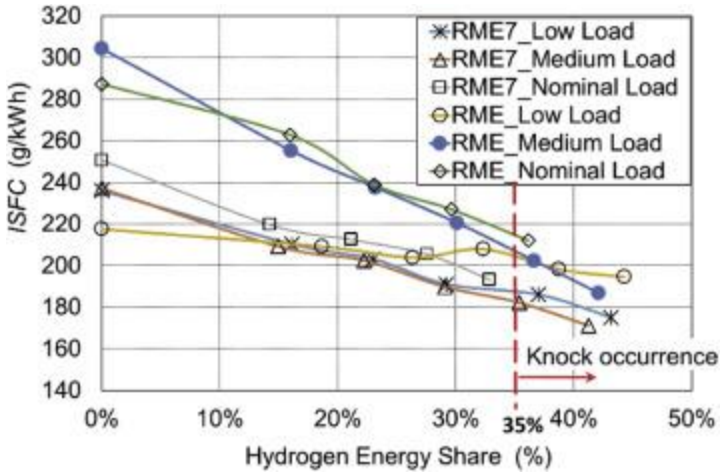

Figure 9: ISFC at various engine loads against HES.

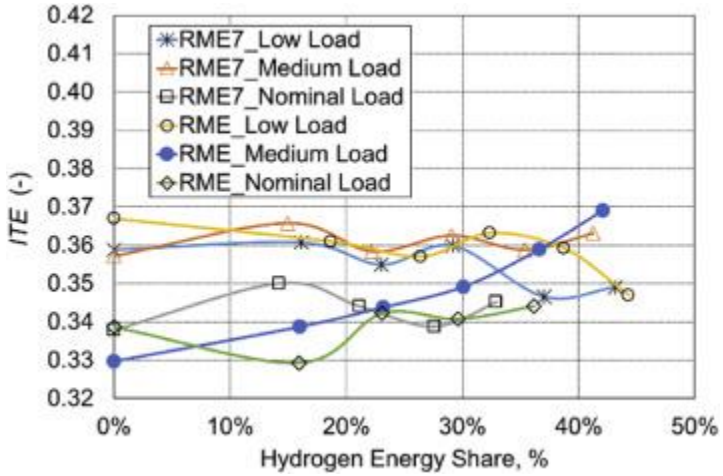

Figure 10: ITE vs. HES at various engine loads.

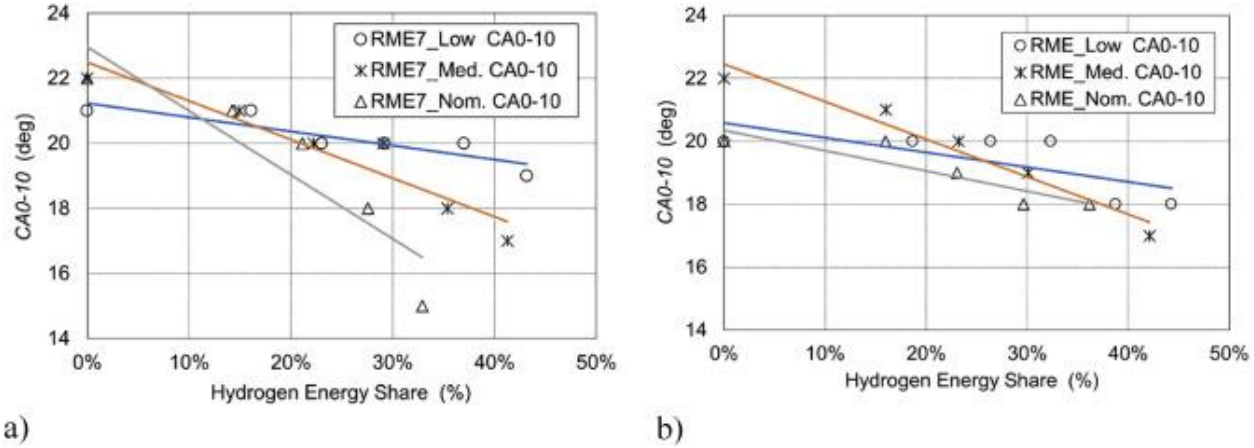

Figure 11: The combustion phase CA0-10 vs. HES for a) RME7 and b) RME.

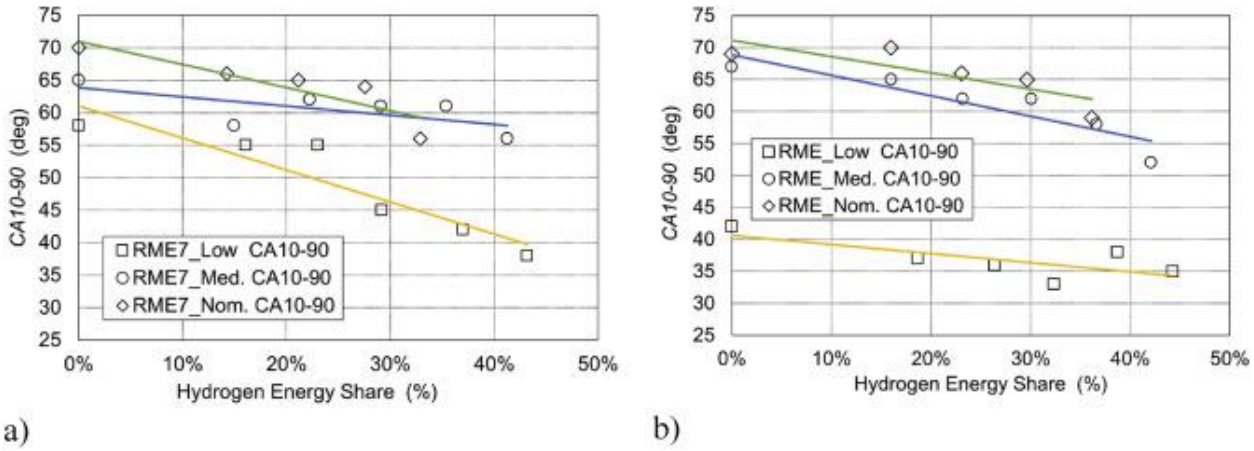

Figure 12: The main combustion phase CA10-90 vs. HES for a) RME7 and b) RME.

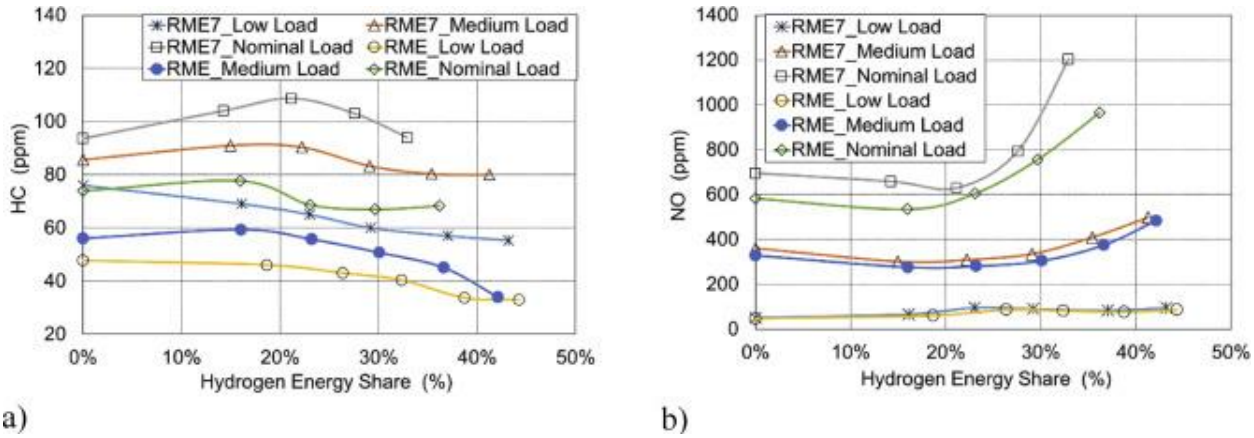

Figure 13: a) HC and b) NO against HES at various engine loads.

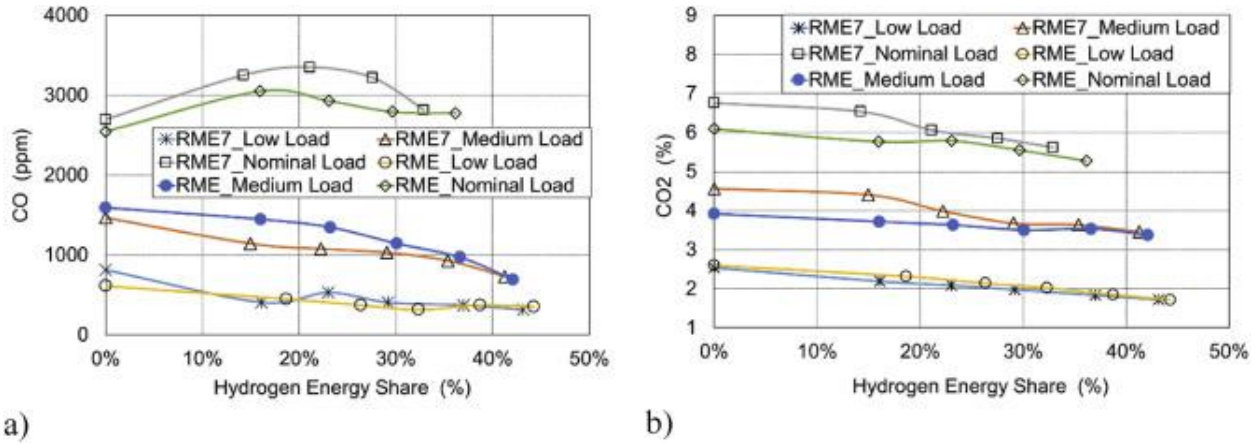

Figure 14: a) CO b) CO2 vs. HES at various engine loads.

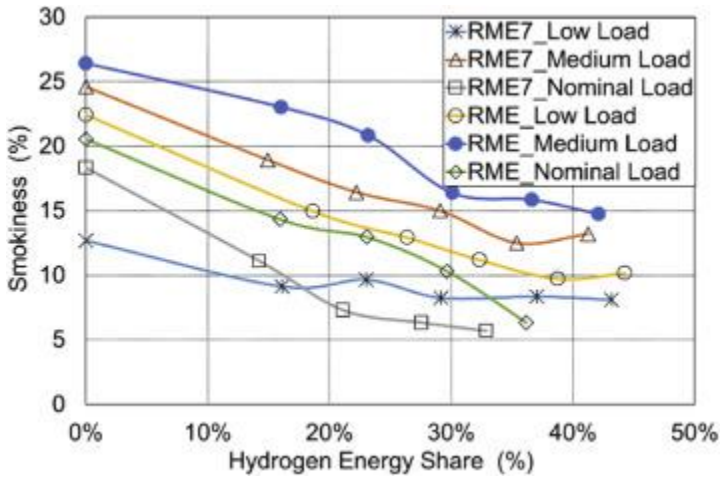

Figure 15: The smokiness vs. HES at various engine loads.

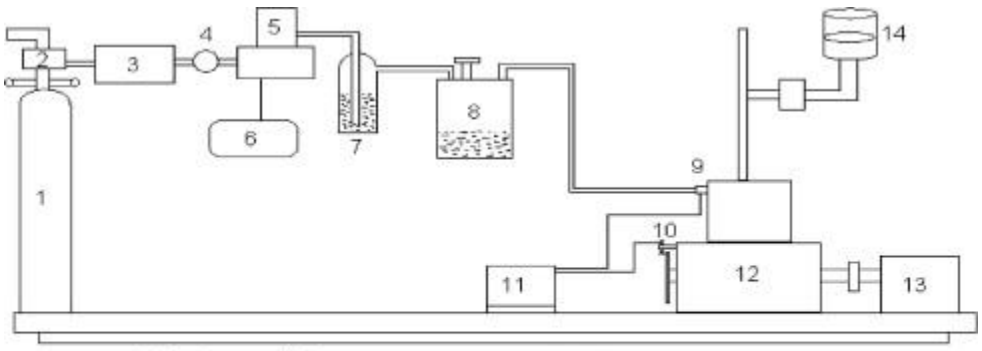

Figure 16: Schematic layout of the experimental set up.

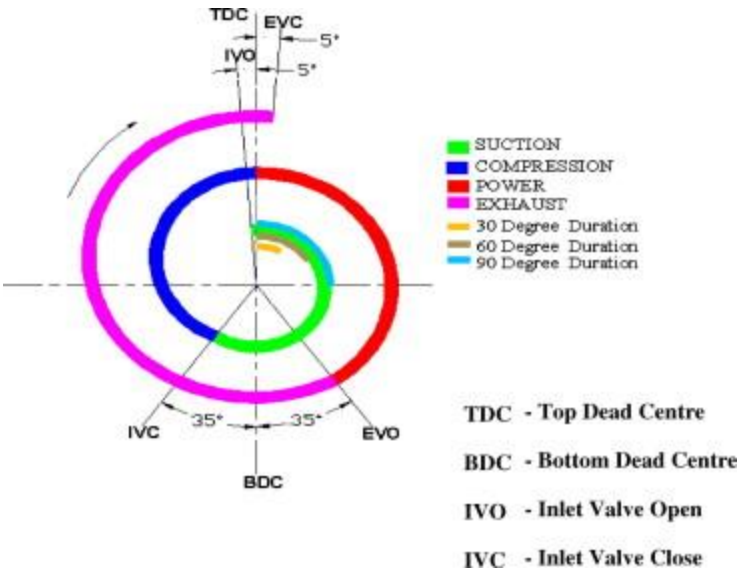

Figure 17: Valve timing diagram of single cylinder Diesel engine for different hydrogen injection timings.

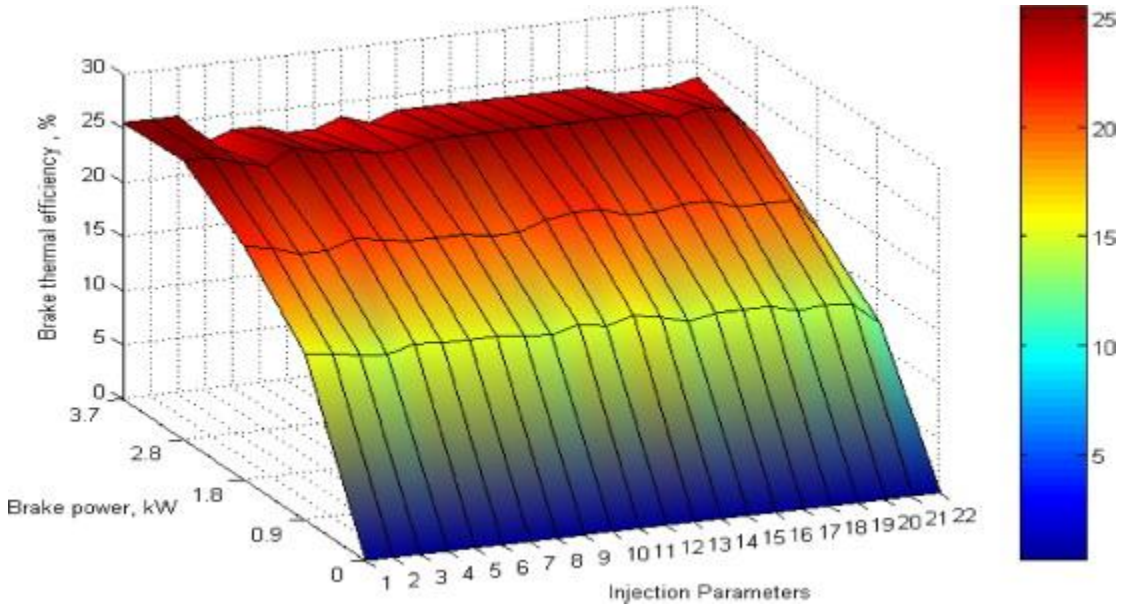

Figure 18: Variation of brake thermal efficiency with brake power for different injection timings and duration.

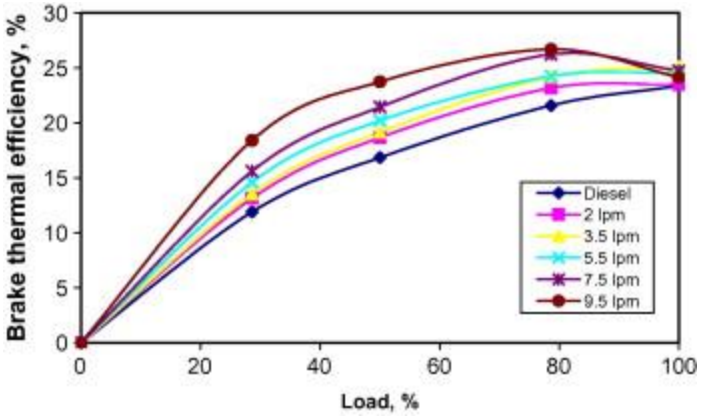

Figure 19: Variation of brake thermal efficiency with load for different hydrogen flow rates in port injection.

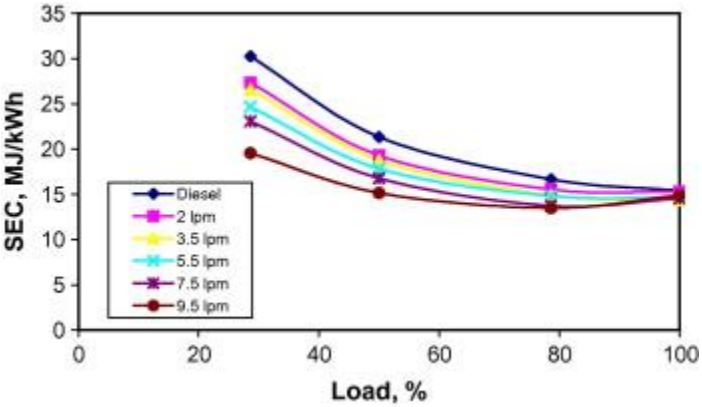

Figure 20: Variation of specific energy consumption with load for different hydrogen flow rates in port injection.

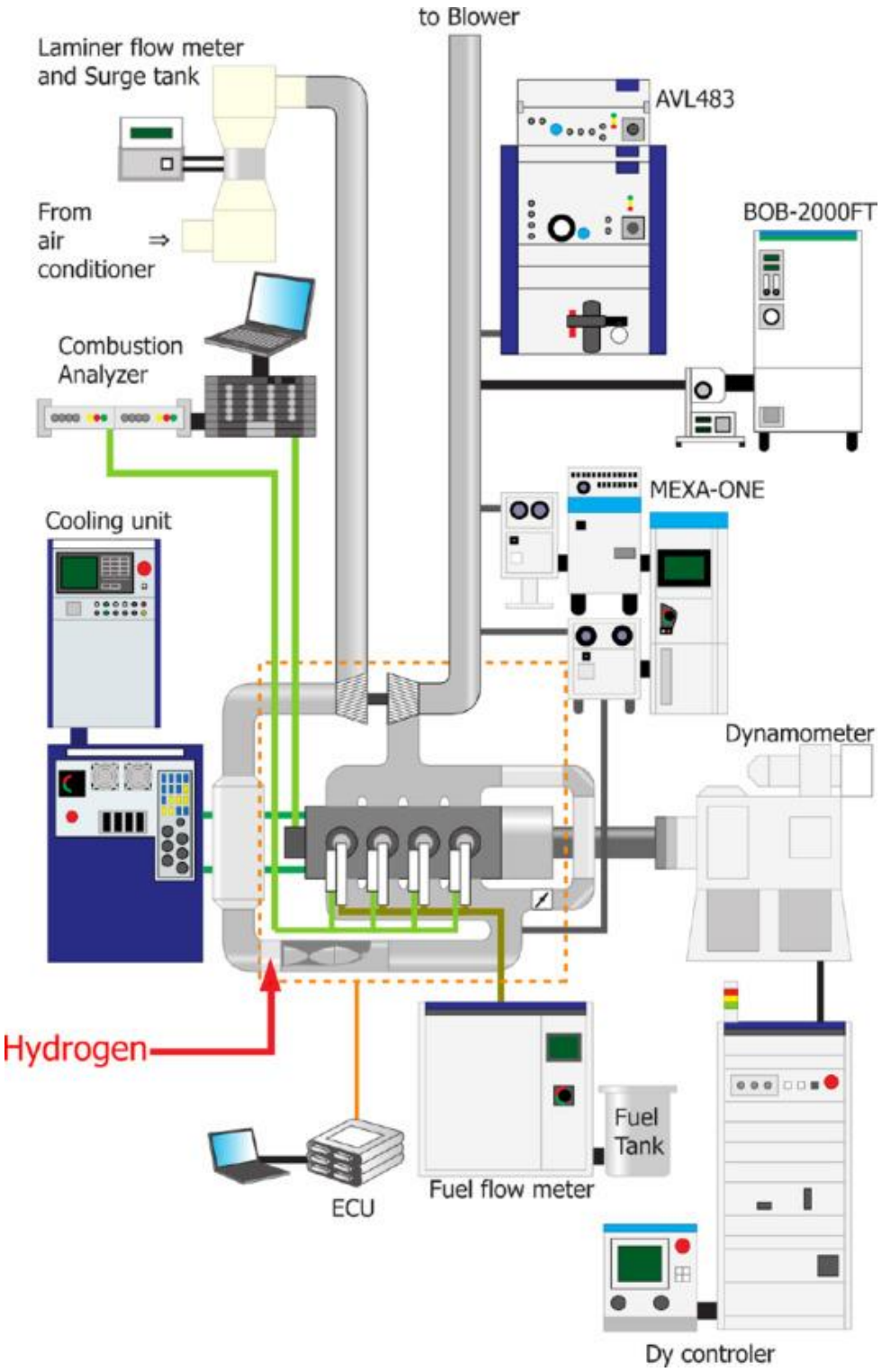

Figure 21: Overview of the experimental apparatus.

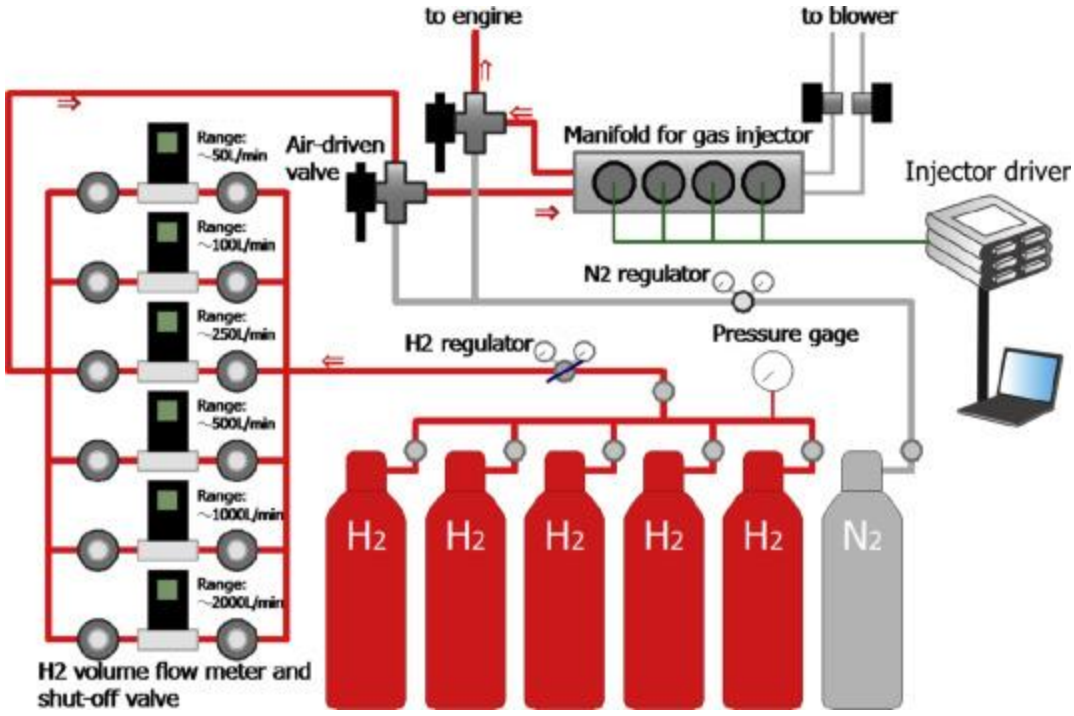

Figure 22: Overview of the hydrogen supply system.

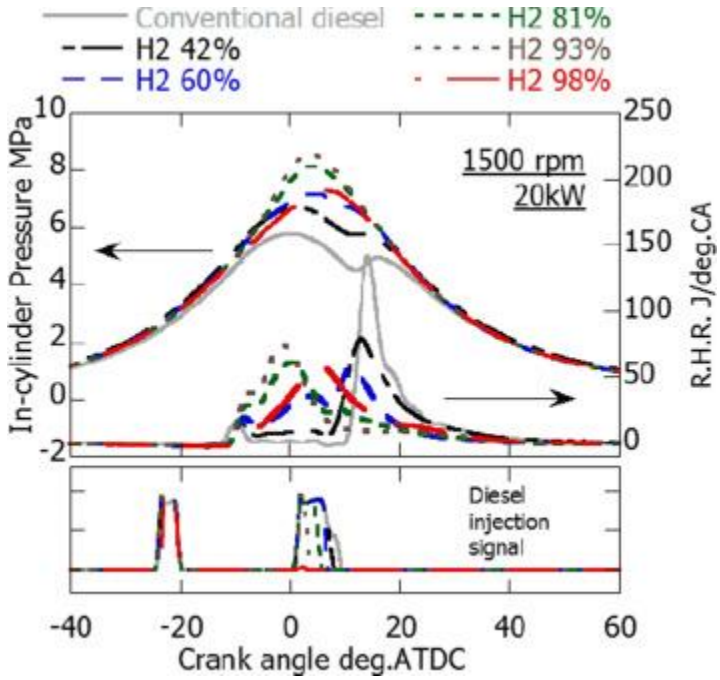

Figure 23: In-cylinder pressure and heat release fate for different H2 energy share ratios, 20 kW.

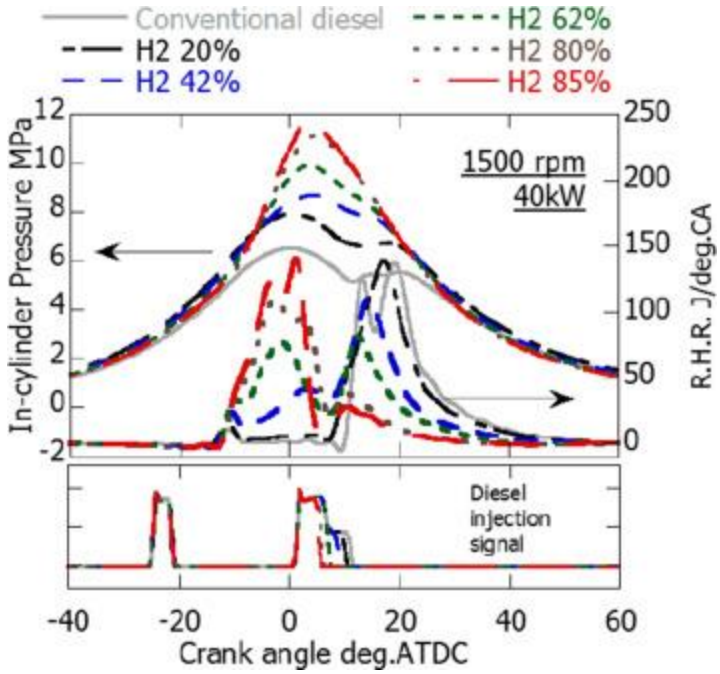

Figure 24: In-cylinder pressure and heat release fate for different H2 energy share ratios, 40 kW.

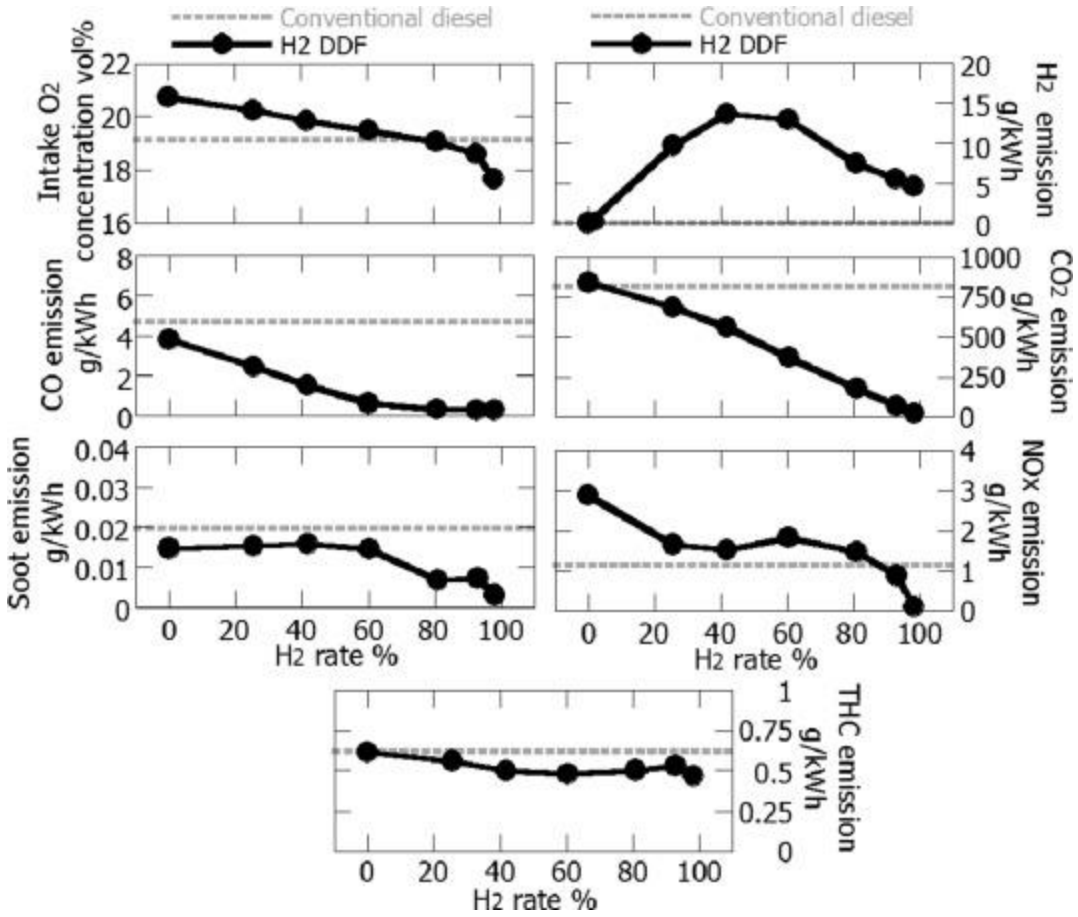

Figure 25: Engine-out emissions for different H2 energy share ratios, 20 kW.

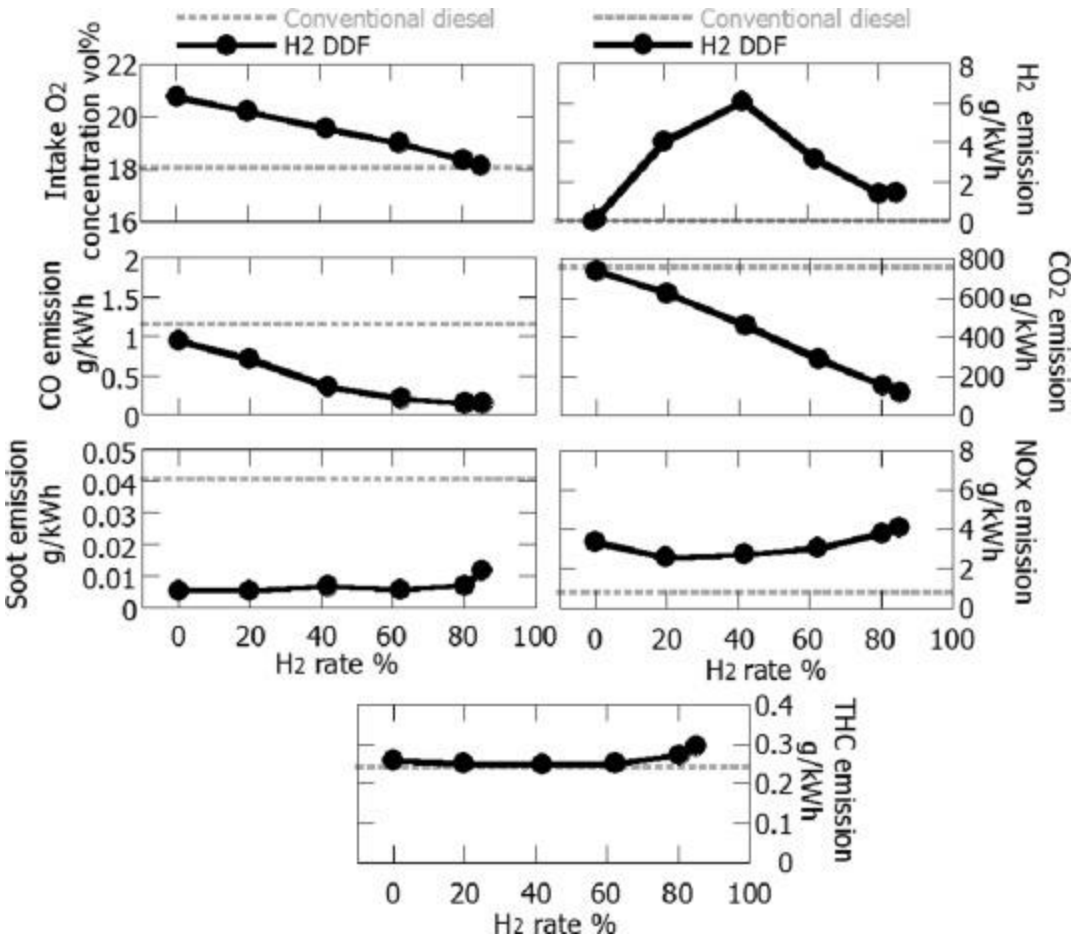

Figure 26: Engine-out emissions for different H2 energy share ratios, 40 kW.

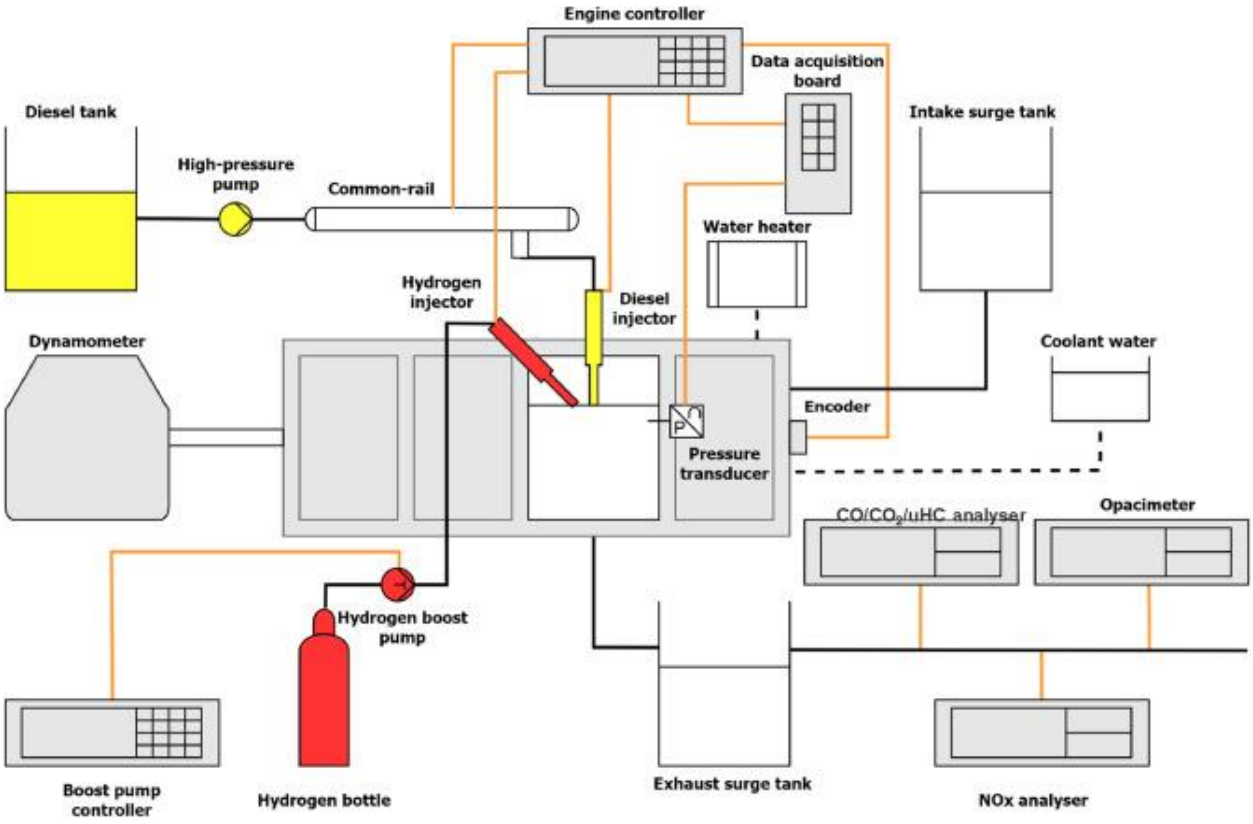

Figure 27: Schematic diagram of the hydrogen-diesel dual direct-injection (H2DDI) engine setup.

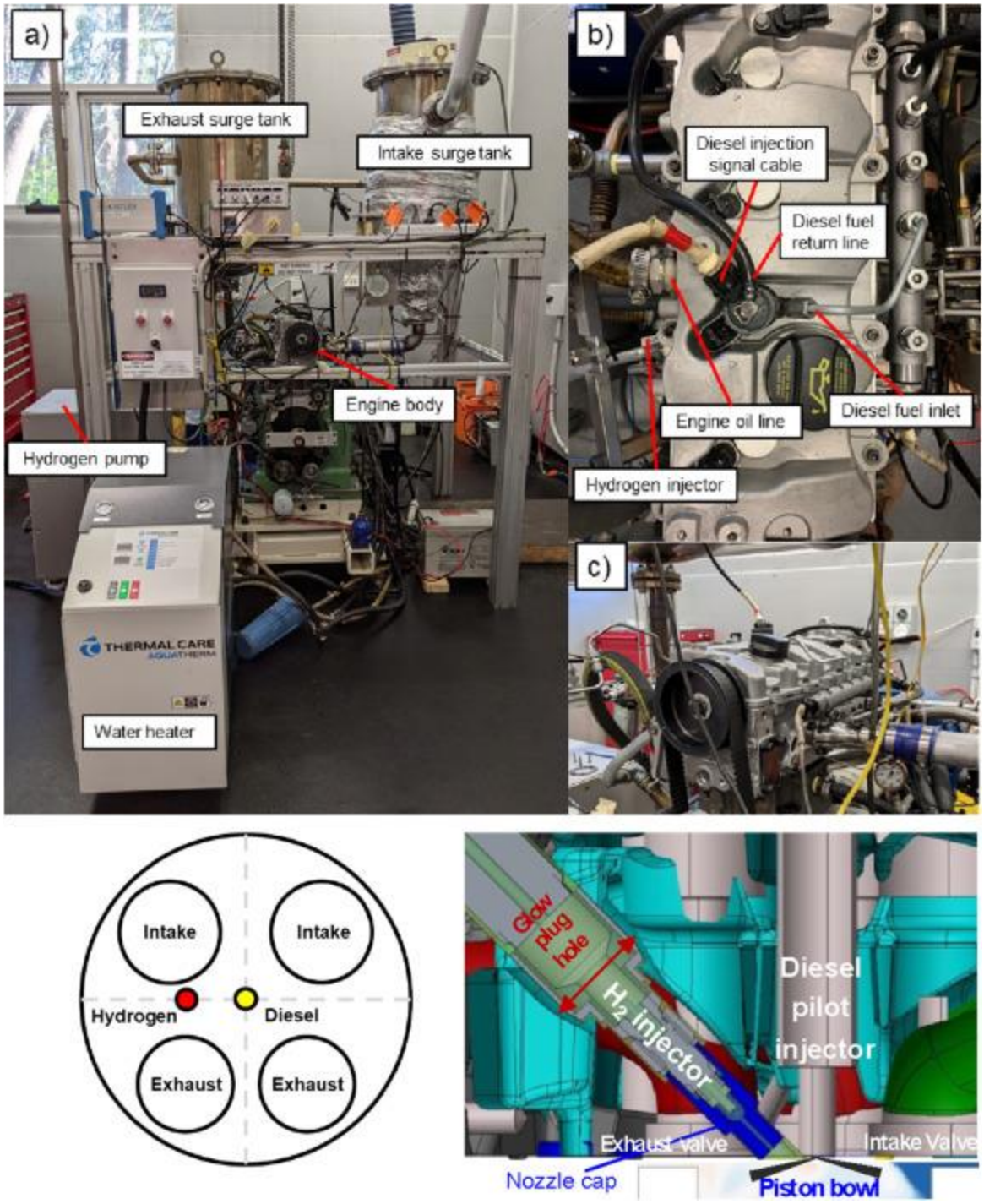

Figure 28: Photographs of the engine setup (top) and a schematic for injector arrangement (bottom).

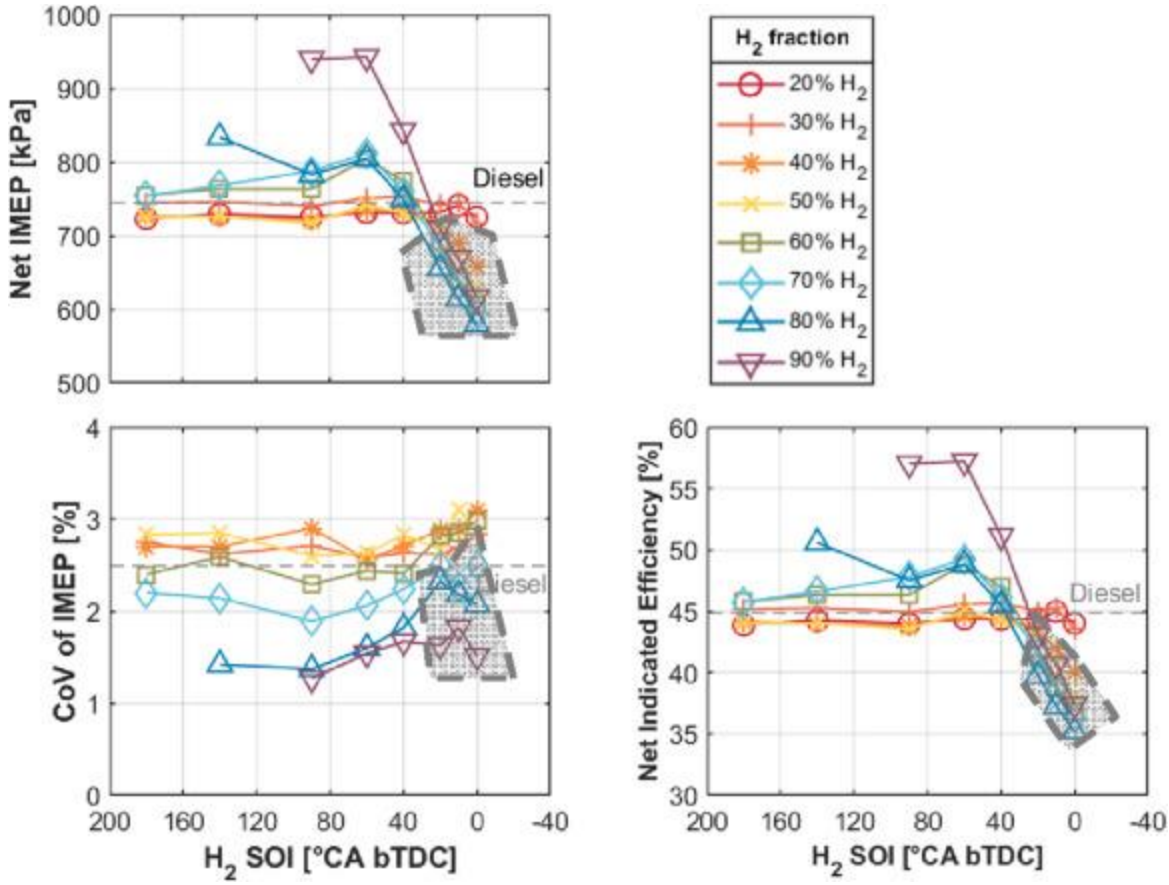

Figure 29: Effect of hydrogen energy fraction and injection timing on indicated mean effective pressure (IMEP), coefficient of variation of IMEP, and indicated efficiency.

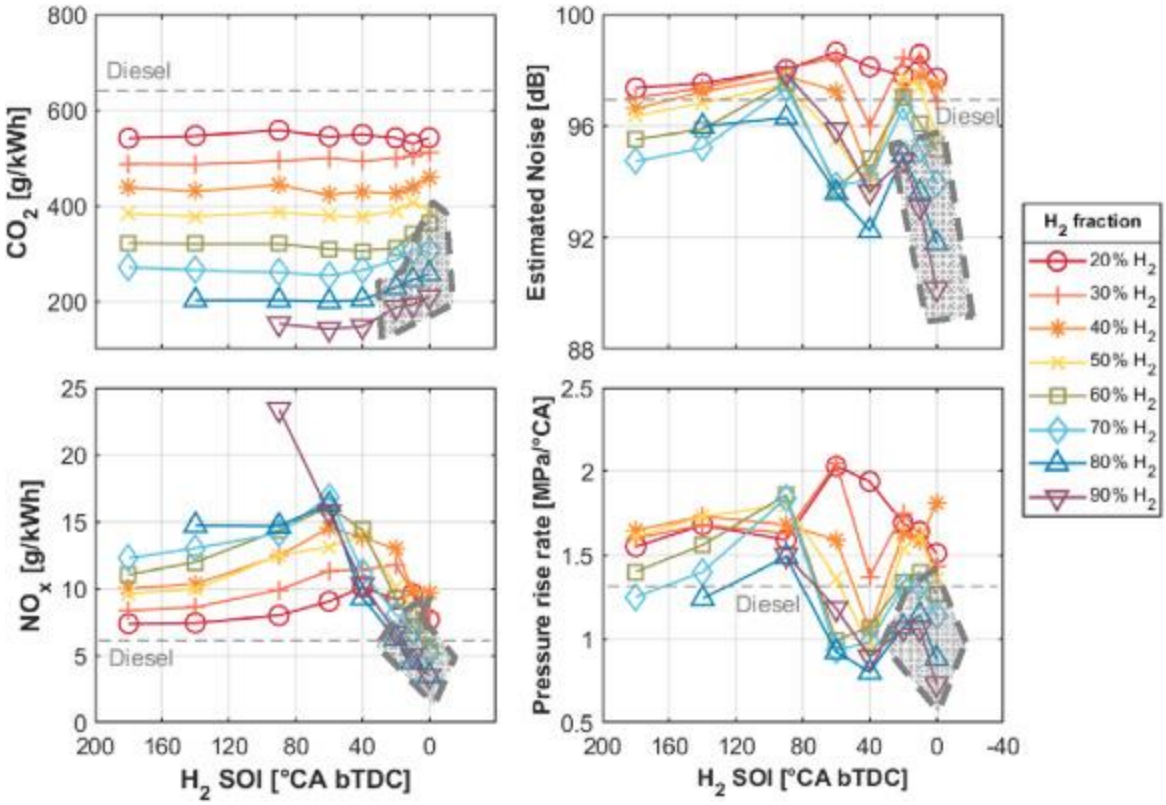

Figure 30: Engine-out emissions of carbon dioxide (CO2), nitrogen oxides (NOx), estimated combustion-induced noise as well as peak pressure rise rate (PRR) for a variation of hydrogen energy fraction and hydrogen injection timing.

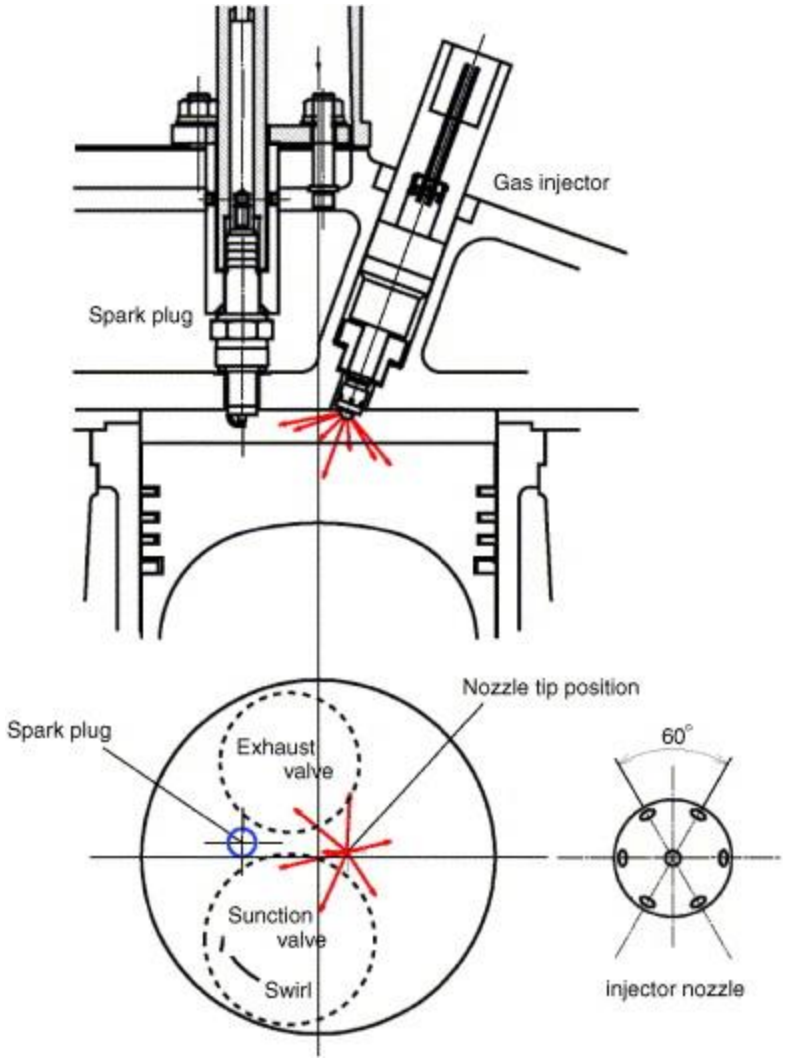

Figure 31: Combustion chamber geometry and gas jet arrangement.

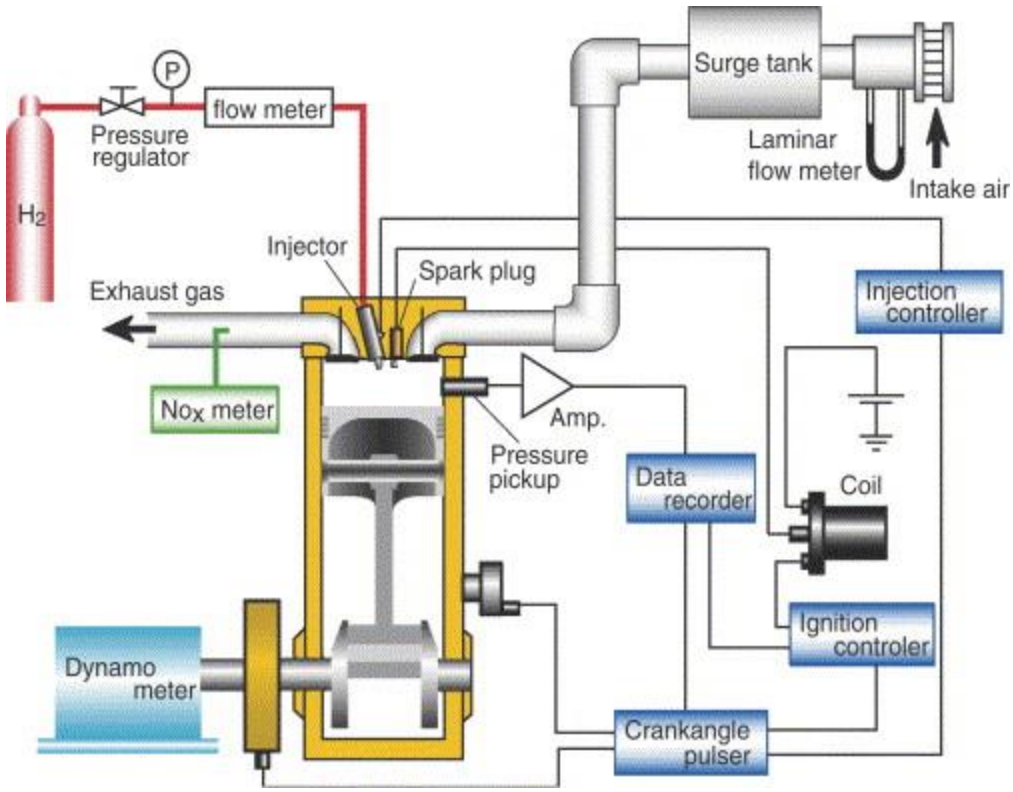

Figure 32: Experimental setup.

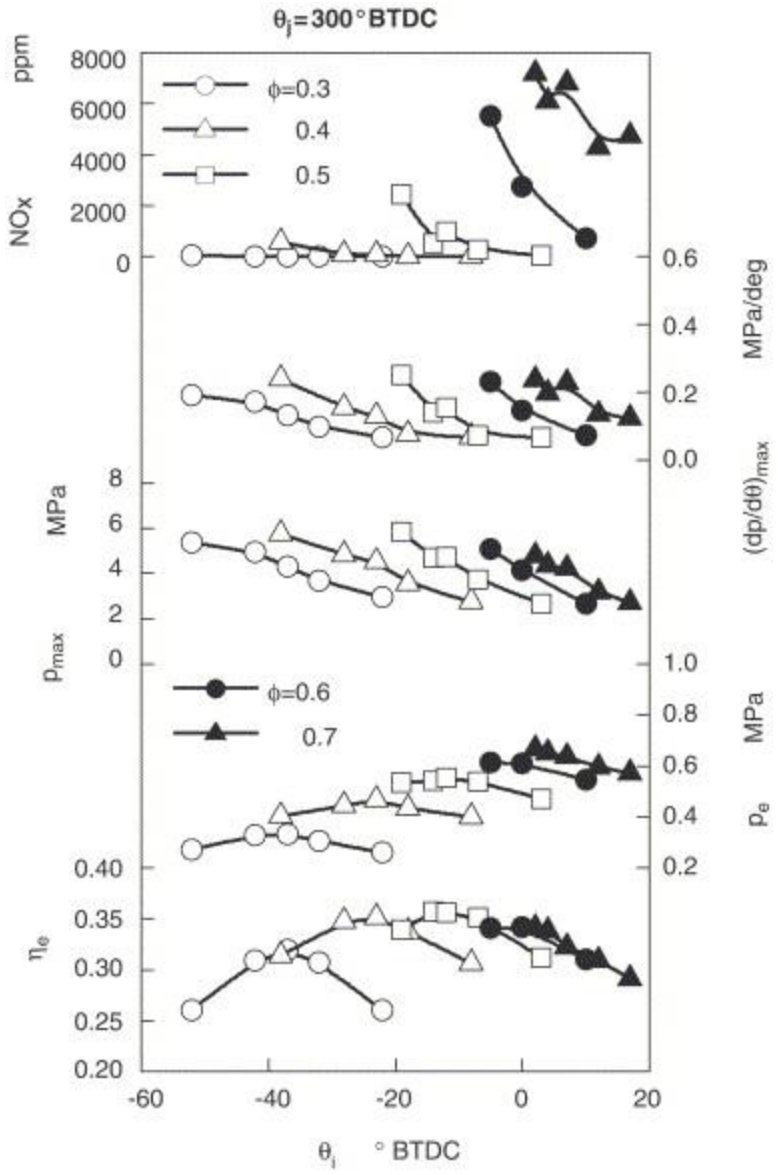

Figure 33: Hydrogen injection during intake stroke.

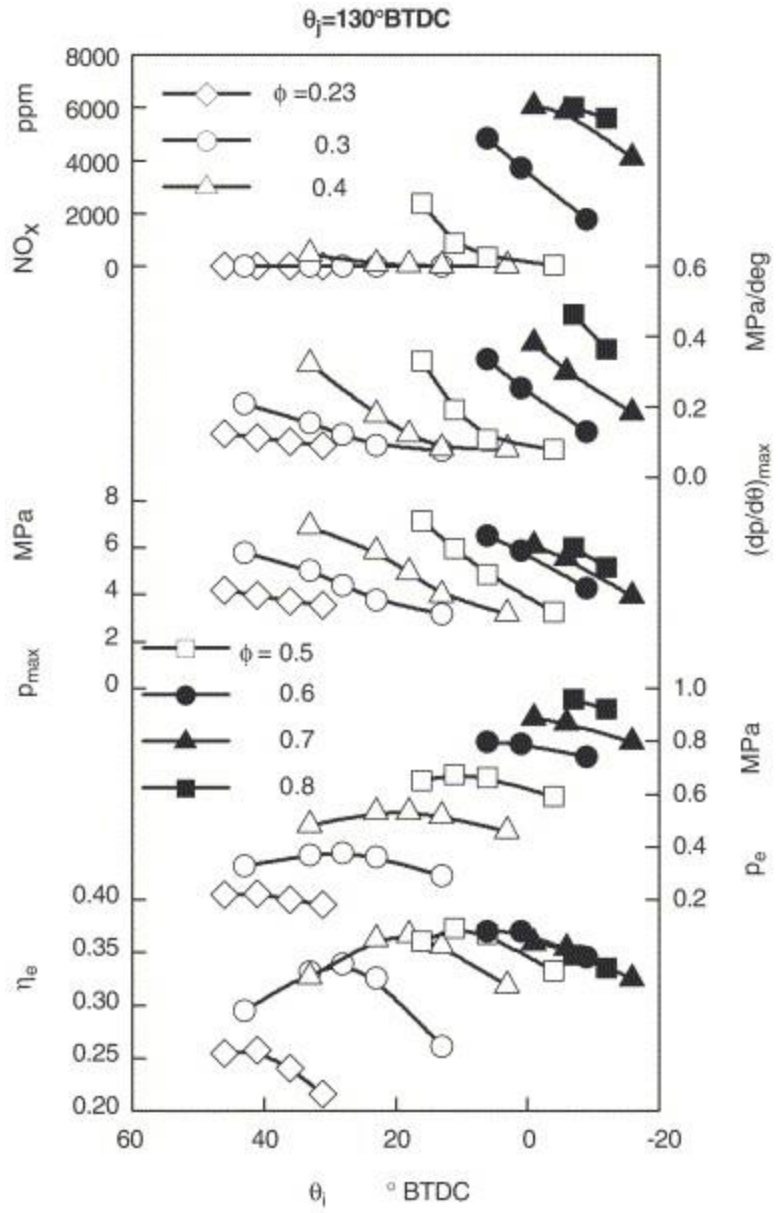

Figure 34: Hydrogen injection during compression stroke.

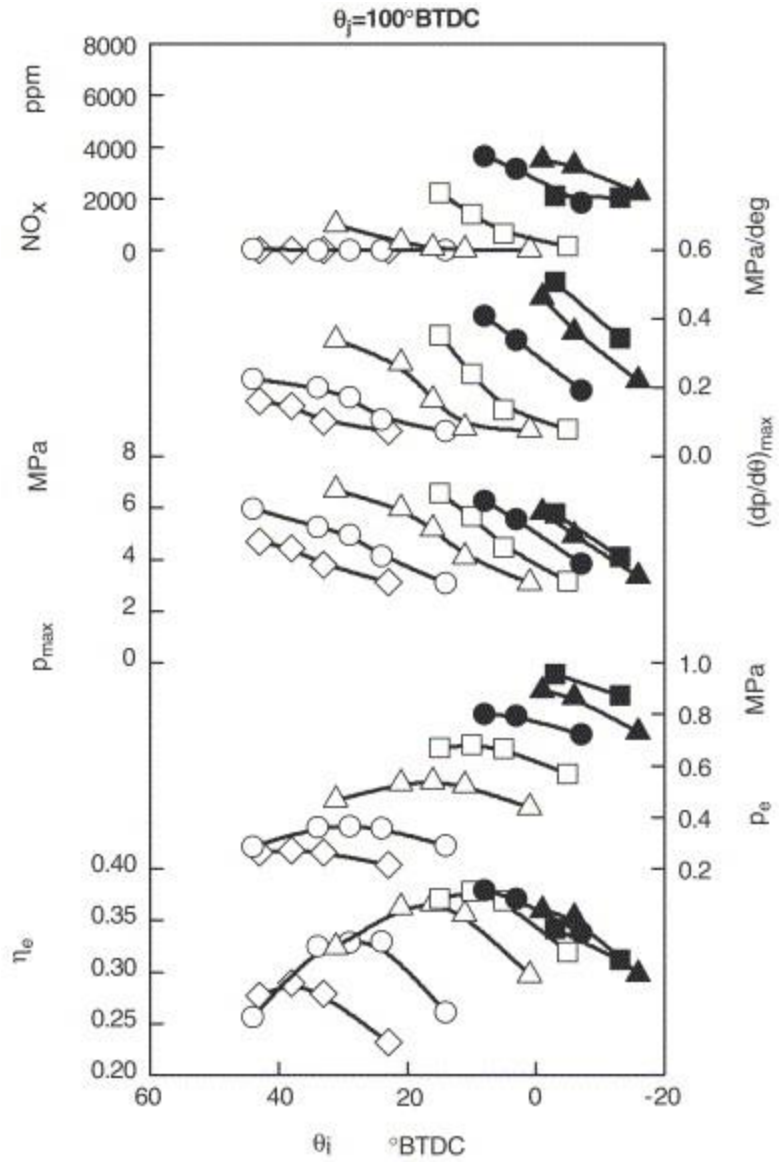

Figure 35: Hydrogen injection during compression stroke.

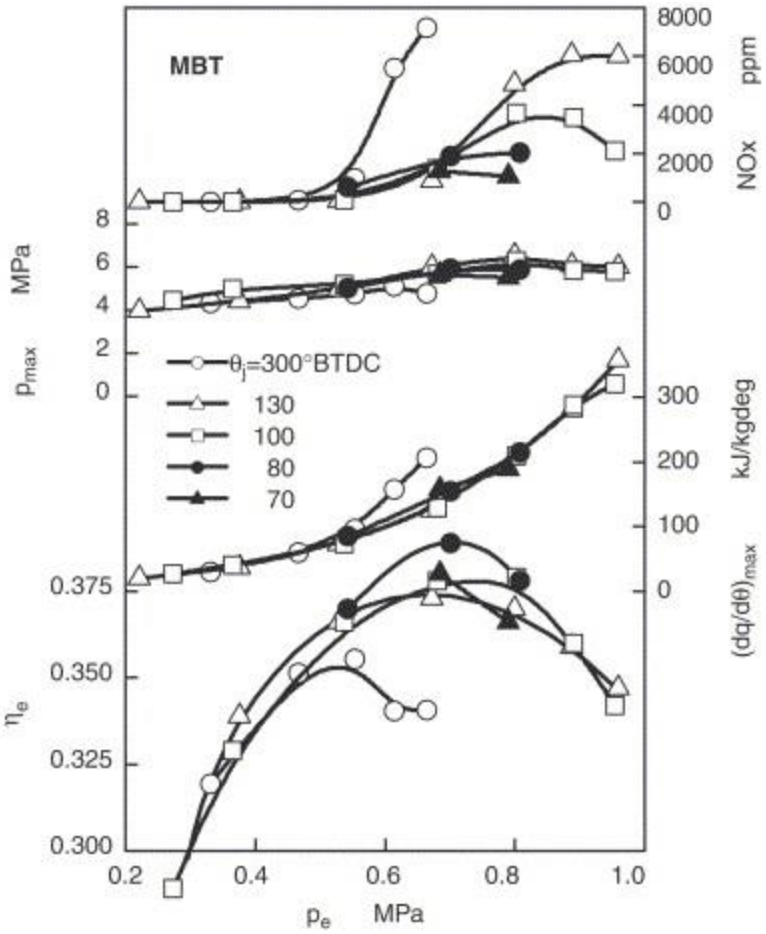

Figure 36: Optimization of injection timing under various equivalence ratios.

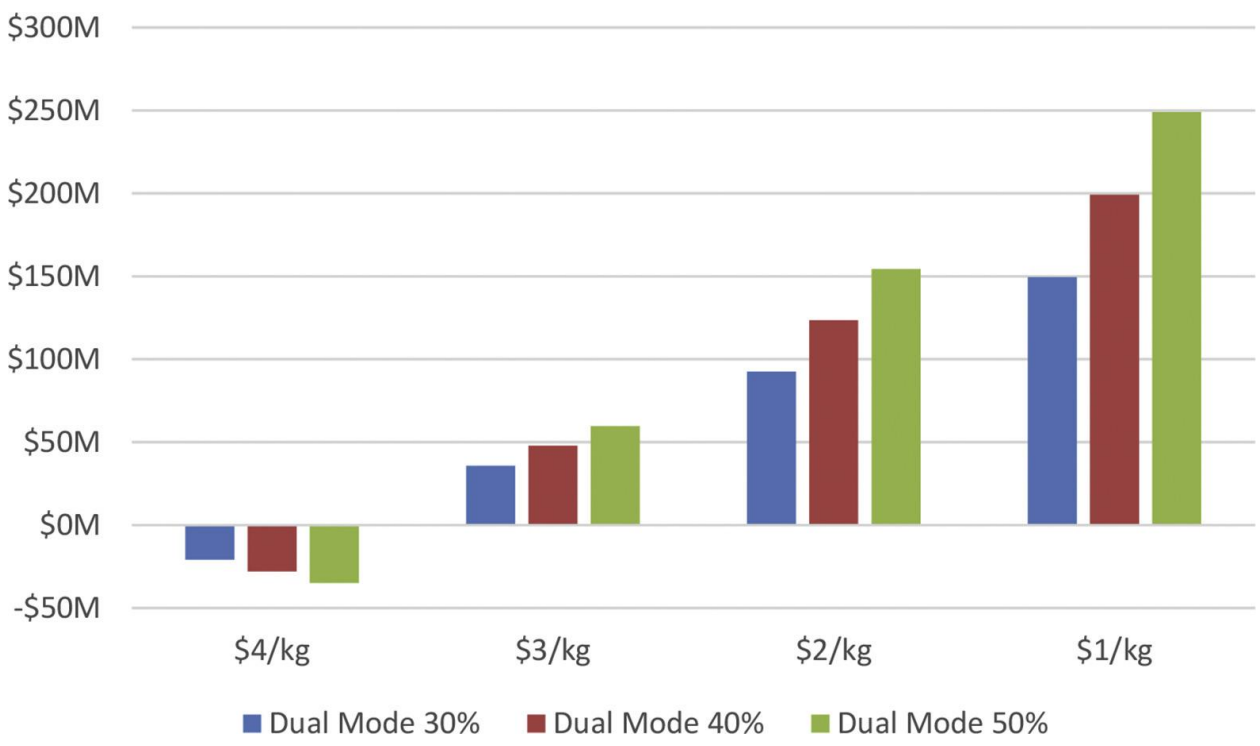

Figure 37: Savings in total cost when using dual-fuel mode for different displacement ratios and prices of waste hydrogen.

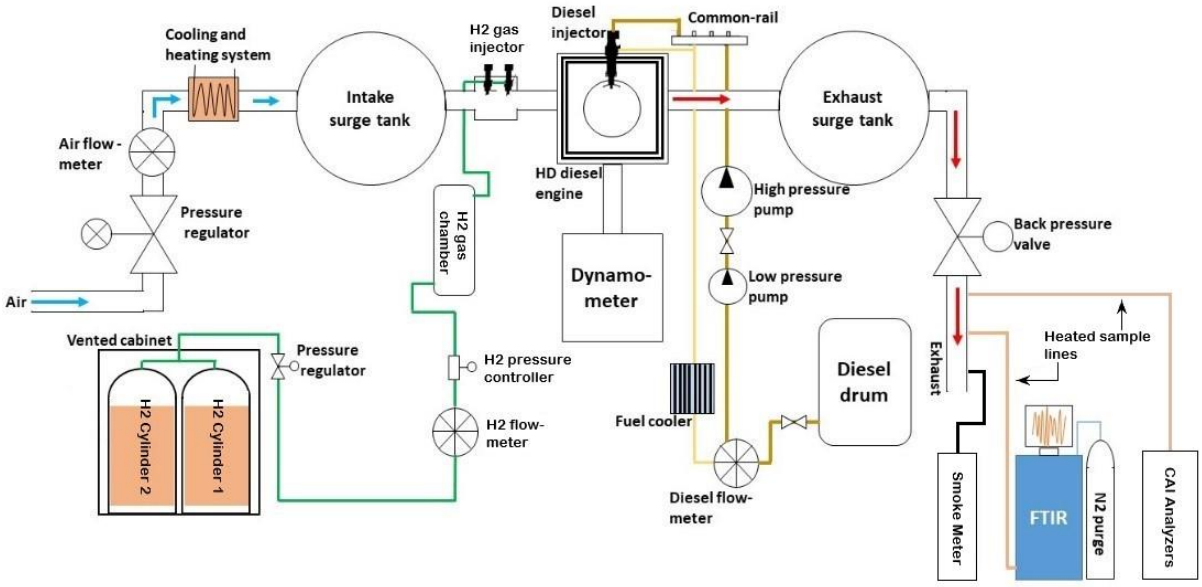

Figure 38: Schematic diagram of engine test setup.

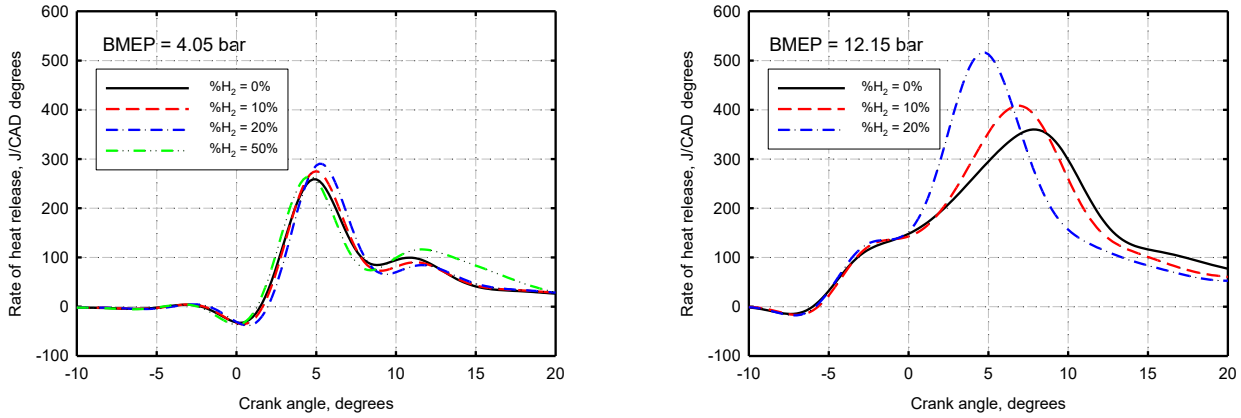

Figure 39: Net heat release rate with changing hydrogen energy fraction.

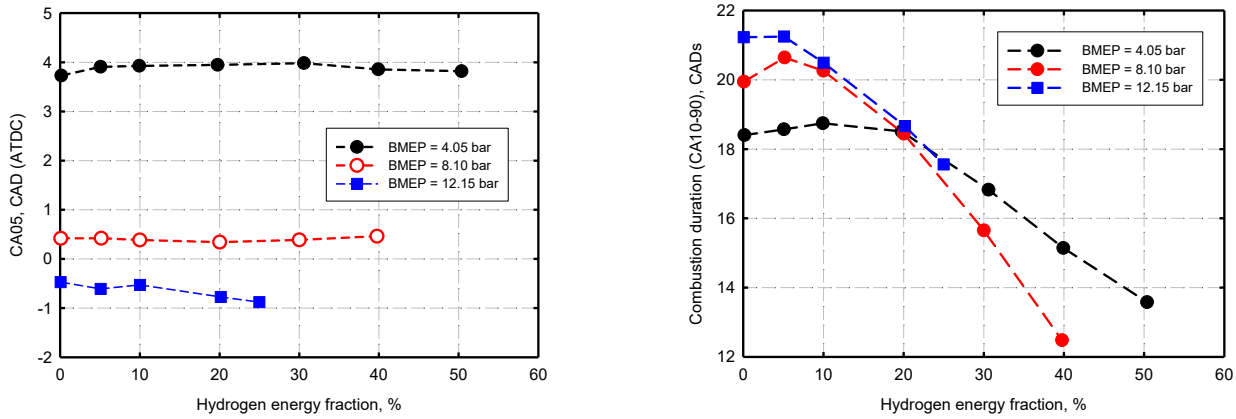

Figure 40: Variations of CA05 and CA10-90 with changing hydrogen energy fraction.

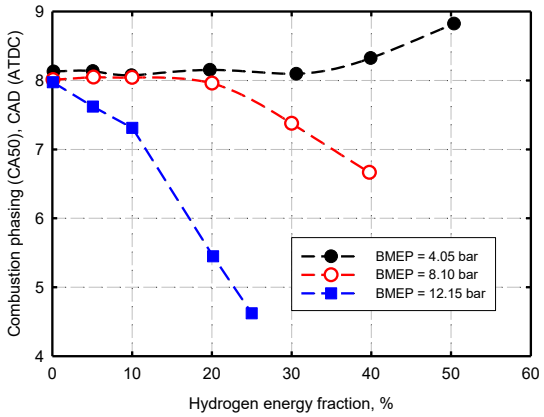

Figure 41: Variation of CA50 with changing hydrogen energy fraction.

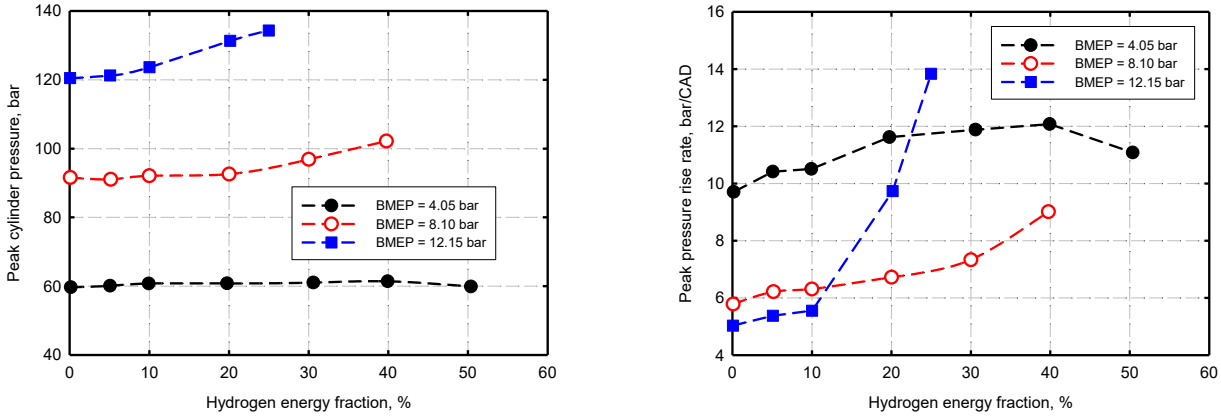

Figure 42: Variation of peak pressure and peak pressure rise rate with changing hydrogen energy fraction.

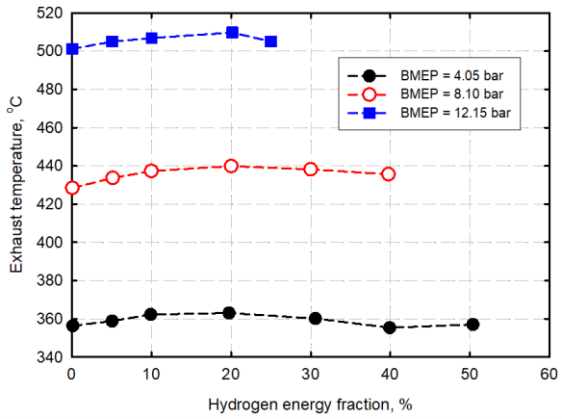

Figure 43: Variation of exhaust temperature with changing hydrogen energy fraction.

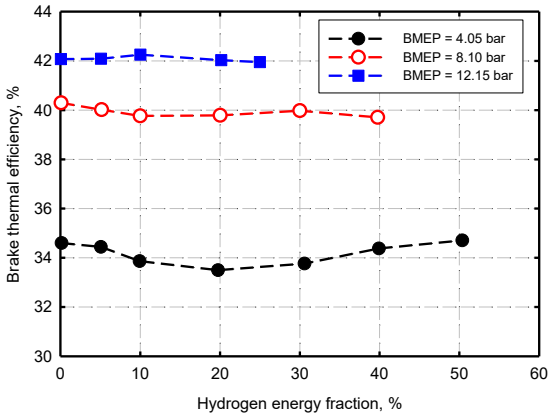

Figure 44: Variation of brake thermal efficiency with changing hydrogen energy fraction.

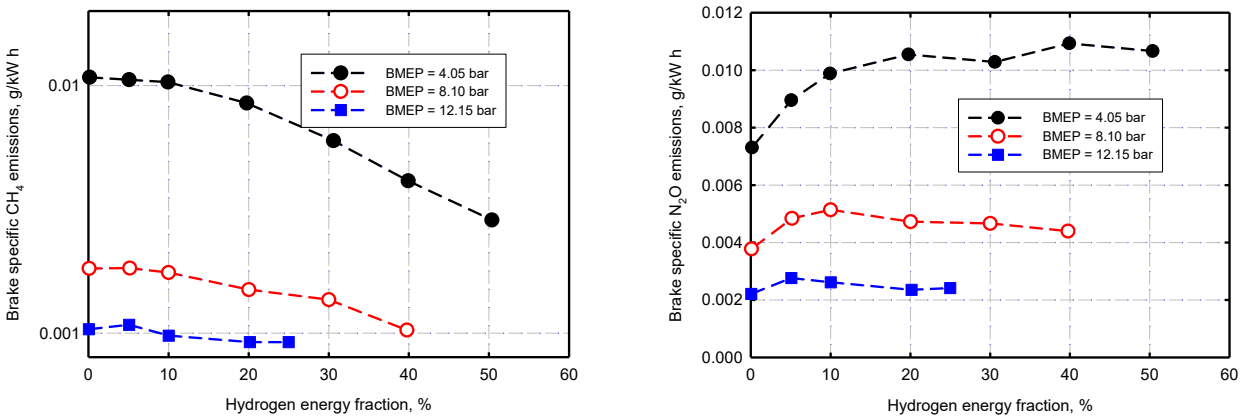

Figure 45: Variations of CH4 and N2O emissions with changing hydrogen energy fraction.

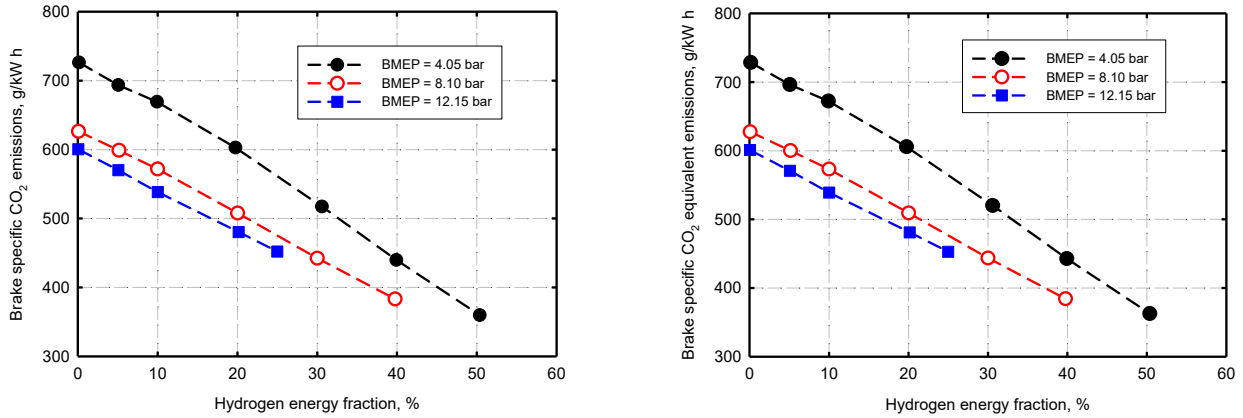

Figure 46: Variations of CO2 and CO2 equivalent emissions with changing hydrogen energy fraction.

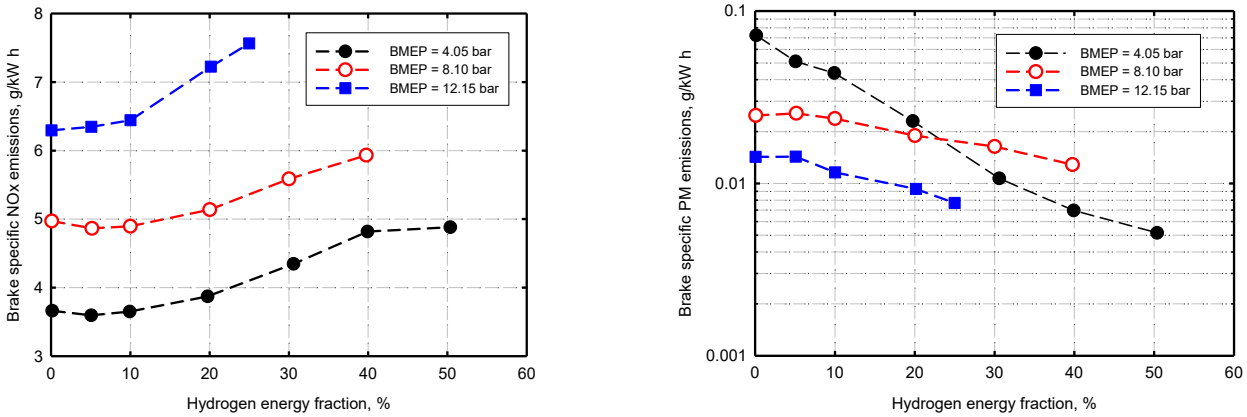

Figure 47: Variations of NOx and PM emissions with changing hydrogen energy fraction.

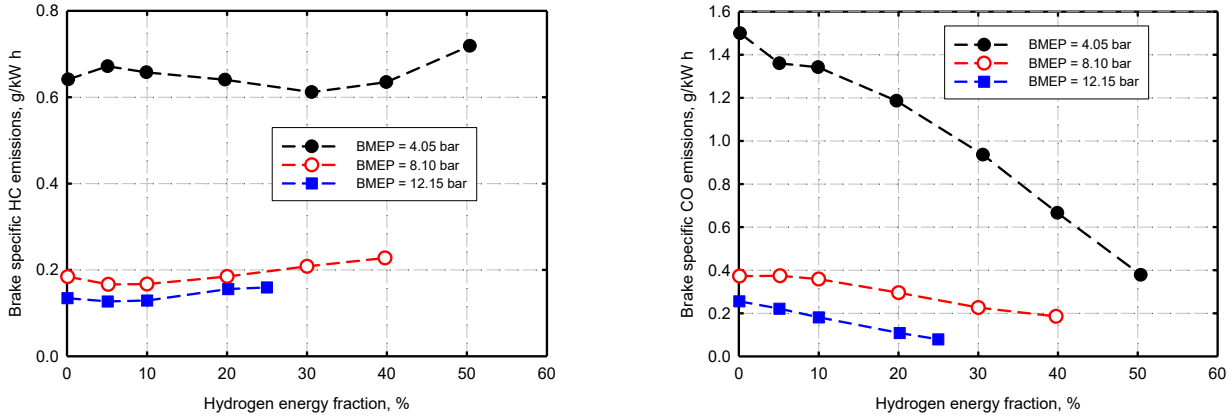

Figure 48: Variations of HC and CO emissions with changing hydrogen energy fraction.

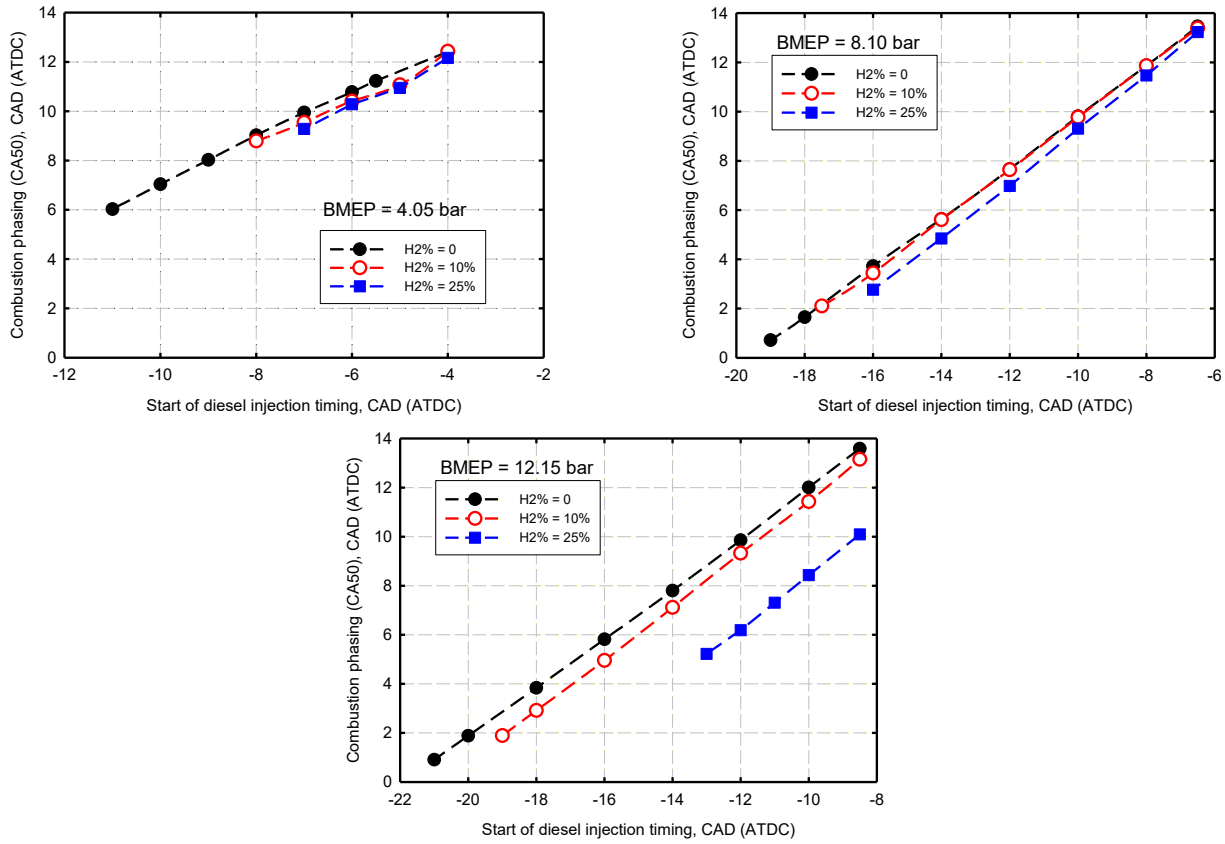

Figure 49: Variation of combustion phasing with changing SODI.

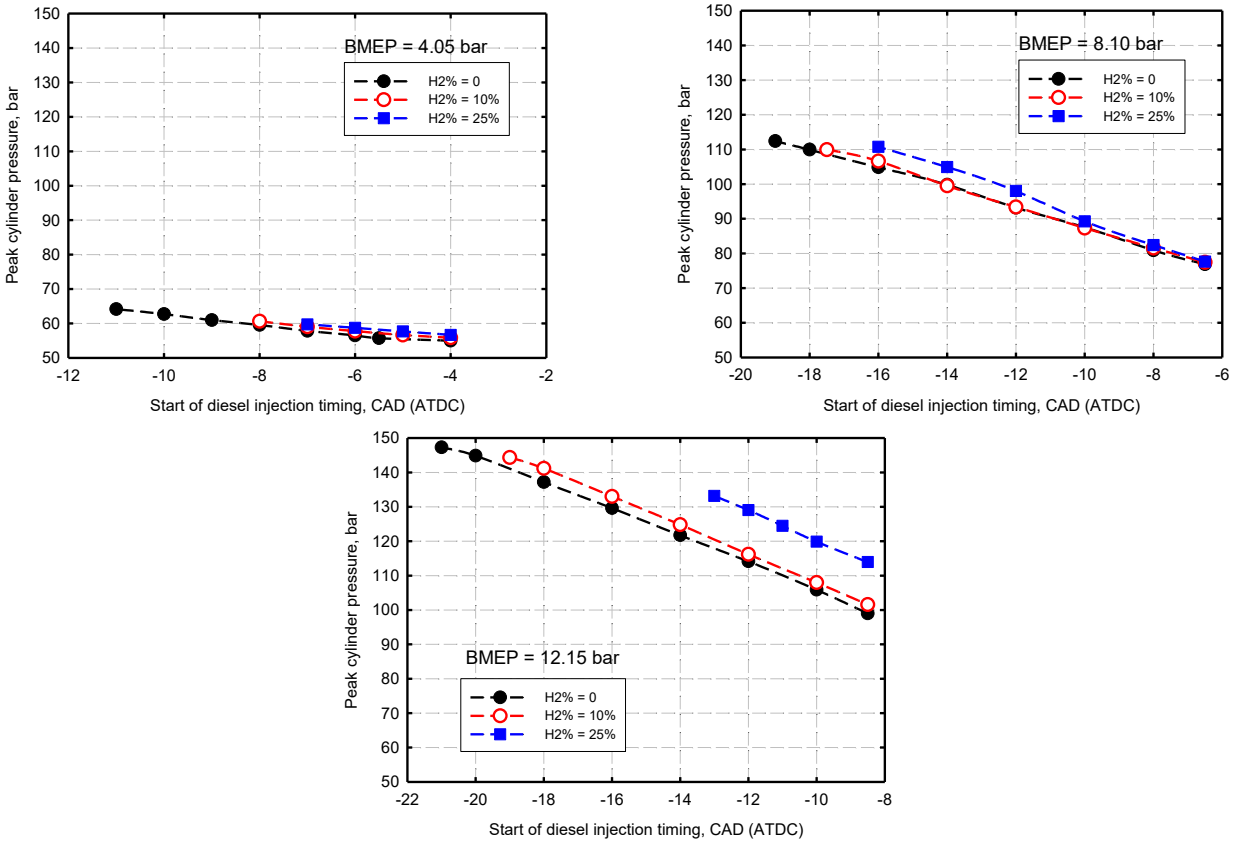

Figure 50: Variation of peak cylinder pressure with changing SODI.

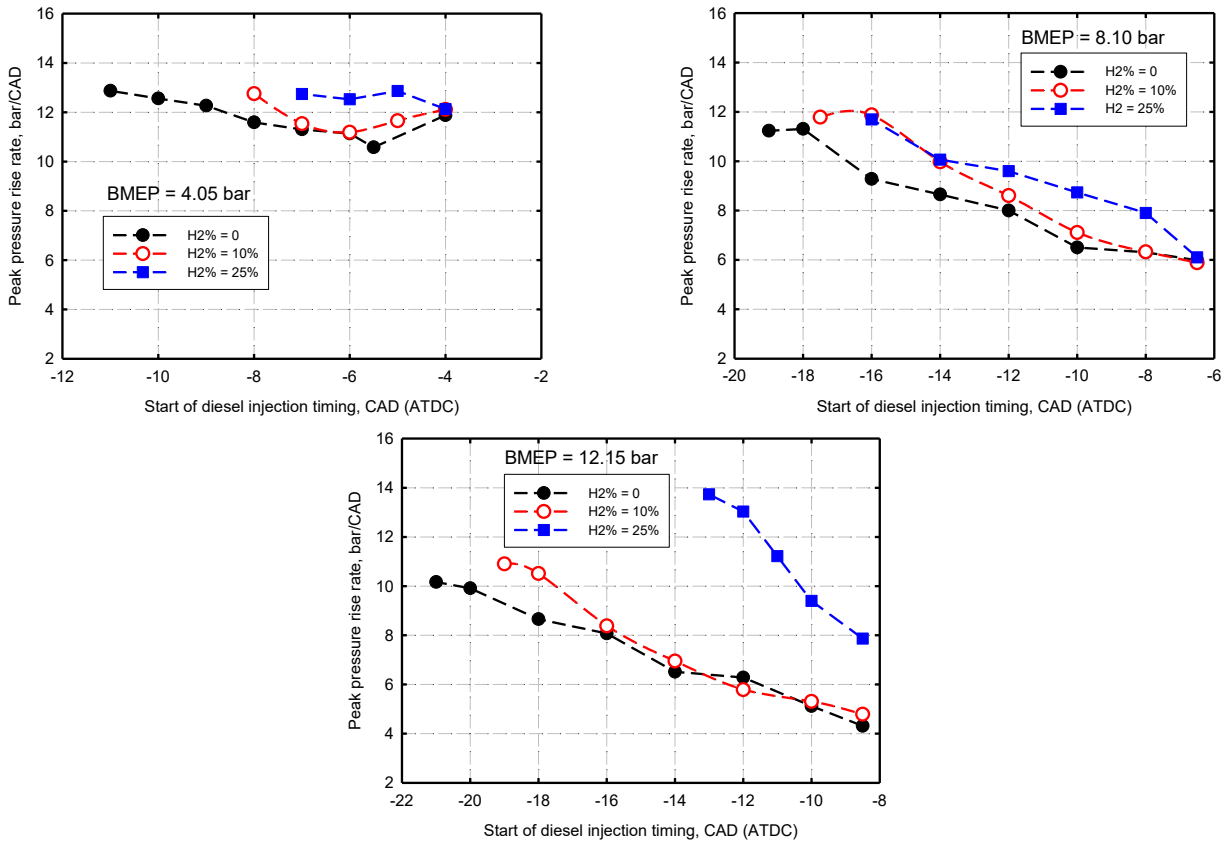

Figure 51: Variation of peak pressure rise rate with changing SODI.

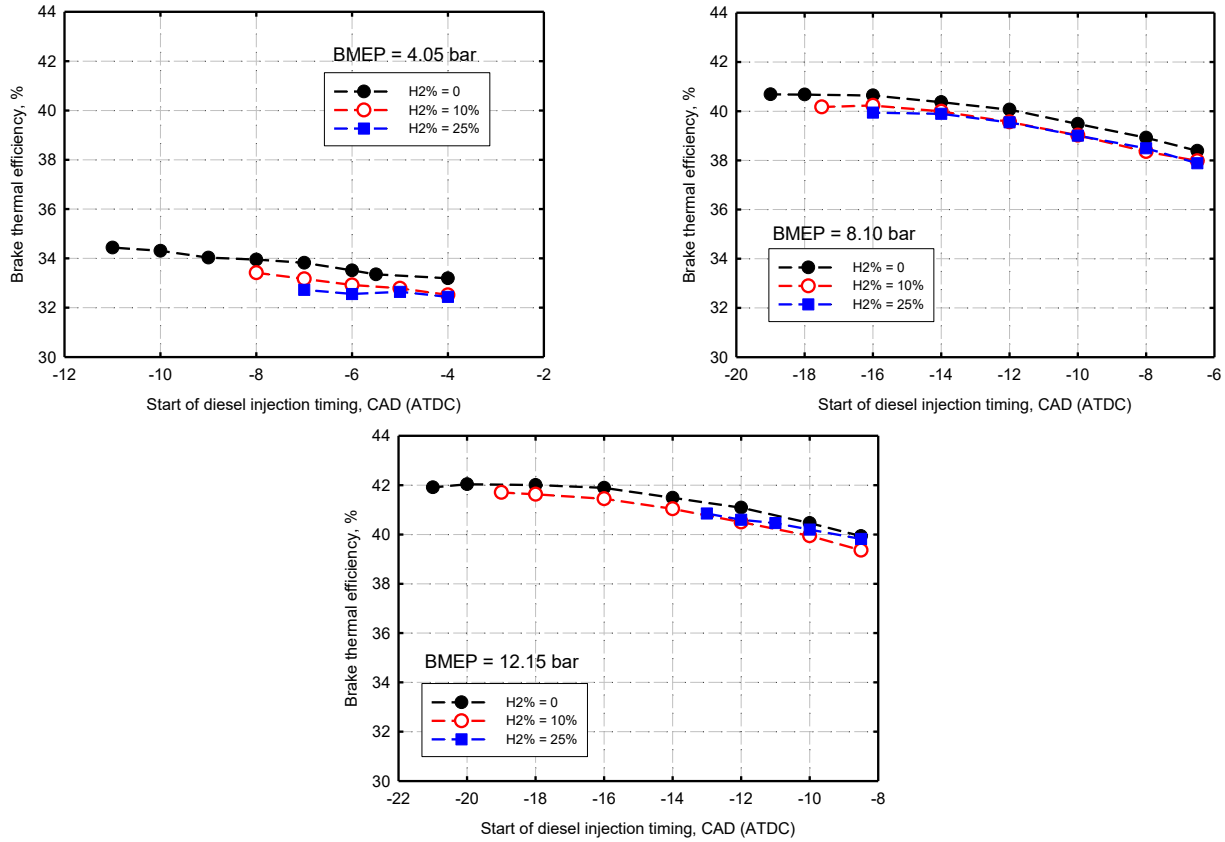

Figure 52: Variation of brake thermal efficiency with changing SODI.

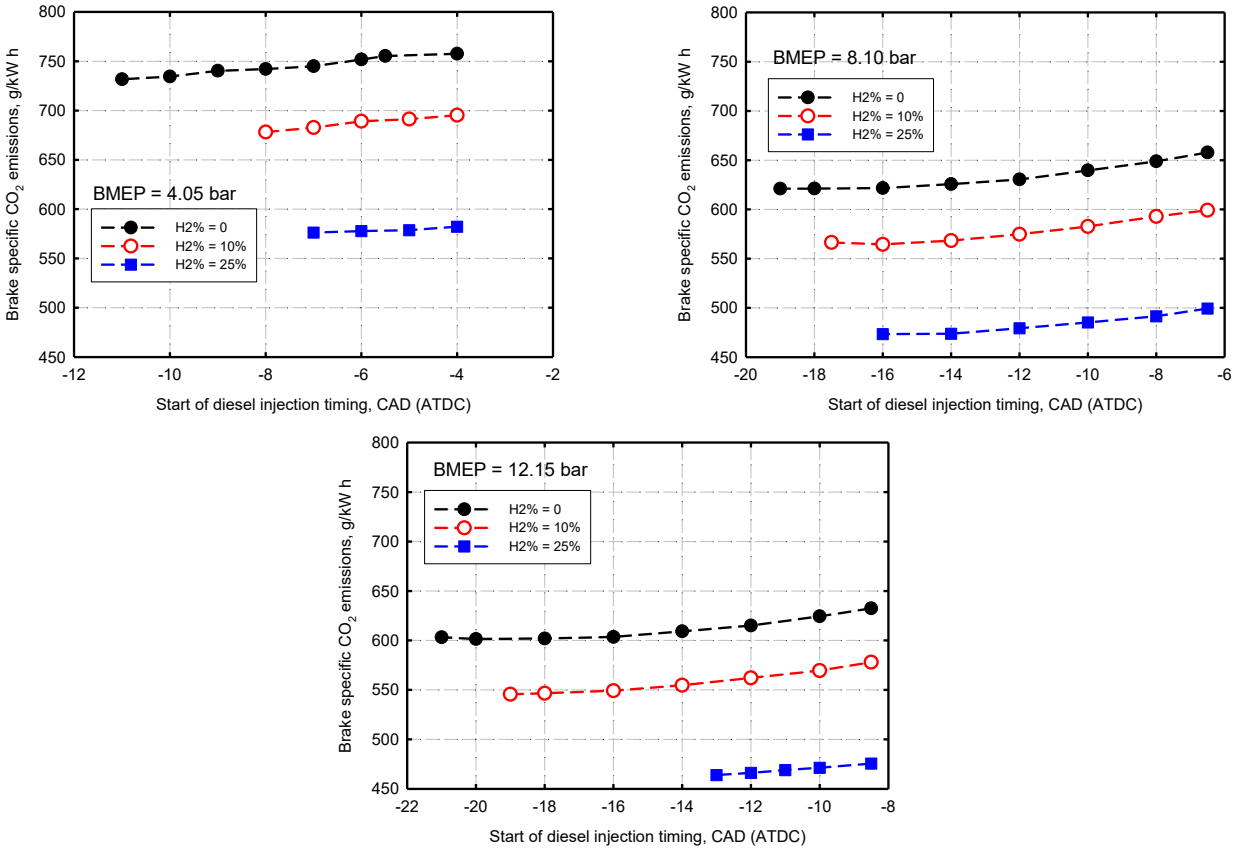

Figure 53: Variation of brake specific CO2 emissions with changing SODI.

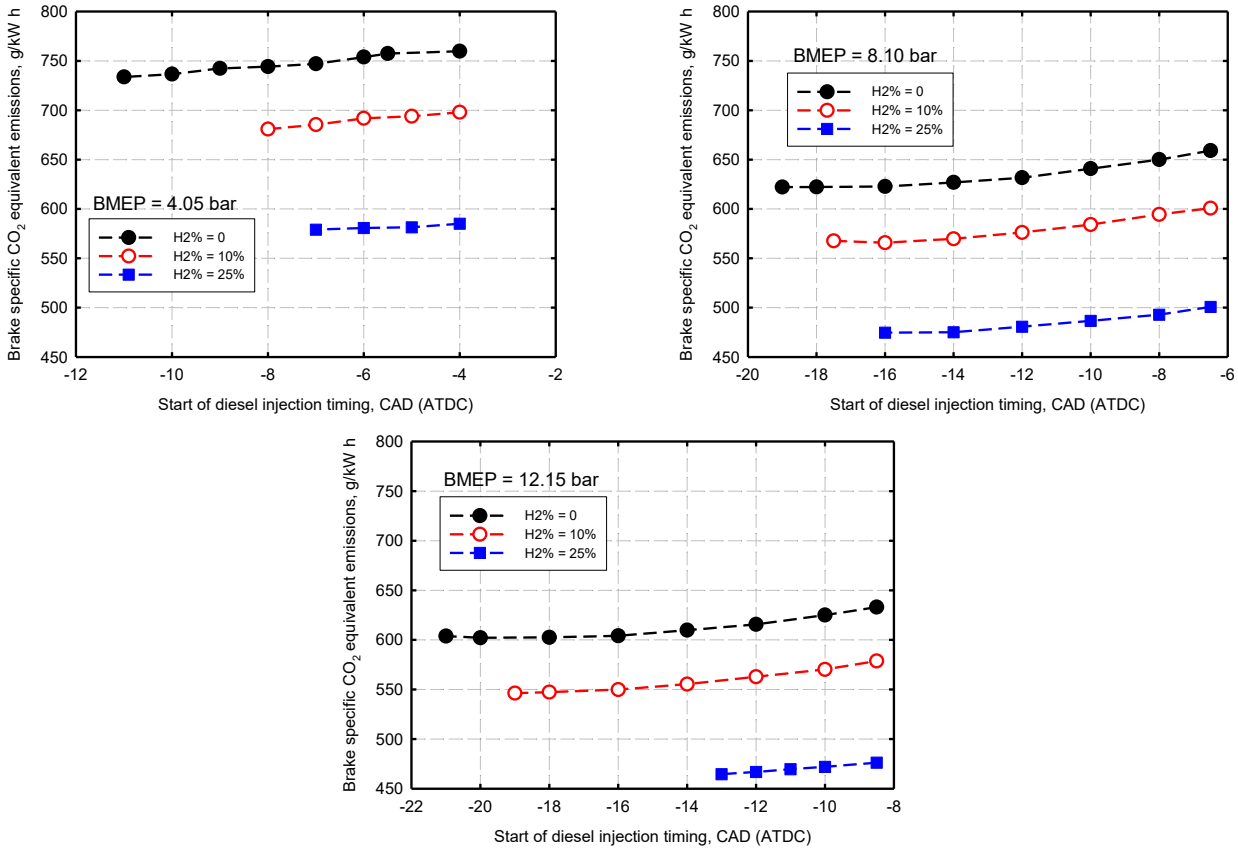

Figure 54: Variation of brake specific CO2 equivalent emissions with changing SODI.

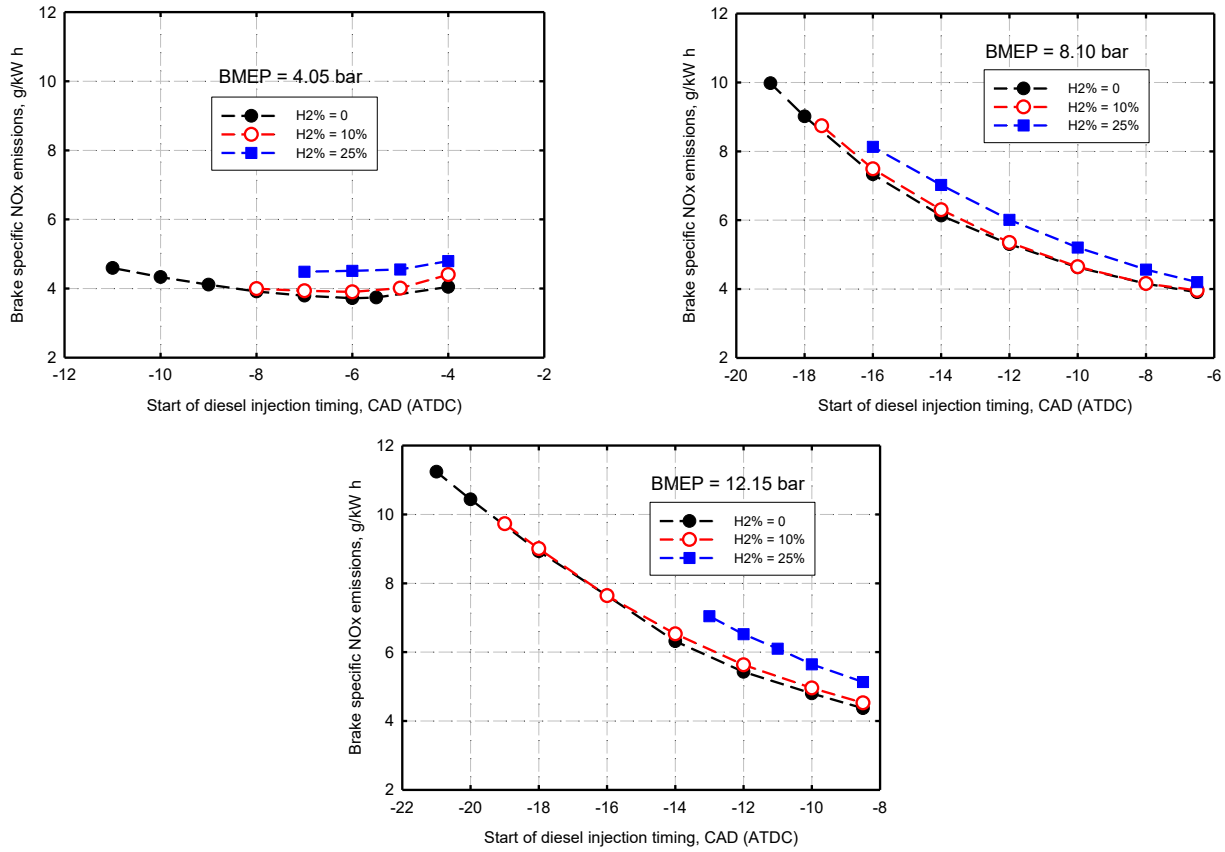

Figure 55: Variation of NOx emissions with changing SODI.

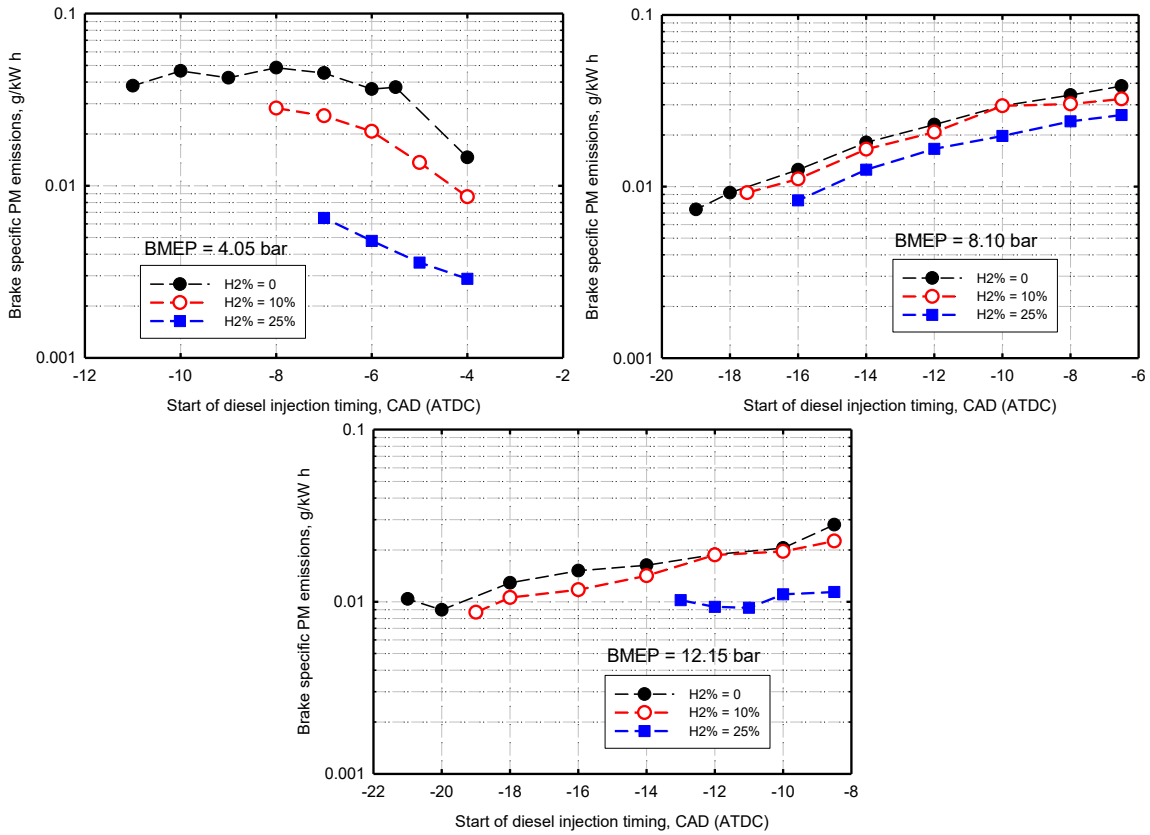

Figure 56: Variation of PM emissions with changing SODI.

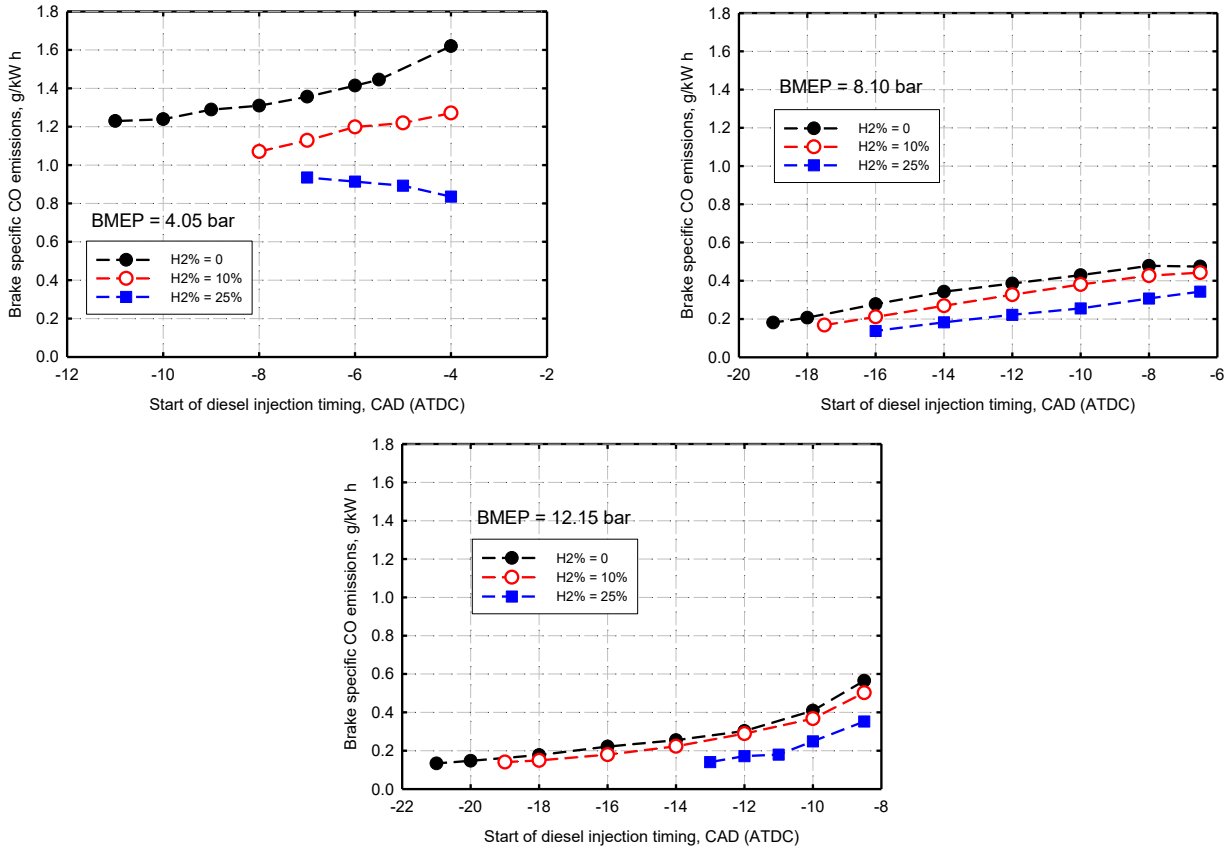

Figure 57: Variation of CO2 emissions with changing SODI.